Diogo Severino Gorgulho

MECANISMO DE PRODUÇÃO RESSONANTE DE PARTÍCULAS DURANTE A INFLAÇÃO

Dissertação no âmbito do Mestrado em Física orientada pelo Professor Doutor João Pedro Trancoso Gomes Rosa e apresentada ao Departamento da Física da Faculdade de Ciências e Tecnologia da Universidade de Coimbra.

Setembro de 2024

Faculty of Sciences and Technology

University of Coimbra

A mechanism of resonant particle production during inflation

Diogo Severino Gorgulho

A thesis written in fulfilment of the requirements for the degree of Master of Science in Physics.

Supervised by Prof. Dr. João Rosa.

September 2024

Agradecimentos

Antes de mais, gostaria de deixar um profundo agradecimento ao meu orientador, Professor Doutor João Rosa, pelo apoio e aconselhamento contínuos ao longo destes anos, direcionados não apenas a este projeto, mas a todo o meu percurso académico, e pela valiosa partilha de conhecimento, graças à qual este trabalho existe.

Quero agradecer aos meus pais, Cláudia e Américo, pela curiosidade e interesse com que seguiram todo o meu percurso, e pelo amparo e encorajamento que me deram ao longo dele, mesmo nos momentos em que as dúvidas me venciam.

Agradeço também aos meus amigos e colegas, e em especial ao Felipe, por me incentivarem, por me tirarem da minha zona de conforto e por tornarem estes anos (e certos dias em particular) mais toleráveis.

Deixo também um agradecimento à Fundação Calouste Gulbenkian, pelo apoio financeiro e por me ter dado a oportunidade de iniciar este projeto no contexto das suas Bolsas Novos Talentos, e ao Centro de Física da Universidade de Coimbra, pelo apoio financeiro também.

Abstract

The standard inflationary paradigm typically places the reheating period strictly after the slow-roll regime of the inflaton field comes to an end. Several proposals for particle production mechanisms during the slow-roll phase have appeared over the years, one argument in their favour being the possibility of having observable signatures of those particles in the Cosmic Microwave Background (CMB) spectrum. In this thesis, we develop and analyse a novel mechanism that allows for production of scalar particles χ during the slow-roll regime due to a narrow parametric resonance found in the equation of motion for the Fourier modes of their associated quantum field. Approximate analytical expressions for the comoving number density and the physical energy density of the produced particles are obtained. The backreaction on the classical inflaton and on its quantum fluctuations is obtained using the Hartree approximation, and its effects on the curvature power spectrum, the scalar spectral index and the tensor-to-scalar ratio are computed. We then perform a numerical analysis of the model including backreaction, considering in particular the efficiency of the particle production process and the effects on the inflaton field and on the CMB observables. We also compare a few analytical results to numerical simulations. We show that an appreciable energy density of χ particles can be generated through this mechanism without it becoming the dominant contribution to the Friedmann equation, thus preserving the underlying inflationary paradigm. We also show that under these conditions we obtain a modification of the curvature power spectrum which includes features that may fall within the range of future observations.

Keywords: *Cosmology, Inflation, Inflationary Epoch, Particle Production, Parametric Resonance.*

Resumo

Tipicamente, o paradigma inflacionário padrão coloca o periodo de *reheating* estritamente após o término do regime de *slow-roll* do inflatão. Várias propostas de mecanismos de produção de partículas durante a fase de *slow-roll* têm surgido ao longo dos anos, sendo um argumento em seu favor a possibilidade de ter assinaturas observáveis dessas partículas no espetro da Radiação Cósmica de Fundo (CMB, do inglês *Cosmic Microwave Background*). Nesta tese, é desenvolvido e analisado um novo mecanismo que possibilita a produção de partículas escalares χ durante o regime de *slow-roll* devido a uma ressonância paramétrica estreita (*narrow* em inglês) encontrada na equação de movimento dos modos de Fourier do campo quântico a elas associado. São obtidas expressões analíticas aproximadas para a densidade comóvel de número e para a densidade física de energia das partículas produzidas. A *backreaction* no inflatão clássico e nas suas flutuações quânticas é obtida usando a aproximação de Hartree, e os seus efeitos no *curvature power spectrum*, no *scalar spectral index* e no *tensor-to-scalar ratio* são determinados. É depois realizada uma análise numérica do modelo incluindo *backreaction*, considerando em particular a eficiência do processo de produção de partículas e os efeitos no inflatão e nos observáveis do CMB. Alguns resultados analíticos são também comparados com simulações numéricas. É mostrado que através deste mecanismo é possível gerar uma densidade de energia apreciável de partículas χ sem que esta se torne a contribuição dominante para a equação de Friedmann, assim preservando o paradigma inflacionário subjacente. É mostrado também que, sob estas condições, são obtidas modificações ao *curvature power spectrum* que podem ser observadas futuramente.

Palavras-chave: *Cosmologia, Inflação, Época Inflacionária, Produção de Partículas, Ressonância Paramétrica.*

There is a theory which states that if ever anyone discovers exactly what the Universe is for and why it is here, it will instantly disappear and be replaced by something even more bizarre and inexplicable.

There is another which states that this has already happened.

— Douglas Adams
The Restaurant at the End of the Universe

Contents

List of Figures

List of Abbreviations

ΛCDM Lambda Cold Dark Matter 2, 7

CMB Cosmic Microwave Background 1, 7–10, 16, 19, 21, 25, 26, 57, 58, 66–68, 74, 80–82, 84, 85, 89, 93, 94, 100, 104, 108

CW Coleman-Weinberg 52, 54, 120, 121

EFE Einstein's Field Equation 2, 5

EMT Energy-Momentum Tensor 4

EoM Equation of Motion 11, 20, 24, 31, 52–54, 56, 62, 73, 78, 109

EoS Equation of State 3, 4

FLRW Friedmann-Lemaître-Robertson-Walker 2, 3, 14, 29

GR General Relativity 1, 2

GUT Grand Unified Theory 9, 10

GW Gravitational Wave 17, 25, 81, 109

HBB Hot Big Bang 2, 7–10, 16, 25

KGE Klein-Gordon Equation 12

QFT Quantum Field Theory 1, 11, 89, 117

SET Stress-Energy Tensor 3, 4

SM Standard Model (of Particle Physics) 2, 5, 22, 109

TT Transverse-Traceless 20

Notation and Conventions

- Natural units $\hbar = c = k_{\rm B} = 1$ are always assumed, unless specifically mentioned;
- Einstein's summation convention will always be assumed, unless mentioned otherwise;
- The metric signature $(+, -, -, -)$ will be used throughout this text;
- The Minkowski metric will be denoted as $\eta_{\mu\nu}$, while for a generic metric $g_{\mu\nu}$ will be used;
- The reduced Planck mass will be denoted as $M_{\rm P} = \frac{1}{\sqrt{8\pi G}}$;
- We write $\ln(x)$ for the natural logarithm (base-e) and $\log_y(x)$ for a base-y logarithm.

1 Introduction

The inception of modern Cosmology in the early 20th century, greatly motivated by the observations of Edwin Hubble – namely the discovery of galaxies and of the expansion of the Universe – and by the newly established theory of general relativity, led to a drastic shift on our understanding of the Universe and its evolution. In little more than a century, we have gone from the idea of a static, scarcely populated Universe, to the notion of a rather crowded one, that is expanding at an accelerated rate [1, 3].

In fact, over the years, our models for cosmological evolution have seen countless updates based on new experimental evidence, as well as new theoretical tools and frameworks. Current models usually involve the placement of *cosmological fluids* (with both quantum and thermal properties) in a geometrical background in order to determine how both those fluids and that background behave and evolve in time, and thus require the combination of concepts and techniques from general relativity (GR), thermodynamics and statistical mechanics, and quantum field theory (QFT) [1, 3]. These models are then tested against data from experiments like the European Space Agency's satellite observatory *Planck* [4], in order to, for instance, set constraints on theoretical parameters and provide evidence for hypothesised phenomena.

One thing, however, that has remained more or less unchanged between cosmological models is the notion that the Universe is homogeneous and isotropic on large scales, which is otherwise known as the *cosmological principle*. This statement was initially a mere approximation in order to simplify theoretical calculations, but was later found to be well-founded, as observations showed, for example, that the temperature of the Cosmic Microwave Background (CMB) radiation displays fluctuations of just $\mathcal{O}(10^{-5}\,\mathrm{K})$ around its average value of 2.73 K, making it an extremely uniform spectrum [1, 3]. We will soon find that facing trouble explaining these particular observations is *also* a common factor to several cosmological models.

1.1 The Hot Big Bang model

Currently, the standard model of Cosmology is the Lambda Cold Dark Matter (ΛCDM) model [1, 5], whose designation will be clarified by the end of § 1.1.1. Nonetheless, we shall refer to it simply as the Hot Big Bang (HBB) model, in keeping with its theorised hot beginning [3]. Its theoretical predictions on cosmic evolution have been tested to be valid up to about 10^{-2} seconds after the Big Bang, but sensible speculations can be made for earlier times also, as long as some kind of extension to the Standard Model of Particle Physics (SM) is assumed [3]. In the following subsection, we establish the tools used by this paradigm and mention some of its greatest successes.

1.1.1 Overview and main results

We shall start by reviewing some of the fundamental equations of the HBB model, namely Einstein's field equations (EFEs) from GR [1]. These can be compactly written as a tensor equation

$$G_{\mu\nu} = M_{\mathrm{P}}^{-2}\, T_{\mu\nu}\,, \tag{1.1.1}$$

where $G_{\mu\nu} = R_{\mu\nu} - \frac{1}{2}Rg_{\mu\nu}$ is the Einstein tensor ($R_{\mu\nu}$ and R being the Ricci tensor and scalar, respectively), $T_{\mu\nu}$ is an energy-momentum (or stress-energy) tensor, which may include a contribution from a cosmological constant Λ ($T^{\Lambda}_{\mu\nu} \equiv M_{\mathrm{P}}^2\,\Lambda\, g_{\mu\nu}$), and M_{P} is the reduced Planck mass. This set of equations establishes a relation between the geometry of spacetime, described by $G_{\mu\nu}$, and the energy content of the Universe, encoded into $T_{\mu\nu}$.

The metric $g_{\mu\nu}$ that describes a homogeneous, isotropic and expanding Universe is the maximally symmetric Friedmann-Lemaître-Robertson-Walker (FLRW) metric, for which the line element ds^2 can be written in spherical coordinates as

$$ds^2 = dt^2 - a^2(t)\,\gamma_{ij}\,dx^i dx^j = dt^2 - a^2(t)\left[\frac{dr^2}{1-kr^2} + r^2 d\Omega^2\right], \tag{1.1.2}$$

where the scale factor $a(t)$ accounts for the expansion of space, and where k denotes the local spatial curvature of spacetime: in particular, the local geometry of the Universe would be hyperbolic (or open) for $k < 0$, Euclidean (or flat) for $k = 0$ and spherical (or closed) for $k > 0$. The spatial coordinates appearing in this definition are known as *comoving coordinates*, while the time coordinate is called *physical* or *cosmic time*, and these are the coordinates measured by an observer moving together with the expansion. Sometimes, it proves useful to instead

work in *conformal time*, $d\tau = dt/a(t)$, in which case the general FLRW metric simply becomes a conformal transformation of the non-expanding case (for $k = 0$, it becomes a conformal transformation of the Minkowski metric).

Due to the cosmological principle and the maximally symmetric metric associated with it, the only properties of the various constituents of the Universe (i.e. different types of matter, radiation, ...) that are required to specify a stress-energy tensor (SET) are the mean energy density ρ and the pressure p. This means that the universal constituents can effectively be modelled as perfect (cosmological) fluids, which are described by the equation of state (EoS)

$$p = w\rho\,, \tag{1.1.3}$$

with constant w, and have a SET given in a general frame by

$$T^{\mu\nu} = (\rho + p)\, u^\mu u^\nu - p g^{\mu\nu}\,, \tag{1.1.4}$$

where u^μ is the four-velocity of the fluid. This expression results in $T^{00} = \rho$, $T^{0i} = T^{i0} = 0$ and $T^{ij} = p\, a^{-2}\, \gamma^{ij}$ in the fluid's rest frame, where $u^\mu = (1, 0, 0, 0)$. Examples of cosmological fluids include pressureless matter ($w = 0$), radiation ($w = \frac{1}{3}$) and a cosmological constant ($w = -1$). Note that pressureless matter includes any type of non-relativistic massive particles (e.g. baryons and cold[1] dark matter), while radiation refers to both photons and any other (ultra)relativistic species (e.g. neutrinos and hot[2] dark matter).

Using the metric (1.1.2) and the rest-frame version of (1.1.4), the 00 component of (1.1.1) becomes

$$H^2 \equiv \left(\frac{\dot{a}}{a}\right)^2 = \frac{1}{3M_{\rm P}^2}\,\rho - \frac{k}{a^2}\,, \tag{1.1.5}$$

which is known as the Friedmann equation. Here, $H \equiv \frac{\dot{a}}{a}$ is the Hubble parameter, and ρ is the total energy density of the Universe (including Λ contributions). The term proportional to k can itself be absorbed into ρ, in which case it is interpreted as the fraction of the energy density that is linked to the curvature of spacetime. The Friedmann equation is of major importance in the context of Cosmology, as it establishes a direct relation between the energy content of the Universe and the latter's rate of expansion.

[1] Here, "cold" means that the species is heavier than the temperature scale of the Universe, $m \gg T$.

[2] Similarly, "hot" refers to particles lighter than the temperature scale, $m \ll T$.

Another equation of great use is obtained using the ij components of (1.1.1) and the Friedmann equation, as well as $T^{ij} = p\, a^2\, \gamma^{ij}$, and is known as the Raychaudhuri (or acceleration) equation

$$\frac{\ddot{a}}{a} \;=\; -\frac{1}{6M_{\rm P}^2}(\rho + 3p)\,, \tag{1.1.6}$$

which in particular shows that to a positive value of Λ corresponds a positive energy density $\rho_\Lambda = M_{\rm P}^2\,\Lambda$ and a negative pressure $p_\Lambda = -\rho_\Lambda$, leading to a positive contribution to the acceleration: this result is what motivates the argument that the observed accelerated expansion of spacetime is due to a cosmological constant[3].

From the covariant conservation of the energy-momentum tensor (EMT), $T^{\mu\nu}{}_{;\nu} = 0$, one finds, for the $\mu = 0$ component, the following conservation equation

$$\frac{\dot{\rho}}{\rho} \;=\; -3\frac{\dot{a}}{a}(1+w)\,, \tag{1.1.7}$$

with solution

$$\rho(t) = \rho_0 \left(\frac{a(t)}{a_0}\right)^{-3\,(1+w)}\,, \tag{1.1.8}$$

where $\rho_0 = \rho(t_0)$ and $a_0 = a(t_0)$, for some pivot t_0 which is usually taken to be the present time. This allows us to conclude that, given an EoS (i.e. a certain value of w), we find different scaling behaviours of ρ with respect to a: in other words, distinct fluids should evolve differently throughout the cosmic history, as they become diluted by different powers of the scale factor. For instance, the energy density of pressureless matter scales with a^{-3}, whereas for radiation the scaling is with a^{-4} (the additional factor of a^{-1} is interpreted as coming from the redshift of the wavelength); in turn, the cosmological constant has a constant energy density, in accordance with the definition of its SET.

We may also plug Eq. (1.1.8) into the flat Friedmann equation and integrate it to get

$$a(t) = \left(\frac{t}{t_0}\right)^{\frac{2}{3\,(1+w)}} \qquad \text{for} \quad w \neq -1\,, \tag{1.1.9}$$

where t_0 contains all multiplicative factors. This expression shows how the scale factor behaves in time for flat Universes dominated by different kinds of cosmological fluids. The particular

[3] A Universe whose energy density is dominated by that of a positive cosmological constant driving accelerated expansion is described by the *de Sitter metric* and may be called a *de Sitter Universe* [6, 7].

case of $k = 0$ is interesting because observations strongly suggest that our Universe is itself flat, which as we will see in § 1.1.2 is a troublesome detail for standard cosmology.

The above equations are sometimes expressed in terms of (time-dependent) dimensionless density parameters Ω_s, given by

$$\Omega_s(t) \equiv \frac{\rho_s(t)}{\rho_{\rm cr}(t)}\,, \tag{1.1.10}$$

where the subscript s refers to the different species that populate the Universe (photons, electrons, neutrons, ...), and where $\rho_{\rm cr}(t)$ is the critical density at time t, which is defined by setting $k = 0$ in Eq. (1.1.5), giving $\rho_{\rm cr}(t) \equiv 3\,M_{\rm P}^2 H^2(t)$. That is, $\rho_{\rm cr}$ is the value of ρ corresponding to a flat, Euclidean Universe. The total density parameter Ω is simply given by the sum of the Ω_s for all particle species.

The field equations can also be found from an action formalism [6], which is often useful, especially when dealing with matter fields. This is achieved by defining the action

$$S \;=\; S_{\rm EH} \,+\, S_M \;=\; -\frac{M_{\rm P}^2}{2}\int d^4x\,\sqrt{-g}\,R \,+\, S_M\,, \tag{1.1.11}$$

where $S_{\rm EH}$ is known as the Einstein-Hilbert action, with $\sqrt{-g} \equiv \sqrt{|\det(g_{\mu\nu})|}$, and S_M is the action for matter fields. We may vary S with respect to $g^{\mu\nu}$ in order to obtain Eq. (1.1.1), which reduce to the vacuum EFEs when $S_M = 0$, using also the following definition for the stress-energy tensor

$$T^{\mu\nu} \equiv -\frac{2}{\sqrt{-g}}\frac{\delta S_M}{\delta g_{\mu\nu}}\,. \tag{1.1.12}$$

It is important to note that Eq. (1.1.4) is related only to the macroscopic properties of the cosmological fluids. However, it is the microscopic particle dynamics that dictate the average behaviour of the fluid, and so these must be taken into consideration. The link between these two scales comes from statistical mechanics, for both equilibrium and out-of-equilibrium states. The equilibrium behaviour of the SM particle species is well studied [1, 8, 9] and it has been found that particles of a certain species s in thermal equilibrium at a temperature T are distributed in energy $E(p) = \sqrt{p^2 + m^2}$ according to

$$f_s[E(p)] = \frac{1}{e^{\frac{E(p)-\mu_s}{T}} \pm 1}\,, \tag{1.1.13}$$

where μ is the chemical potential of the species, and $+$ and $-$ refer to fermions and bosons, respectively, making the distribution function either a Fermi-Dirac or a Bose-Einstein distribution. These functions can be used to express quantities like the number density n_s, the energy density ρ_s or the pressure p_s, written here for a gas of free particles with degeneracy g

$$n_s = g \int \frac{d^3p}{(2\pi)^3} f_s[E(p)] \tag{1.1.14a}$$

$$\rho_s = g \int \frac{d^3p}{(2\pi)^3} f_s[E(p)]\, E(p) \tag{1.1.14b}$$

$$p_s = g \int \frac{d^3p}{(2\pi)^3} f_s[E(p)]\, \frac{p^2}{3\,E(p)}\,, \tag{1.1.14c}$$

which are then expressed in terms of the equilibrium temperature T. This temperature can be related with the cosmic time t via the conservation equation (1.1.7)[4]. In particular, it can be shown that the number density is diluted by the expansion of the Universe as $n_s \propto a^{-3}$. As stated before, these results describe species in thermal equilibrium and can be used to determine, for instance, the epoch at which the energy densities of two of those species are equal, the most notable one being the *matter-radiation equality*, found to have occurred at about $z_{\rm eq} \sim 3000$ (z being the redshift parameter), which has strong implications in the generation of large-scale structure [1, 8].

However, particles interact with each other and are not always in a state of equilibrium. These out-of-equilibrium interactions are described by the Boltzmann equation

$$\frac{dn_s(t)}{dt} + 3H\, n_s(t) = \int \frac{d^3p}{(2\pi)^3}\, C[f_s]\,, \tag{1.1.15}$$

which is reminiscent of a conservation equation, giving the time evolution of the particle number density for each species s. The right-hand side of the equation is a *collision term*, containing information on any type of physical process that the particles may undergo, namely scattering, pair creation, annihilation and particle decay. When this term is zero, the solution for n_s simply scales as a^{-3} due to the expansion, in accordance with the equilibrium theory. Collision terms are normally related with the cross sections of the processes that generate them and thus with the rate Γ at which they occur. In particular, there exists a competition between the interaction rate Γ and the expansion rate H: if $\Gamma \gtrsim H$, thermal equilibrium can be reached via interactions, whereas if $\Gamma \lesssim H$, the expansion does not allow thermal equilibrium to be attained [1, 8].

[4] This equation also implies that the entropy density of the Universe $s(T) \equiv \frac{\rho+p}{T} \propto a^{-3}$ satisfies $s(T)\,a^3 =$ const., which states that the entropy in a comoving volume $S \propto s(T)\,a^3$ is conserved.

Using the toolkit described above, the HBB paradigm has provided us with several interesting and successful results. To begin with, as was mentioned before, the observed accelerated expansion of the Universe is accounted for by means of a cosmological constant Λ, which is interpreted within this paradigm as an unidentified form of energy known as *dark energy*, which makes up about 68% of the total energy density of today's observable Universe [1, 3, 5]; this, together with the fact that currently the second most abundant form of energy in the observable Universe (at about 26% of the total density) is the also unidentified *cold dark matter* [5], motivates the designation of the standard cosmological model as ΛCDM. Prior to the current Λ-*dominated era*, the ΛCDM model predicts that two other eras have taken place in cosmic history, as is summarised in Figure 1.1.1: the *radiation-dominated era*, shortly after the Big Bang, and the *matter-dominated era*, situated between the other two, and from which we have "just" exited [1, 3, 8]. Moreover, the Big Bang nucleosynthesis described by this model correctly predicts the measured primordial mass abundances of light-element nuclei, namely a mass abundance of $\sim 25\%$ for ^{4}He [1, 3]. The model also accurately predicts the existence of the CMB, which should have had its origin during the matter-dominated era, while also predicting some of its observed characteristics, in particular its black-body spectrum, average temperature and polarisation [1, 3]. Other successes include the prediction of the observed large-scale structure of the Universe, i.e. the observed statistical distribution of galaxies and other large-scale bodies, and of the existence of the baryon acoustic oscillations [1, 3, 8].

1.1.2 Shortcomings of the Hot Big Bang model

In spite of the substantial amount of observational data from our Universe that the HBB model is able to adequately predict and describe, there are a few aspects that it fails to properly explain, which we shall now present with some detail.

The flatness problem

One of the conundrums that the HBB model fails to tackle is known as the flatness problem [2, 3, 10, 11]. It consists in the fact that the current energy density of the Universe, ρ_0, is measured to be very close to the current critical density, $\rho_{\mathrm{cr},0}$, which is the energy density in the case of a flat Universe, thus resulting in a total density parameter $\Omega_0 = \frac{\rho_0}{\rho_{\mathrm{cr},0}} \approx 1$. This of course means that the Universe is essentially flat. Using the Friedmann equation, it is possible to show that

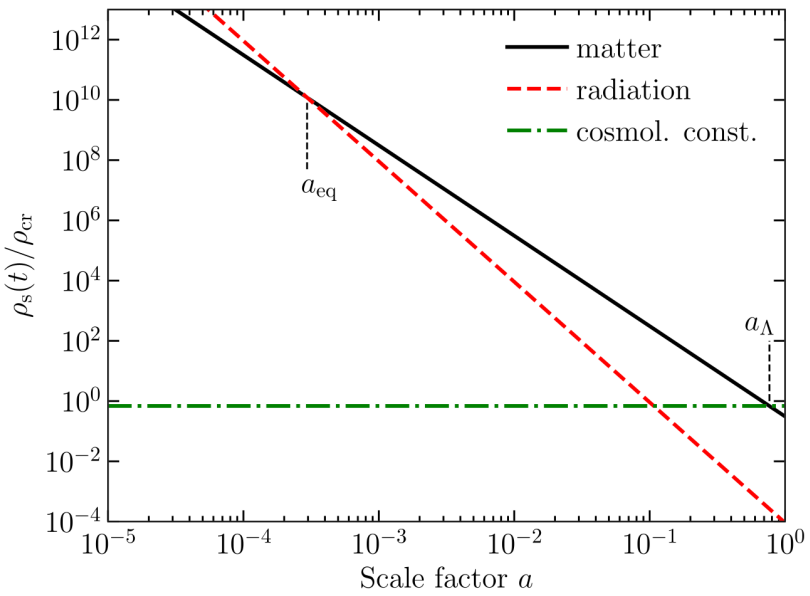

Figure 1.1.1: Evolution of the energy density (normalised against the current critical density, as per Eq. (1.1.8)) for different constituents of the Universe: pressureless matter ($\propto a^{-3}$), radiation ($\propto a^{-4}$) and a cosmological constant ($\propto a^0$). The *matter-radiation equality* and the *matter-*Λ *equality* are identified with $a_{\rm eq}$ and a_Λ, respectively. Taken from Ref. [1].

$$\Omega^{-1} - 1 \;=\; -\frac{3M_{\rm P}^2 k}{\rho\, a^2(t)}\,, \tag{1.1.16}$$

so that, for matter- and radiation-dominated Universes ($\rho \propto a^{-3}$ and $\rho \propto a^{-4}$, respectively), deviations from unity in the value of Ω grow with the scale factor, whose value increases over time. Hence, in order for $\Omega_0 \approx 1$ to be true, one can show that we must have, for example, $|\Omega - 1| \lesssim \mathcal{O}(10^{-60})$ at the Planck scale, at about 10^{-43} seconds after the Big Bang [3], which means that the initial value of Ω has to be markedly fine-tuned. In summary, the observed flatness of the Universe appears to exist only through a delicate arrangement of parameters in the early stages of the cosmological evolution, which surely is a bothersome prediction of the working paradigm.

The horizon problem

Another noteworthy issue with the HBB model is dubbed the horizon problem [2, 3, 10, 11]. As stated before, the CMB spectrum has been found to be very uniform, with all the radiation being in thermal equilibrium, having in principle attained it by means of causal processes (e.g. Compton scattering). Since their emission at the time of last scattering, the CMB photons have moved freely across the Universe, which implies that all points in the last scattering surface

must have been in thermal equilibrium too. If that were the case, at the time of emission, all regions of the last scattering surface from which we receive CMB radiation at $a = a(t_0)$ ought to be in causal contact with each other. In particular, the separation distance at the time of emission

$$d_{\rm sep}(t_e) \;=\; a(t_e) \int_{a(t_e)}^{a(t_0)} \frac{da'}{a'^2\, H(a')}\,, \tag{1.1.17}$$

between two regions in opposite points in the sky from which we receive CMB radiation must be *smaller* than the physical causal horizon distance at that time, $d_H(t_e)$, with [1, 10]

$$d_H(t) \;\equiv\; a(t) \int_{a(t_i)}^{a(t)} \frac{da'}{a'^2\, H(a')}\,, \tag{1.1.18}$$

where $H(a) = \frac{\dot{a}}{a}$ and t_i marks the Big Bang singularity. Working in the HBB paradigm, one can show that the ratio between these two distances is given in terms of the redshift parameter z by

$$\frac{d_{\rm sep}(t_e)}{d_H(t_e)} \;=\; 2\left((1+z)^{1/2} - 1\right)\,, \tag{1.1.19}$$

with $z \sim 1000$ at the time of emission, making $d_{\rm sep}(t_e) \gg d_H(t_e)$. Hence, according to the HBB model, at the time of recombination there were regions in the last scattering surface that were not in causal contact, but were necessarily in thermal equilibrium with one another. There are no physical processes that could lead to the observed thermal homogeneity between causally disconnected regions, so the Universe must have been thermally homogeneous already at the Big Bang, which is again indicative of a fine-tuned Universe.

Other problems

In addition to these two problems, one may point out several more, albeit of less importance, e.g. the predicted existence of unobserved topological defects (like magnetic monopoles) by some Grand Unified Theories (GUTs), which the HBB model has no mechanism to dispose of, and also the origin and structure of the CMB temperature anisotropies, which the HBB model fails to explain satisfactorily [1–3, 7, 8, 11].

1.2 The inflationary solution

A possible solution to the aforementioned problems is found by modifying the HBB model to include a period of accelerated expansion just before the radiation-dominated era, dubbed the *inflationary epoch* [1–3, 7, 8, 11–16].

It is straightforward to see, looking at the Raychaudhuri equation (1.1.6), that an accelerated expansion corresponds to $w < -\frac{1}{3}$. Since $\rho \propto a^{-3(1+w)}$, as was shown using the conservation equation (1.1.7), we conclude that in Eq. (1.1.16), for $w < -\frac{1}{3}$, we have $\rho a^2 \propto a^{-3(1+w)} a^2 \propto a^r$, with $r > 0$, so that deviations from flatness would be smoothed out in a period of accelerated expansion, thereby solving the flatness problem [3].

Furthermore, if $a \propto t^p$, we have $H = \frac{p}{t} \propto a^{-1/p}$. The physical causal horizon distance in Eq. (1.1.18) thus diverges if $p > 1$, which, from $\ddot{a} \propto p(p-1)t^{p-2}$, is also the condition for accelerated expansion. Hence, such a period would be associated with an infinite causal horizon, so that during it all regions could be in causal contact with each other, thus being allowed to reach thermal equilibrium through conventional physical processes. In a posterior epoch, the causal horizon can eventually become finite, thereby removing the causal connection between some of these regions, which, however, will all remain in thermal equilibrium. In other words, we have successfully solved the horizon problem [1].

Additionally, a period of accelerated expansion would cause the topological defects predicted by the GUTs to dilute away, thereby explaining their observational absence (provided no others would be produced after this period ends) [3]. Similarly, other issues with the HBB model can be solved by postulating the existence of this period of cosmological *inflation* – in particular, we shall see that quantum effects linked to inflation generate a solution to the CMB anisotropies [3, 7].

The duration of inflation can be quantified using the number of e-folds, defined as

$$N_e = \ln \frac{a_f}{a_i} \,, \tag{1.2.1}$$

where a_i and a_f are the values of the scale factor at the beginning and at the end of inflation, respectively. Throughout this text, we will use N_e to designate both the e-folds variable and the duration of inflation in that variable. In order to solve the flatness and the horizon problems, it is possible to show that N_e should be around 50-60, which we shall treat as the reference range for the duration of inflation [3, 7].

We shall now initiate a brief exploration of the main concepts within this paradigm.

1.2.1 Standard picture of inflation

Inflationary models are based in QFT. However, if we neglect quantum fluctuations, we may consider a classical description of the *inflaton* field, which is then modelled as a real scalar field, $\phi(t, \mathbf{x})$. The discussion contained in this section is primarily based on [2, 3, 7, 11]. The inflaton is usually modelled as a scalar field because scalar fields are invariant under Lorentz transformations, which means that even if they attain a non-zero (classical) vacuum expectation value the local Lorentz invariance of the vacuum [17, 18] is maintained, which would not happen for spinor and vector fields[5]; moreover, scalar fields are the simplest to treat mathematically, so it is only logical to try and devise a mechanism based on one. In this work, we will assume a single-field inflation scenario [22].

The classical inflaton

Following an action formalism, we write a Lagrangian density and an action for $\phi(t, \mathbf{x})$, from which we can obtain the equation of motion (EoM) and the stress-energy tensor. Using the latter, we can determine the energy density, ρ_ϕ, and the pressure, p_ϕ, of the field

$$\rho_\phi = \frac{1}{2}\dot{\phi}^2 + \frac{1}{2}\frac{(\nabla\phi)^2}{a^2} + V(\phi) \tag{1.2.2a}$$

$$p_\phi = \frac{1}{2}\dot{\phi}^2 - \frac{1}{6}\frac{(\nabla\phi)^2}{a^2} - V(\phi)\,, \tag{1.2.2b}$$

where we have introduced a potential energy $V(\phi)$ for the inflaton. From (1.2.2), ρ_ϕ and p_ϕ do not seem to be related by the equation of state (1.1.3), with $w < -\frac{1}{3}$ in order to get an accelerated expansion. However, if the potential energy dominates, we have indeed $p_\phi \approx -\rho_\phi$, so that $w \approx -1 < -\frac{1}{3}$, in which case the inflaton field approximately mimics a cosmological constant; as such, during inflation, the Universe exists in a *quasi*-de Sitter space [1, 2, 7]. From equation (1.1.7), it is clear that ρ_ϕ is approximately constant in time and in this case, if we take it to dominate the energy density of the Universe, we may write the Friedmann equation as

$$H^2 = \frac{1}{3M_\mathrm{P}^2}\,\rho_\phi \implies \frac{\dot{a}}{a} = H = \frac{1}{M_\mathrm{P}}\sqrt{\frac{\rho_\phi}{3}} \approx \text{const.}\,, \tag{1.2.3}$$

where we have already assumed a flat Universe (i.e. $k = 0$), which we will continue to assume for the remainder of this text. From (1.2.3), it follows that the scale factor grows at an almost

[5] In spite of this, inflationary scenarios where the inflaton is modelled either as a fermion field [19] or as a vector field [20, 21] have been proposed.

exponential rate, being given by $a(t) = a_0\, e^{Ht}$, with $H \approx$ const. while inflation lasts. Hence, we may consider that the term $\frac{(\nabla\phi)^2}{a^2}$ is quickly diluted away, which is equivalent to saying that the inflaton field is in fact homogeneous and thus exclusively time-dependent, $\phi = \phi(t)$. With this, in order to have $p_\phi \approx -\rho_\phi$ we just need to ensure that $\frac{1}{2}\dot{\phi}^2 \ll V(\phi)$, which translates into saying that the inflaton is rolling slowly (or *slow-rolling*) down its potential, which is then approximately flat (constant). This is what we shall dub the first slow-roll condition.

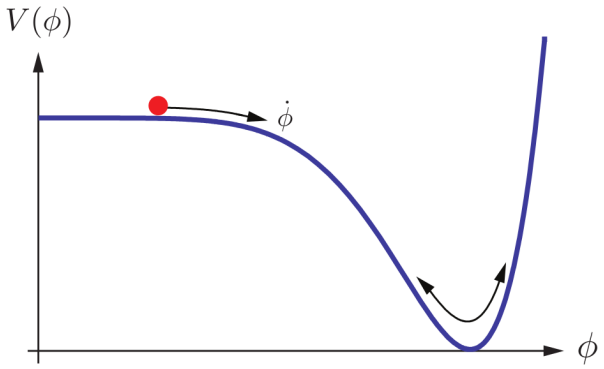

Figure 1.2.1: Generic representation of an inflationary potential $V(\phi)$, down which the field ϕ is *slow-rolling* with velocity $\dot{\phi}$. The right part of the potential is explained in § 1.2.2. Taken from Ref. [2].

Moreover, neglecting gradients, the equation of motion for the inflaton is a Klein-Gordon equation (KGE) given by

$$\ddot{\phi} + 3H\dot{\phi} + V_{,\phi}(\phi) = 0\,, \tag{1.2.4}$$

which we can use to establish a second slow-roll condition: $\ddot{\phi} \ll 3H\dot{\phi}$. This one ensures that the first condition is verified for a long enough time to allow inflation to solve the flatness and the horizon problems.

In the slow-roll regime, the Friedmann equation (1.2.3) and the Klein-Gordon equation (1.2.4) can thus be rewritten, respectively, as

$$3M_{\rm P}^2 H^2 \approx V(\phi) \tag{1.2.5a}$$

$$3H\dot{\phi} \approx -V_{,\phi}(\phi)\,. \tag{1.2.5b}$$

We may rephrase the two slow-roll conditions in terms of two slow-roll parameters, ϵ_V and η_V, which we shall define as

$$\begin{cases} \frac{1}{2}\dot{\phi}^2 \ll V(\phi) \\ |\ddot{\phi}| \ll 3H|\dot{\phi}| \end{cases} \iff \begin{cases} \epsilon_V \equiv \frac{1}{2}M_{\rm P}^2 \left(\frac{V_{,\phi}(\phi)}{V(\phi)}\right)^2 \ll 1 \\ |\eta_V| \equiv \left| M_{\rm P}^2 \frac{V_{,\phi\phi}(\phi)}{V(\phi)} \right| \ll 1 \end{cases} , \tag{1.2.6}$$

so that inflation ends once $\epsilon_V \sim 1$ (and $|\eta_V| \sim 1$). These quantities can be thought of as a measure of how much the Universe departs from an exact de Sitter space during inflation [1]. Alternative ways to express the slow-roll parameters are often found in the literature: one that only depends on the Hubble parameter H is given by

$$\epsilon_H \equiv -\frac{\dot{H}}{H^2} \tag{1.2.7a}$$

$$\eta_H \equiv 2\epsilon_H - \frac{1}{2}\frac{\dot{\epsilon}_H}{\epsilon_H H} = \epsilon_H - \frac{1}{2}\frac{\ddot{H}}{\dot{H}H} , \tag{1.2.7b}$$

which can be shown to be equivalent to the parameters in Eq. (1.2.6) in the slow-roll regime (i.e. when all parameters are small). The first Hubble slow-roll parameter ϵ_H is always defined in the same manner, but there exist different conventions for the second parameter η_H. We chose this definition for η_H in order to make it coincide with the definition of η_V (i.e. we simply rewrote η_V solely in terms of H), which is not the most common convention; for instance, in Refs. [2, 7, 11, 23], the parameter η_H is actually defined as $\eta_H \equiv 2\epsilon_H + \frac{2\ddot{\phi}}{\dot{\phi}H}$, while in Ref. [24] it is given by $\eta_H \equiv -\frac{\ddot{\phi}}{\dot{\phi}H}$, with the exact relation $\frac{\ddot{\phi}}{\dot{\phi}H} = \frac{1}{2}\frac{\ddot{H}}{\dot{H}H}$.

It is also useful to express the number of e-folds in terms of the potential $V(\phi)$, so that we are able to compare different inflationary models in this domain; an approximate expression one can arrive at using Eq. (1.2.1) and $a(t) = a_0\, e^{Ht}$ is

$$N_e \;=\; \int_{t_i}^{t_e} H\, dt \;\approx\; -\frac{1}{M_{\rm P}^2}\int_{\phi_i}^{\phi_f} \frac{V(\phi)}{V_{,\phi}(\phi)}\, d\phi , \tag{1.2.8}$$

where ϕ_i and ϕ_f are the values of the inflaton field at the beginning and at the end of inflation, respectively. From this relation, we also conclude that $dN_e = H\, dt$, which is quite a useful relation. This last result implies in particular that $\epsilon_H = -\frac{H'}{H}$, with the prime denoting differentiation with respect to N_e, which shows that H varies very little during inflation, since $\epsilon_H \ll 1$ then. In fact, within an e-fold and during slow-roll, we have

$$H(N_e + 1) = H(N_e)\, e^{-\int \epsilon_H\, dN_e} \approx H(N_e)\, e^{-\epsilon_H} \approx H(N_e)\,(1 - \epsilon_H) \approx H(N_e) , \tag{1.2.9}$$

where we used the fact that ϵ_H varies little during slow-roll, as per $\left|\frac{\epsilon'_H}{\epsilon_H}\right| = 2\,|\eta_H - 2\epsilon_H| \ll 1$, which is obtained directly from Eq. (1.2.7b).

Choosing a potential $V(\phi)$ allows us to calculate explicit expressions for the slow-roll parameters and for the number of e-folds, to which we can apply, respectively, the slow-roll conditions and the reference range of values, and thereby estimate the values for which quantities like ϕ_i and ϕ_f the chosen potential may be an interesting candidate to describe the dynamics of the inflaton field. Common choices for $V(\phi)$ include the family of monomial potentials $V(\phi) = \lambda\phi^n$ and the family of hilltop potentials $V(\phi) = V_0\left[1 - \frac{\kappa}{n}\left(\frac{\phi}{M_\mathrm{P}}\right)^n\right]$, but other possibilities are also widely found in the literature [3, 22].

It is pertinent to point out that the derivative $V_{,\phi\phi}(\phi)$ is often associated with the squared mass of the inflaton field, m_ϕ^2, meaning that the second slow-roll condition, $|\eta_V| \ll 1$, can give information on the value of that quantity: in particular, it bounds the inflaton mass from above, since, using the Friedmann equation (1.2.5a),

$$|\eta_V| = \left|M_\mathrm{P}^2\frac{V_{,\phi\phi}(\phi)}{V(\phi)}\right| \approx \frac{1}{3}\left|\frac{V_{,\phi\phi}(\phi)}{H^2}\right| \ll 1 \implies m_\phi \ll H\,, \tag{1.2.10}$$

which, thinking of the solution to equation (1.2.4) in the case where $V_{,\phi}(\phi) \approx m_\phi^2\phi$, translates to the inflaton field behaving as an over-damped harmonic oscillator, whose damping is due to the expansion of the Universe, accounted for in H. The condition $m_\phi \ll H$ can also be interpreted as the inflaton being a *light* scalar field.

The quantum inflaton

Now, so far we have only concerned ourselves with the classical description of the inflaton field. If we introduce quantum fluctuations into the mix, the field may be described as $\phi(t,\mathbf{x}) = \bar{\phi}(t) + \varphi(t,\mathbf{x})$, where $\bar{\phi}(t)$ designates the classical inflaton field we have been working with. The fluctuations are described to linear order by the equation

$$\Box\,\varphi = -V_{,\bar{\phi}\bar{\phi}}\left(\bar{\phi}\right)\,\varphi\,, \tag{1.2.11}$$

which, in the case of a light inflaton field ($V_{,\bar{\phi}\bar{\phi}} \sim m_{\bar{\phi}}^2 \ll H^2$), may be simplified to

$$\ddot{\varphi} + 3H\,\dot{\varphi} - \frac{1}{a^2}\nabla^2\varphi = 0\,, \tag{1.2.12}$$

i.e. a homogeneous wave equation in FLRW spacetime. This equation may be rewritten in conformal time τ (with $\varphi_{,\tau} \equiv \varphi'$) as

$$\varphi'' + 2\,\frac{a'}{a}\,\varphi' - \nabla^2\varphi = 0\,, \tag{1.2.13}$$

the solution of which can be expressed in operator form as a sum of Fourier modes $\varphi_{\mathbf{k}}(\tau, \mathbf{x}) = \varphi_k(\tau)\, e^{i\mathbf{k}\cdot\mathbf{x}}$, leading to

$$\hat{\varphi}(\tau, \mathbf{x}) = \int \frac{d^3k}{(2\pi)^3}\,\frac{1}{\sqrt{2k}}\left[\hat{a}_{\mathbf{k}}\,\varphi_k^{+}(\tau)\, e^{i\mathbf{k}\cdot\mathbf{x}} + \hat{a}_{\mathbf{k}}^{\dagger}\,\varphi_k^{-}(\tau)\, e^{-i\mathbf{k}\cdot\mathbf{x}}\right], \tag{1.2.14}$$

where $k = |\mathbf{k}|$, with $\mathbf{k}$ being the comoving 3-momentum, and $\varphi_{\mathbf{k}}^{\pm}(\tau) = \frac{1}{a(\tau)}\left(1 \mp \frac{i}{k\tau}\right) e^{ik\tau}$. The operators $\hat{a}_{\mathbf{k}}$ and $\hat{a}_{\mathbf{k}}^{\dagger}$ are the creation and annihilation operators, respectively. The Bunch-Davies vacuum state [2, 7, 11] is defined as $\hat{a}_{\mathbf{k}}|0\rangle \equiv 0$.

Each Fourier mode has a corresponding physical wavelength given by $\lambda_{k,\mathrm{phys}}(t) = \frac{2\pi}{k}a(t)$, which of course grows *quasi*-exponentially with expansion. If the physical wavelength associated with a certain mode k becomes larger than the Hubble horizon H^{-1}, that mode will become causally disconnected and so its amplitude will freeze, since no physical process will be able to alter it then. The amplitude of a superhorizon mode is constant and is given by $|\varphi_{\mathbf{k}}^{\pm}| \approx \frac{H}{k}$. Upon exiting the horizon and freezing in amplitude, the fluctuation associated with the k mode will then be stretched to macroscopic scales by expansion.

If we calculate the vacuum expectation value of the variance of the field fluctuations at $\mathbf{x} = 0$, $\langle 0|\hat{\varphi}^2(\tau, 0)|0\rangle$, we get

$$\langle 0|\hat{\varphi}^2(\tau, 0)|0\rangle = \int d\ln k\,\left(\frac{H}{2\pi}\right)^2 \approx \left(\frac{H}{2\pi}\right)^2 N_e\,, \tag{1.2.15}$$

where we regularised the integral by considering only super-horizon modes and used the fact that at horizon-crossing $k = aH$. This result indicates that the average amplitude of the inflaton fluctuations grows as inflation progresses, specifically with the square-root of the number of e-folds. Moreover, each logarithmic momentum scale contributes with the same factor $\left(\frac{H}{2\pi}\right)^2$ to the integral, making this spectrum of fluctuations scale-invariant; rigorously, the scale-invariance is only approximate, since H varies adiabatically in time due to slow-roll [3]. These quantum fluctuations of the inflaton induce perturbations in its stress-energy tensor, which in turn induce scalar perturbations in the metric tensor and the curvature of spacetime, as described by Einstein's field equations, ϕ being the dominant fluid in the Universe during the inflationary epoch [7]. These metric and curvature perturbations act as inhomogeneities in the fabric of spacetime and will be subject to the same process as the inflaton fluctuations: upon horizon-crossing, their amplitudes will freeze and they will be stretched to macroscopic sizes, thus becoming observable

(Figure 1.2.2). These inhomogeneities will then be passed on to the fluids that at some point will fill the Universe, thus providing the seeds to the observed large-scale structure. In particular, they will be the origin of the temperature fluctuations encountered in the CMB, whose structure the inflationary paradigm is able to satisfactorily account for as well, thereby solving yet another conundrum of the HBB model [1, 2, 7, 11].

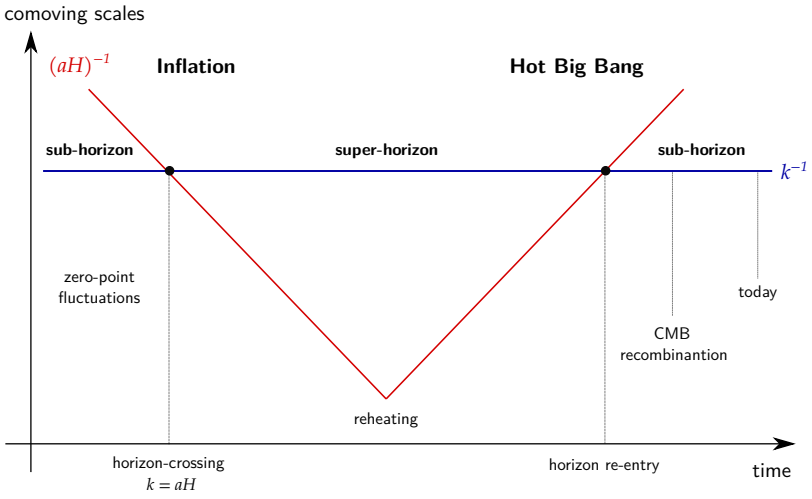

Figure 1.2.2: Diagrammatic illustration of the evolution of a perturbation during and after inflation. The perturbation freezes in amplitude and is stretched to macroscopic sizes once the corresponding mode becomes superhorizon. When inflation ends and standard cosmology ensues, the Hubble horizon grows and the perturbation reenters it. Image adapted from [2].

The perturbations of the inflaton are normally described by the power spectrum $\mathcal{P}_\varphi(k)$, defined from Eq. (1.2.15) as [1]

$$\langle 0|\hat{\varphi}^2(\tau,0)|0\rangle \equiv \int \frac{d^3k}{(2\pi)^3}\,\mathcal{P}_\varphi(k) \quad \Rightarrow \quad \mathcal{P}_\varphi(k) = \frac{H^2}{2k^3}\,, \tag{1.2.16}$$

which in turn habilitates the definition of the *dimensionless* power spectrum of inflaton fluctuations

$$\Delta^2_\varphi(k) \equiv \frac{k^3}{2\pi^2}\,\mathcal{P}_\varphi(k) = \left(\frac{H}{2\pi}\right)^2, \tag{1.2.17}$$

which of course is the nearly scale-invariant spectrum appearing in the variance integral (notice that we are keeping the momentum scale k in the argument of Δ^2_φ precisely to highlight the slight scale dependence of this quantity). We will understand the importance of this spectrum shortly.

As mentioned earlier, the quantum fluctuations of the inflaton field are able to source scalar perturbations of the metric. To see how this occurs in practice, we start by perturbing Einstein's field equations to some order in perturbation theory. Working in first-order, the perturbed metric $\tilde{g}_{\mu\nu} = g_{\mu\nu} + h_{\mu\nu}$, assuming $|h_{\mu\nu}| \ll |g_{\mu\nu}|$, may be written as

$$\tilde{g}_{00}(t, \mathbf{x}) = +1 + h_{00}(t, \mathbf{x}) \tag{1.2.18a}$$

$$\tilde{g}_{0i}(t, \mathbf{x}) = a(t)\, h_{0i}(t, \mathbf{x}) = a(t)\, h_{i0}(t, \mathbf{x}) \tag{1.2.18b}$$

$$\tilde{g}_{ij}(t, \mathbf{x}) = -a^2(t)\, [\delta_{ij} + h_{ij}(t, \mathbf{x})] \ , \tag{1.2.18c}$$

with $h_{ij} = h_{ji}$. The perturbation components are decomposed according to their behaviour under spatial rotations, as per the scalar-vector-tensor decomposition [1, 7, 8, 25, 26]

$$h_{00} = 2A \tag{1.2.19a}$$

$$h_{0i} = h_{i0} = -B_{,i} - B_i \tag{1.2.19b}$$

$$h_{ij} = 2D\delta_{ij} - 2E_{,ij} + V_{i,j} + V_{j,i} + h_{ij}^{\mathrm{TT}} \, , \tag{1.2.19c}$$

where A, B, D and E are 3-scalars, B_i and V_i are divergenceless 3-vectors ($B_i{}^{,i} = V_i{}^{,i} \equiv \frac{\partial V_i}{\partial x^i} = 0$), and h_{ij}^{TT} is a transverse ($\frac{\partial h_{ij}^{\mathrm{TT}}}{\partial x^i} = 0$) and traceless ($g^{ij} h_{ij}^{\mathrm{TT}} = 0$) tensor, typically identified with gravitational waves (GWs). Likewise, the energy-momentum tensor for a perfect fluid (cf. Eq. (1.1.4)) may also be perturbed to first-order [1, 8, 25, 26]

$$\delta T_{00} = -\rho\, h_{00} + \delta\rho \tag{1.2.20a}$$

$$\delta T_{i0} = p\, a\, h_{i0} - (\rho + p) \left(\delta u_{,i} + \delta u_i^{\mathrm{V}}\right) \tag{1.2.20b}$$

$$\delta T_{ij} = a^2 \left[p\, h_{ij} + \delta_{ij}\, \delta p + \Pi_{,ij}^{\mathrm{S}} + \Pi_{i,j}^{\mathrm{V}} + \Pi_{j,i}^{\mathrm{V}} + \Pi_{ij}^{\mathrm{T}}\right] \ , \tag{1.2.20c}$$

where $\delta u^\mu \equiv \delta(g^{\mu\nu} u_\nu)$ is the velocity perturbation, whose spatial components are decomposed as $\delta u_i = \delta u_{,i} + \delta u_i^{\mathrm{V}}$, with δu being the velocity potential (a 3-scalar) and δu_i^{V} denoting a divergenceless 3-vector, while the terms denoted with a Π are the components of the anisotropic stress, which is absent in an unperturbed perfect fluid (these quantities satisfy a set of conditions that is detailed in Ref. [8]). Plugging these decompositions into Eq. (1.1.1), one is able to find

that, at linear order, the scalar, vector and tensor perturbations of the metric satisfy decoupled differential equations and so evolve independently [1, 7], which greatly simplifies the calculations.

When working with these decompositions, however, one must be wary, as they depend on the choice of coordinates. Hence, we must define gauge-invariant combinations of the above quantities in order to link them with observables. A useful choice, as we will see in a moment, is called the *comoving curvature perturbation*, which normally appears expressed in conformal-Newtonian gauge variables, under which $A \equiv \Phi$ and $D \equiv -\Psi$ are the only non-vanishing components of the perturbation and are respectively the Newtonian gravitational potential and a local curvature perturbation [1, 2, 7, 8, 11]. Using this gauge, the gauge-invariant comoving curvature perturbation is then written as

$$\mathcal{R} \equiv -\Psi + H\,\delta u\,, \tag{1.2.21}$$

where during inflation $\delta u = \frac{\varphi}{\dot{\bar{\phi}}}$ and Ψ is negligible compared to the other term. This quantity is of course defined using both the metric perturbations and the perturbations of the energy-momentum tensor, and acts as a measure of how much the curvature of spacetime is deformed, in this case due to the fluctuations of the inflaton field.[6] Considering an expansion of $\mathcal{R}$ in Fourier modes, we thus have

$$\langle \mathcal{R}^2 \rangle \;=\; \int d\ln k \left(\frac{H}{\dot{\bar{\phi}}}\right)^2 \Delta^2_\varphi(k) \;\equiv\; \int d\ln k\;\, \Delta^2_{\mathcal{R}}(k) \tag{1.2.22a}$$

$$\Delta^2_{\mathcal{R}}(k) = \left(\frac{H}{\dot{\bar{\phi}}}\right)^2 \left(\frac{H}{2\pi}\right)^2 , \tag{1.2.22b}$$

where $\Delta^2_{\mathcal{R}}(k)$ is the dimensionless power spectrum of the curvature perturbations and is thus aptly called the *dimensionless curvature power spectrum*, with the quantity $\mathcal{P}_{\mathcal{R}}(k) \equiv \frac{2\pi^2}{k^3}\,\Delta^2_{\mathcal{R}}(k)$ being the *curvature power spectrum*; however, henceforth we shall refer to $\Delta^2_{\mathcal{R}}(k)$ simply as the curvature power spectrum. Like $\Delta^2_\varphi(k)$, the curvature power spectrum is also a nearly scale-invariant quantity; its slight scale dependence is found to described by the power law [1, 2, 7, 11]

$$\Delta^2_{\mathcal{R}}(k) = \Delta^2_{\mathcal{R}}(k_*) \left(\frac{k}{k_*}\right)^{n_s - 1} , \tag{1.2.23}$$

where k_* is a pivot comoving momentum scale at which the amplitude $\Delta^2_{\mathcal{R}}(k_*)$ is defined and n_s is called the *scalar spectral index*. The latter satisfies

[6] The evolution of $\mathcal{R}$ is described by the Mukhanov-Sasaki equation [8, 27, 28].

$$n_s - 1 = \frac{d \ln \Delta^2_{\mathcal{R}}(k)}{d \ln k} \tag{1.2.24}$$

and characterises how the curvature power spectrum deviates from scale-invariance, which would be attained at $n_s = 1$. For $n_s > 1$, the spectrum would be *blue tilted*, as there would be more power on higher momenta, whereas for $n_s < 1$ it would be *red tilted*, as the power would be concentrated in lower momenta.

The power spectrum of curvature perturbations has been observed by satellites such as *Planck* [4], by analysing the spectrum of CMB temperature fluctuations. The power law behaviour predicted by Eq. (1.2.23) has been identified and the observables $\Delta^2_{\mathcal{R}}(k_*)$ (usually denoted by A_s) and n_s have been measured at the CMB scales, corresponding to modes that exited the horizon during a period of about 8 to 10 e-folds, placed 50 to 60 e-folds before the end of inflation [3], and with one of which k_* is identified; note that to these modes correspond the largest length scales observable in the CMB, as they were stretched for almost the entirety of the inflationary epoch. At $k_* = 0.05$ Mpc^{-1}, these observables were found to assume the values [29][7]

$$\ln\left(10^{10}\, A_s\right) = 3.044 \pm 0.014 \tag{1.2.25a}$$

$$n_s = 0.9649 \pm 0.0042\,, \tag{1.2.25b}$$

making the curvature power spectrum very slightly red tilted.

Within single-field inflation, the amplitude $\Delta^2_{\mathcal{R}}(k_*)$, which is defined by evaluating Eq. (1.2.22b) at the pivot scale, i.e. $\Delta^2_{\mathcal{R}}(k_*) = \left(\frac{H_*}{\dot{\bar{\phi}}_*}\right)^2 \left(\frac{H_*}{2\pi}\right)^2$, can be approximated during slow-roll by

$$\Delta^2_{\mathcal{R}}(k_*) \approx \frac{1}{24\pi^2} \frac{V(\bar{\phi}_*)}{M_{\rm P}^4} \frac{1}{\epsilon_{V_*}}\,, \tag{1.2.26}$$

where ϵ_{V_*} is obtained by evaluating Eq. (1.2.6) at $\bar{\phi}_*$. This last expression is important since it can be used to constrain parameters of the inflationary potential via the measured value for the amplitude, Eq. (1.2.25a), thereby allowing us to scrap candidate functions that violate those constraints [1, 3]. Moreover, using Eq. (1.2.24), one can show that during slow-roll

$$n_s - 1 \;\approx\; 2\eta_V - 6\epsilon_V\,, \tag{1.2.27}$$

[7] For the *Planck* likelihood TT,TE,EE+lowE+lensing and at 68% C.L..

which is valid for all single-field inflation models [2, 7, 11].

Although scalar curvature perturbations are the only ones induced by the inflaton fluctuations (at least in first-order perturbation theory [25, 26, 30, 31]), it is pertinent to also investigate other types of metric perturbations. In particular, it can be shown that quantum vacuum fluctuations of the gravitational field generate a stochastic spectrum of gravitational waves; let us briefly see how. The transverse-traceless (TT) component of the metric perturbation, h_{ij}^{TT}, can be found to obey a first-order EoM that is identical to the one satisfied by inflaton fluctuations, Eq. (1.2.11), in the homogeneous limit[8] [2, 7, 11, 25, 26, 31, 32]

$$\Box\, h_{ij}^{\mathrm{TT}} = 0\,, \tag{1.2.28}$$

which allows us to reuse the results previously obtained for φ; we need only take into account a relative normalisation between the two quantities, as can be understood from the action in Eq. (1.1.11), as well as the existence of two possible polarisations for h_{ij}^{TT}.[9] In fact, we could have obtained Eq. (1.2.28) directly from the Einstein-Hilbert action by perturbing the latter to first-order and then variating it with respect to h_{ij}^{TT} [26]. Hence, the variances of $\hat{h}_{ij}^{\mathrm{TT}}$ and $\hat{\varphi}$ are related by

$$\langle (\hat{h}_{ij}^{\mathrm{TT}})^2 \rangle \;=\; 2 \times \left(\frac{2}{M_{\mathrm{P}}} \right)^2 \langle \hat{\varphi}^2 \rangle\,, \tag{1.2.29}$$

leading to the definition of the *dimensionless power spectrum of tensor perturbations*

$$\Delta_t^2(k) = \frac{2}{\pi^2} \frac{H^2}{M_{\mathrm{P}}^2}\,, \tag{1.2.30}$$

for which we have used Eqs. (1.2.16) and (1.2.17). Like the previous spectra, this one is nearly scale-invariant as well and, despite not having been observed yet, it is expected to follow a similar power law, for which we may write the following *ansatz*

$$\Delta_t^2(k) = \Delta_t^2(k_*) \left(\frac{k}{k_*} \right)^{n_t}\,, \tag{1.2.31}$$

where the *tensor spectral index* n_t satisfies

[8] In first-order perturbation theory, perfect fluids (like the inflaton) do not generate anisotropic stress, and so they do not lead to the appearance of a term on the right-hand side of the EoM for h_{ij}^{TT}, which would act as a classical source of gravitational waves.

[9] Note that this does not mean that the tensor perturbations are induced by φ (which is entirely not the case), only that the equations of motion followed by the two quantities are the same.

$$n_t = \frac{d \ln \Delta_t^2(k)}{d \ln k} \,. \tag{1.2.32}$$

As stated before, neither $\Delta_t^2(k_*)$ nor n_t have been measured, but some bounds have been set on both of these parameters, in particular via another CMB parameter called the *tensor-to-scalar ratio* [2, 7, 11, 29]

$$r \equiv \frac{\Delta_t^2(k_*)}{\Delta_{\mathcal{R}}^2(k_*)} \,, \tag{1.2.33}$$

which relates the weight or power contained in the tensor and in the scalar perturbations of the CMB spectrum. The current bounds on $r_{0.002}$ (corresponding to $k_* = 0.002$ Mpc^{-1}) and on the derived parameter $n_{t,0.01}$ are [29][10]

$$r_{0.002} < 0.044 \tag{1.2.34a}$$

$$-0.55 < n_{t,0.01} < 2.54 \,, \tag{1.2.34b}$$

which means that there is considerably more power on scalar perturbations and that true scale-invariance ($n_t = 0$) appears to still be compatible with observations, as does a red titled ($n_t < 0$) or a blue tilted ($n_t > 0$) spectrum. It is interesting to note that an accurate measurement of the amplitude of the power spectrum of tensor perturbations would directly allow us to obtain an experimental value for H during inflation (since $\Delta_t^2(k_*) = \frac{2}{\pi^2}\frac{H_*^2}{M_{\rm P}^2}$) and thus discover the energy scale of this process, which is currently unknown; nonetheless, an upper bound may be imposed on H using Eq. (1.2.34a)

$$H \,<\, \pi M_{\rm P} \sqrt{\frac{0.044}{2} \Delta_{\mathcal{R},0.002}^2} \,\sim\, 10^{13} \text{ GeV} \,, \tag{1.2.35}$$

where $\Delta_{\mathcal{R},0.002}^2 \equiv \Delta_{\mathcal{R}}^2(k_* = 0.002 \text{ Mpc}^{-1})$ was computed using Eqs. (1.2.23) and (1.2.25).

An expression for r in terms of the field velocity $\frac{d\bar{\phi}}{dN_e}$ can be found by dividing Eq. (1.2.22b) by Eq. (1.2.30), giving

$$r \,=\, \frac{8}{M_{\rm P}^2} \left(\frac{d\bar{\phi}}{dN_e} \right)^2 \,, \tag{1.2.36}$$

[10] For the *Planck* TT,TE,EE+lowE+lensing+BK15 likelihood and at 95% C.L. for $r_{0.002}$, and at 95% C.L. for the derived parameter $n_{t,0.01}$.

where the derivative is to be evaluated at k_*. Moreover, from Eqs. (1.2.30) and (1.2.32), it can be found that during single-field slow-roll inflation

$$n_t \approx -2\,\epsilon_V \tag{1.2.37a}$$

$$r \approx 16\,\epsilon_V\,, \tag{1.2.37b}$$

which indicates that $n_t < 0$, making the power spectrum of tensor perturbations red tilted, and from where we also find the following bound on ϵ_V

$$\epsilon_V \lesssim 3 \times 10^{-3}\,, \tag{1.2.38}$$

making it a small value, as expected. Moreover, Eq. (1.2.37) leads to the well-known *consistency relation* of single-field inflation[11]

$$r \approx -8\,n_t\,, \tag{1.2.39}$$

which is deemed to be the ultimate test (the smoking gun) of the theory: if both r and n_t are measured accurately and are found to satisfy Eq. (1.2.39), inflation will then likely be confirmed [2, 7, 11].

1.2.2 Pre-heating and reheating

Inflation ends when the slow-roll conditions stop being verified, at which point the solution to equation (1.2.4) describes under-damped oscillations near the minimum of $V(\phi)$, since H would have decreased considerably by then, as per $|\eta_V| \gtrsim 1$; the classical inflaton thus behaves as pressureless matter [2, 11]. After inflation, standard cosmology must be recovered. This means that the energy lost by the inflaton field must ultimately be converted into the familiar SM particles, allowing the usual cosmological evolution to proceed. This is accomplished by means of a *reheating* period [2, 11, 33–35].

The process of reheating is typically divided into three stages. In the first one, dubbed *pre-heating*, the inflaton field decays into scalar particles due to parametric resonance, normally of the broad (explosive) kind. In general, this process is incomplete, as the resonance eventually becomes *narrow* and inefficient. Moreover, the particles that result from it are far from thermal

[11] Other inflationary paradigms (e.g. multi-field inflation) lead to different consistency relations [22].

equilibrium and have large occupation numbers. The second stage of reheating is the decay of the previously produced particles and of the part of the inflaton field that survived pre-heating. The third and final stage is the thermalisation of the newly produced particles, by which they reach a state of thermal equilibrium [33].

In the stage of pre-heating, the classical inflaton field ϕ, which is oscillating with a decreasing amplitude $\Phi(t)$, couples with e.g. a quantum scalar field $\hat{\chi}$, thus introducing an oscillatory mass term for these particles. For a quadratic inflationary potential $V(\phi) \sim \frac{1}{2}\, m^2(\phi - \sigma)^2$ (here written in a way to allow spontaneous symmetry breaking), an interaction term $-\frac{1}{2}g^2\phi^2\chi^2$ and neglecting expansion (i.e. setting $a = 1$), the equation of motion for a mode $\chi_k(z)$, with $z = \frac{m\,t}{2}$, can then be written as a Mathieu equation [33, 36–39]

$$\chi_k''(z) \,+\, [A_k \,-\, 2q\,\cos(2z)]\;\chi_k(z) \;=\; 0\;, \qquad \begin{cases} A_k = 4\,\frac{k^2+g^2\sigma^2}{m^2} \\ q = \frac{4g^2\sigma\Phi}{m^2} \end{cases} . \tag{1.2.40}$$

This equation is notable for the fact that its solutions develop parametric resonances (which can either be *narrow*, for $q \ll 1$, or *broad*, for $q \gg 1$) in the form of exponential instabilities $\chi_k(z) \propto e^{\mu_k(z)\,z}$, the instability being attained when $\mu_k(z)$ is real [33, 36–40]. Using these unstable solutions, one can obtain the number of produced particles with momentum k (denoted n_k), as well as the total number density of produced particles (denoted n_χ), since [33]

$$n_k = \frac{\omega_k}{2}\left(\frac{|\dot{\chi}_k|^2}{\omega_k^2} + |\chi_k|^2\right) - \frac{1}{2} \tag{1.2.41a}$$

$$n_\chi = \int \frac{d^3k}{(2\pi)^3}\; n_k\,, \tag{1.2.41b}$$

with $\omega_k^2(t) = k^2 + g^2\sigma^2 + 2g^2\sigma\Phi\,\sin(mt)$, so that the exponential growth can be interpreted in this context as explosive particle production (rigorously, the production is explosive only in the case of a broad resonance). A thorough account of the theory of pre-heating can be found in [33]. Note that preheating is not limited to the decay of the inflaton field into other scalar fields: for example, a theory of preheating with fermions was developed in [41] and one with Abelian gauge fields was proposed in [42].

The subsequent decay of the particles produced during pre-heating and of the remaining inflaton field, as well as the thermalisation of their decay products, is described by methods similar to those used in the elementary theory of reheating [2, 11, 33, 43, 44]. Let us briefly explore this theory using a phenomenological description, in the particular case where the rapidly oscillating inflaton couples with a scalar field χ and a spinor field ψ, considering also a quadratic

inflationary potential and recovering the expansion of space. The effects of these interactions can be encompassed in a friction term $\Gamma\dot{\phi}$ that is added to the EoM for ϕ, Eq. (1.2.4) [45], whose solution then becomes

$$\phi(t) \;=\; \Phi(t)\, e^{imt} \;\approx\; \phi_0\, e^{imt}\, e^{-\frac{1}{2}(3H+\Gamma)t}\,, \tag{1.2.42}$$

where $\Gamma = \Gamma(\phi \to \chi\chi) + \Gamma(\phi \to \psi\psi)$ is the total decay rate of the inflaton, which coincides with its flat-space limit. Thus, the damping of the oscillations of ϕ can be attributed to both the expansion of the Universe and particle production due to the decay of the inflaton. In fact, given that $\rho_\phi = \frac{1}{2}|\dot{\phi}|^2 + \frac{1}{2}m^2|\phi|^2 \approx \frac{1}{2}m^2\Phi^2$ (for $m^2 \gg H^2$, which is true at the end of inflation, and $m^2 \gg \Gamma^2$, which is verified as well since at this stage $H > \Gamma$) and $n_\phi = \rho_\phi/m$, and since the solution in Eq. (1.2.42) obeys

$$\frac{d}{dt}(a^3\Phi^2) = -\Gamma\, a^3\Phi^2\,, \tag{1.2.43}$$

we find that the comoving energy density $\sim a^3\rho_\phi$ decays exponentially with Γ, as does the comoving number density $\sim a^3 n_\phi$. Moreover, if we multiply Eq. (1.2.4) (with the added friction term) by $\dot{\phi}$, we obtain a conservation equation like Eq. (1.1.7) but with a decay term proportional to Γ on the right-hand side; the particles produced during reheating then follow a similar conservation equation, but with a flipped-sign on the right-hand side term, ensuring that the total energy density is conserved during this stage. Thus, reheating can be described by the following set of differential equations

$$\dot{\rho}_\phi + 3H(\rho_\phi + p_\phi) \;=\; -\Gamma\rho_\phi \tag{1.2.44a}$$

$$\dot{\rho}_M + 3H(\rho_M + p_M) \;=\; \Gamma\rho_\phi \tag{1.2.44b}$$

$$3M_{\rm P}^2H^2 \;=\; \rho_\phi + \rho_M\,, \tag{1.2.44c}$$

which reproduces the same behaviour for $a^3\rho_\phi \propto e^{-\Gamma t}$ when $p_\phi \approx 0$, while also predicting the evolution of ρ_M for different types of fluid (the subscript M refers to "matter" of any kind and so it can include radiation, which is particularly important in order to obtain the radiation-dominated era after inflation) [3, 8].

Particle production ends (and so reheating stops) when H becomes smaller than the decay rate Γ, allowing thermalisation to occur; this defines a *reheating temperature*, which can be found

to be $T_r \approx 0.2\sqrt{\Gamma M_{\rm P}}$ if the decay products of ϕ are ultra-relativistic and if thermal equilibrium is achieved rapidly after reheating completes [33].

After these processes, standard cosmology ensues and the HBB model can be applied.

1.3 Particle production during inflation

Apart from the usual models of pre-heating and reheating discussed in § 1.2.2, in which particle production occurs strictly after inflation ends, there have been several proposals of mechanisms for production of particles *during* the slow-roll phase of inflation [46–51]. These models are interesting and may have a few advantages over the standard paradigm of reheating for a number of reasons.

The most important one is the fact that these models can give rise to observational data in the CMB, as they may introduce features in the otherwise nearly scale-invariant curvature power spectrum, $\Delta^2_{\mathcal{R}}$, and they may provide a contribution to the power spectrum of tensor perturbations, Δ^2_t. The presence of these additional fields during inflation should in principle cause some backreaction on the dynamics of the classical inflaton and of its quantum fluctuations, both of which are intimately related to the curvature power spectrum, as we saw in § 1.2.1. Hence, if the inflaton acquires some signatures due to the particles produced throughout inflation, some information about the latter may very well be imprinted on the CMB and thus be observable and/or measurable. Something similar does not happen in the usual picture of post-inflation reheating, as the perturbations generated then do not grow to macroscopic sizes. Additionally, the produced particles may generate tensor perturbations of their own, leading to a stochastic GW spectrum that will contribute to Δ^2_t; moreover, this spectrum might eventually be detectable by current or future GW interferometers [25, 26, 32, 47].

A second advantage is the fact that if particle production during inflation is efficient enough, we may have the energy density of the inflaton field be fully converted to that of the produced field by the *end* of inflation, thereby eliminating the need for a post-inflation reheating period. In this case, the recovering of the HBB model should be attained through the decay of the produced field into other particles.

Lastly, a third advantage is the possibility that the produced particles lead to the appearance of a friction term in the equation of motion for the inflaton, which translates into a relaxation of the constraints on the slow-roll parameters and an eventual modification of the inflaton perturbation spectrum. This is the basis of warm inflation models [52–55], so that this mechanism can in fact have a double application (and importance) within the theory of inflation. However,

we will not be exploring this possibility in this work.

It is clear that this type of model has an additional complication, since we must not allow the production of particles to be too efficient to the point where the energy density of the newly produced particles dominates over that of the inflaton field during the slow-roll regime, in which case we would effectively be breaking inflation. Hence, the production must be quite controlled, meaning that some type of compromise in its magnitude and effectiveness has to be attained in order for these models to generate measurable signals whilst not destroying the underlying inflationary mechanism.

1.4 Outline

In the following chapters, we will present and explore the theoretical model developed throughout the duration of this research paper. Our goal is to establish and analyse a mechanism of resonant production of scalar particles, χ, during the inflationary epoch. We intend to check whether this production can be efficient enough to allow the existence of some observational signature of these particles, without them becoming the dominant contribution to the energy density of the Universe, thus forcing inflation to end prematurely.

The outline of the upcoming chapters is as follows. In Chapter 2, we begin in § 2.1.1 by introducing and motivating the Lagrangian for this theoretical model, which we will then use in § 2.1.2 to obtain and discuss the equation of motion for the χ field. In § 2.2 and § 2.3, we calculate the comoving number density and the physical energy density, respectively, of the produced χ particles. In § 2.4, we deal with the backreaction of the χ particles on the inflaton field: the effect on the classical inflaton is discussed in § 2.4.1, while the effect on its quantum fluctuations is discussed in § 2.4.2. In § 2.4.3, we analyse the impact of the backreaction on several CMB observables. In Chapter 3, we start by analysing the parameter space of our model and performing numerical simulations of solutions to the equation of motion of the χ modes, in §§ 3.1 and 3.2, respectively. Then, in § 3.3, we test our theoretical results against observational data, for several choices of the inflationary potential $V(\phi)$. Chapter 4 will be dedicated to the overarching discussion of the derived results, featuring also the concluding remarks regarding the proposed mechanism. Three appendices, §§ A to C, are included as well, where we walk through a few useful calculations in some detail.

2 Resonant particle production during inflation

The following sections will be dedicated to the exploration of our particular model of resonant production of scalar particles during inflation. We shall discover whether the conditions for an efficient production of these particles can be met without breaking inflation, and what observational signatures are possible to obtain then.

2.1 The model

As we shall find shortly, the mechanism presented here is motivated by Warm Little Inflaton scenarios [55–61], which in turn are inspired by Little Higgs models [62–64].

2.1.1 The Lagrangian

Consider the Lagrangian

$$\mathcal{L}_\Phi = \left(D_\mu \Phi_1\right)^\dagger \left(D^\mu \Phi_1\right) + \left(D_\mu \Phi_2\right)^\dagger \left(D^\mu \Phi_2\right) - \frac{1}{4} F_{\mu\nu} F^{\mu\nu} - \mathscr{V}(|\Phi_1|, |\Phi_2|)\,, \tag{2.1.1}$$

where $\Phi_{1,2}$ are complex scalar fields, A_μ is the (massless) U(1) gauge field, $D_\mu \equiv \partial_\mu - ieA_\mu$ is the gauge covariant derivative and $F_{\mu\nu} = \partial_\mu A_\nu - \partial_\nu A_\mu$ is the gauge field strength tensor (the fields $\Phi_{1,2}$ are assumed to have the same charge e).

The potential $\mathscr{V}(|\Phi_1|, |\Phi_2|)$ is the sum of two Higgs potentials (one for each field) and is given by

$$\mathscr{V}(|\Phi_1|, |\Phi_2|) = \frac{\lambda_1}{4}\left(|\Phi_1|^2 - \frac{M^2}{2}\right)^2 + \frac{\lambda_2}{4}\left(|\Phi_2|^2 - \frac{M^2}{2}\right)^2. \tag{2.1.2}$$

This Lagrangian has a U(1) gauge invariance, granted the fields transform as

$$\begin{cases} \Phi_1 \longrightarrow e^{i\alpha}\Phi_1 \\ \Phi_2 \longrightarrow e^{i\alpha}\Phi_2 \\ A_\mu \longrightarrow A'_\mu = A_\mu + \frac{1}{e}\partial_\mu\alpha \end{cases} , \tag{2.1.3}$$

where $\alpha \equiv \alpha(x^\mu)$ (the transformation is local). The potential reaches its minimum $\mathscr{V} = 0$ at

$$\begin{cases} \Phi_1^0 = \frac{M}{\sqrt{2}} e^{i\frac{\phi_1}{M}} \\ \Phi_2^0 = \frac{M}{\sqrt{2}} e^{i\frac{\phi_2}{M}} \end{cases} \iff \begin{cases} \Phi_1^0 = \frac{M}{\sqrt{2}} e^{i\frac{\theta+\phi}{M}} \\ \Phi_2^0 = \frac{M}{\sqrt{2}} e^{i\frac{\theta-\phi}{M}} \end{cases} , \tag{2.1.4}$$

where ϕ_1, ϕ_2, θ and ϕ are real scalar fields, the latter being a relative phase between Φ_1^0 and Φ_2^0. We can add radial perturbations, h_1 and h_2, to these solutions to get an approximate form of the fields near the potential minimum. Additionally, if we set $\alpha = -\frac{\theta}{M}$ in (2.1.3) we can eliminate θ (a Goldstone boson) from the Lagrangian, in which case we will be working in the *unitary gauge* or *unitarity gauge* [55, 62–66]. In this case, we can write the fields as

$$\begin{cases} \Phi_1 = \frac{M+h_1}{\sqrt{2}} e^{i\frac{\phi}{M}} \\ \Phi_2 = \frac{M+h_2}{\sqrt{2}} e^{-i\frac{\phi}{M}} \end{cases} . \tag{2.1.5}$$

Here, h_1 and h_2 are also real scalar fields, each describing a Higgs-like particle. Furthermore, unlike θ, the relative phase ϕ is a physical degree of freedom, which is not absorbed by the unitary gauge; in fact, it is a U(1) gauge-invariant quantity that we identify with the inflaton field [55]. It is simple to show that, in the unitary gauge, the gauge field A_μ acquires a mass $m_A = \sqrt{2}\, eM$ and the Higgs-like fields h_1 and h_2 acquire masses $m_{h_1} = \sqrt{\frac{\lambda_1}{2}}\, M$ and $m_{h_2} = \sqrt{\frac{\lambda_2}{2}}\, M$, respectively.

We can now introduce a third scalar field, χ, which describes the particles we intend to produce. We take it to be real, so that the coupling between χ and the fields Φ_1 and Φ_2 is of the form $\frac{1}{2}g^2|\Phi_1 - \Phi_2|^2\chi^2$, where g is a dimensionless coupling constant that we shall take to be smaller than unity. Since the χ field does not transform under the U(1) group (it being U(1)-neutral), we may add to (2.1.1) the also U(1)-invariant Lagrangian

$$\mathcal{L}_{\chi\Phi} = \frac{1}{2}\partial_\mu\chi\,\partial^\mu\chi - \frac{1}{2}g^2|\Phi_1 - \Phi_2|^2\chi^2 , \tag{2.1.6}$$

which allows us to define the full Lagrangian of our model

$$\begin{aligned} \mathcal{L} = {} & (D_\mu\Phi_1)^\dagger (D^\mu\Phi_1) + (D_\mu\Phi_2)^\dagger (D^\mu\Phi_2) + \frac{1}{2}\partial_\mu\chi\,\partial^\mu\chi - \frac{1}{4}F_{\mu\nu}F^{\mu\nu} \\ & - \mathscr{V}(|\Phi_1|, |\Phi_2|) - \frac{1}{2}g^2|\Phi_1 - \Phi_2|^2\chi^2 , \end{aligned} \tag{2.1.7}$$

where the coupling constant g and the mass scale M are free parameters of the model.

Using (2.1.5), the last term in (2.1.7) can be written as

$$\begin{aligned}\frac{1}{2}g^2|\Phi_1-\Phi_2|^2\chi^2 &= \frac{1}{2}g^2M^2\left[1-\cos\left(\frac{2\phi}{M}\right)\right]\chi^2+... \\ &= \frac{1}{2}\times\underbrace{2g^2M^2\sin^2\left(\frac{\phi}{M}\right)}_{m_\chi^2}\chi^2+\underbrace{...}_{\text{higher order terms}},\end{aligned} \tag{2.1.8}$$

which in turn gives to leading order in χ and excluding all other fields and interactions (in this paper we are only concerned with analysing χ production, so that we may ignore $h_{1,2}$ and A_μ, assuming they are heavier than χ and so should not influence the inflationary dynamics)

$$\mathcal{L}_\chi = \frac{1}{2}\partial_\mu\chi\,\partial^\mu\chi-\frac{1}{2}m_\chi^2\chi^2. \tag{2.1.9}$$

For the time being, we shall ignore any backreaction on ϕ due to χ. Hence, we shall consider ϕ to be well described by its free field solution, which can be found independently, and whose value must depend solely on time, as we saw in § 1.2.1. Notice that we did not include a potential term for ϕ in the original Lagrangian; such a term would in fact be allowed by the U(1) gauge symmetry of our theory, given that the inflaton is a relative phase, and so gauge-invariant, and so we could (and should) have included it. Furthermore, note also that m_χ^2 is a function of ϕ (and thus of time), so that the Lagrangian (2.1.9) simply describes a free real scalar field χ with an oscillating mass $m_\chi^2(t)$. Production of χ particles is a consequence of this time-varying mass, as we shall find later on. Hence, since the fields $h_{1,2}$ and A_μ do not have oscillating masses, but constant ones, there will be no production of particles in their case, which is another argument we can use to neglect them.

We can define an effective action for χ as

$$S_\chi = \int d^4x\,\sqrt{-g}\left(\frac{1}{2}\partial_\mu\chi\,\partial^\mu\chi-\frac{1}{2}m_\chi^2\,\chi^2\right), \tag{2.1.10}$$

with $g_{\mu\nu}=\text{diag}(+1,-a^2,-a^2,-a^2)$, making $\sqrt{-g}\equiv\sqrt{|\det g_{\mu\nu}|}=a^3$, where $a=a(t)\propto e^{Ht}$ is the scale factor. Note that we are considering a flat FLRW metric, as is customary in inflation-related research (we follow in particular Ref. [33]), and that the inflaton energy density is dominant, so that the scale factor does grow *quasi*-exponentially. In the ensuing discussion, we take H to be constant, which we shall see is a good approximation in the context of χ production; recall, however, that in reality H varies adiabatically due to the slow-roll dynamics

of ϕ, although its variation within an e-fold is quite small, cf. Eq. (1.2.9). Setting to zero its variation with respect to χ, one arrives at the equation of motion for χ

$$\ddot{\chi} + 3H\dot{\chi} - \frac{1}{a^2}\nabla^2\chi + m_\chi^2\chi = 0\,. \tag{2.1.11}$$

We can also vary S_χ with respect to the metric and thus find the stress-energy tensor and the energy density for χ, respectively given by

$$T_\chi^{\mu\nu} = -\frac{2}{\sqrt{-g}}\frac{\delta S_\chi}{\delta g_{\mu\nu}} = -g^{\mu\nu}\left(\frac{1}{2}\partial_\alpha\chi\,\partial^\alpha\chi - \frac{1}{2}m_\chi^2\chi^2\right) + \partial^\mu\chi\,\partial^\nu\chi \tag{2.1.12}$$

and

$$\rho_\chi \equiv T_\chi^{00} = \frac{1}{2}\dot{\chi}^2 + \frac{1}{2}\frac{|\nabla\chi|^2}{a^2} + \frac{1}{2}m_\chi^2\chi^2. \tag{2.1.13}$$

2.1.2 The equation of motion

We now turn our attention to equation (2.1.11). We can write its solution as a sum of Fourier modes $\chi_{\mathbf{k}}(t,\mathbf{x}) = \chi_k(t)\,e^{i\mathbf{k}\cdot\mathbf{x}}$, with $k = |\mathbf{k}|$, and promote χ to an operator $\hat{\chi}$, which gives

$$\hat{\chi}(t,\mathbf{x}) = \int \frac{d^3k}{(2\pi)^3}\left[\hat{a}_{\mathbf{k}}\chi_k(t)\,e^{i\mathbf{k}\cdot\mathbf{x}} + \hat{a}_{\mathbf{k}}^\dagger\chi_k^*(t)\,e^{-i\mathbf{k}\cdot\mathbf{x}}\right], \tag{2.1.14}$$

where $\hat{a}_{\mathbf{k}}$ and $\hat{a}_{\mathbf{k}}^\dagger$ are annihilation and creation operators, respectively, satisfying the canonical commutation relations

$$\left[\hat{a}_{\mathbf{k}},\,\hat{a}_{\mathbf{k}'}^\dagger\right] = (2\pi)^3\,\delta^3\left(\mathbf{k}-\mathbf{k}'\right) \tag{2.1.15a}$$

$$\left[\hat{a}_{\mathbf{k}},\,\hat{a}_{\mathbf{k}'}\right] = \left[\hat{a}_{\mathbf{k}}^\dagger,\,\hat{a}_{\mathbf{k}'}^\dagger\right] = 0\,. \tag{2.1.15b}$$

We may define the conjugate momentum of $\hat{\chi}$ as

$$\hat{\pi}_\chi(t,\mathbf{x}) \equiv \frac{\partial\left(\sqrt{-g}\,\mathcal{L}_\chi\right)}{\partial\dot{\hat{\chi}}(t,\mathbf{x})} = \sqrt{-g}\,\dot{\hat{\chi}}(t,\mathbf{x}) = a^3(t)\,\dot{\hat{\chi}}(t,\mathbf{x}) \tag{2.1.16}$$

and impose that the commutators of $\hat{\chi}$ and $\hat{\pi}_\chi$ satisfy the equal-time relations

$$[\hat{\chi}(t,\mathbf{x}),\, \hat{\pi}_\chi(t,\mathbf{y})] \;=\; \frac{i}{\sqrt{-g}}\,\delta^3\left(\mathbf{x}-\mathbf{y}\right) \;=\; \frac{i}{a^3(t)}\,\delta^3\left(\mathbf{x}-\mathbf{y}\right) \tag{2.1.17a}$$

$$[\hat{\chi}(t,\mathbf{x}),\, \hat{\chi}(t,\mathbf{y})] \;=\; [\hat{\pi}_\chi(t,\mathbf{x}),\, \hat{\pi}_\chi(t,\mathbf{y})] \;=\; 0\,, \tag{2.1.17b}$$

which indeed occurs only if the following Wronskian normalisation condition for the mode functions $\chi_k(t)$ is verified

$$\dot{\chi}_k^*(t)\,\chi_k(t) \;-\; \chi_k^*(t)\,\dot{\chi}_k(t) \;=\; \frac{i}{(\sqrt{-g})^2} \;=\; \frac{i}{a^6(t)}\,. \tag{2.1.18}$$

Let us now return to the study of the EoM. Inserting the expression for $\hat{\chi}(t,\mathbf{x})$ in equation (2.1.11), we arrive at

$$\ddot{\chi}_k + 3H\dot{\chi}_k + \frac{k^2}{a^2}\chi_k + m_\chi^2\chi_k = 0\,, \tag{2.1.19}$$

where $k_{\text{phys}} = \frac{k}{a}$ is the physical momentum of each mode k. We define $\omega_k(t) = \sqrt{\frac{k^2}{a^2(t)} + m_\chi^2(t)}$ to be the energy associated with each mode, such that equation (2.1.19) may be rewritten as

$$\ddot{\chi}_k + 3H\dot{\chi}_k + \omega_k^2(t)\chi_k = 0\,, \tag{2.1.20}$$

which greatly resembles the equation of motion for a damped harmonic oscillator with a time-varying frequency, where the damping is due to the expansion of the Universe (accounted for in H). Hence, we now see that each mode in the Fourier expansion (2.1.14) actually behaves like a damped harmonic oscillator with a time-varying frequency.

Since we want to study particle production during inflation, we should consider ϕ to be in the slow-roll regime. In this regime, the time derivatives of ϕ get successively smaller as their order increases, so that we may perform a Taylor expansion of ϕ around some instant t_0 and keep only the first two terms, that is until the first derivative of the field

$$\phi(t) \approx \phi(t_0) + \dot{\phi}(t_0)(t-t_0) \equiv \dot{\phi}t + \delta\,. \tag{2.1.21}$$

Using $m_\chi^2 = 2g^2M^2\sin^2\left(\frac{\phi}{M}\right) \approx 2g^2M^2\sin^2\left(\frac{\dot{\phi}t}{M}\right)$ (where we have set $\delta = 0$ to simplify the calculations, since a phase factor should not impact the underlying physics) and substituting in equation (2.1.19), we get

$$\ddot{\chi}_k + 3H\dot{\chi}_k + \left[\frac{k^2}{a^2} + 2g^2M^2\sin^2\left(\frac{\dot{\phi}t}{M}\right)\right]\chi_k = 0\,. \tag{2.1.22}$$

In order to simplify the equation by removing the effects of the expansion of the Universe (i.e. the $3H\dot{\chi}_k$ factor) we may define a new function $X_k = a^{3/2}\chi_k$ (its Wronskian condition being $\dot{X}_k^* X_k - X_k^* \dot{X}_k = ia^{-3}$) and substitute χ_k in (2.1.22), which leads to

$$\ddot{X}_k + \left[\frac{k^2}{a^2} - \frac{9}{4}H^2 + 2g^2M^2\sin^2\left(\frac{\dot{\phi}t}{M}\right)\right]X_k = 0\,, \tag{2.1.23}$$

where a change of variable $t \longrightarrow z = \frac{|\dot{\phi}|}{M}t$ can be done, allowing us to write

$$X_k'' + \left[\left(\frac{M}{\dot{\phi}}\right)^2\left(\frac{k^2}{a^2} + g^2M^2 - \frac{9}{4}H^2\right) - \left(\frac{M}{\dot{\phi}}\right)^2 g^2M^2\cos(2z)\right]X_k = 0\,, \tag{2.1.24}$$

where the primes denote derivatives with regard to z, which is dimensionless, and where we used the fact that the above equations are invariant under a sign change in $\dot{\phi}$. This equation can be rewritten as

$$X_k'' + \left[A_k(z) - 2q\cos(2z)\right]X_k = 0\,, \tag{2.1.25}$$

with

$$A_k(z) = \left(\frac{M}{\dot{\phi}}\right)^2\left(\frac{k^2}{a^2(z)} - \frac{9}{4}H^2\right) + 2q \tag{2.1.26a}$$

$$q = \frac{1}{2}\left(\frac{M}{\dot{\phi}}\right)^2 g^2M^2\,. \tag{2.1.26b}$$

Equation (2.1.26) is a Mathieu-like equation with a variable parameter $A_k(z)$ [36–39]. Rigorously, both A_k and q vary in time (and so both should be functions of z), since $\dot{\phi}$ is itself a time-varying quantity; however, since we are in the slow-roll regime, we may neglect the variation of $\dot{\phi}$ when compared with the variation of the scale factor, $a(z)$, which is approximately exponential. In this case, we may take q to be a constant and $A_k(z)$ to vary solely due to $a(z)$.

For the theory of Mathieu equations used here, in particular the application of Floquet theory and of Floquet's Theorem, see [2, 33, 36–39]. It should be noted that this theory assumes both parameters A_k and q to be constant in time; we can, however, employ it to some extent even if $A_k = A_k(z)$ and/or $q = q(z)$, as long as we ensure that the variation of these parameters is

slow (or adiabatic) [40]. The variation of q due to the slow-roll dynamics can be shown to be in fact slow (see § 3.3 and Appendix A). The variation of $A_k(z)$ is trickier to analyse; nonetheless, we shall see in a few paragraphs that under some conditions it is also adiabatic. Therefore, we may safely apply the theory of Mathieu equations to (2.1.25).

The main characteristic of these equations is the existence of parametric resonance bands for some values of the parameters A_k and q. We shall only consider the case of a narrow resonance ($q \ll 1$), for which the resonance bands occur for $A_k \sim n^2$, with n a positive integer. In a narrow resonance, particle production is more contained than in a broad resonance ($q \gtrsim 1$), thereby being more likely not to break the underlying inflationary mechanism, which assumes the ϕ field to be dominant. We shall also restrict ourselves to the first ($A_k \sim 1$) and most important of these bands, which occurs for $1 - q \lesssim A_k \lesssim 1 + q$ [36].

Let us briefly focus on the parameter $A_k(z)$. Since we expect the modes being produced, which are the ones inside the resonance band, to be causally connected (i.e. subhorizon), we must impose that for those modes $\frac{k}{a(z)} \gg H$, such that

$$A_k(z) \approx \left(\frac{M}{\dot{\phi}}\right)^2 \left(\frac{k}{a}\right)^2 + 2q\,, \tag{2.1.27}$$

which, using (2.1.26b), is readily written as

$$A_k(z) \approx 2q\left[\left(\frac{k/a}{gM}\right)^2 + 1\right]. \tag{2.1.28}$$

Since at the center of the resonance band (which is where the modes are while they are being produced), we have $A_k \approx 1$, it follows from (2.1.28) that

$$\left(\frac{k/a}{gM}\right)^2 \approx \frac{1}{2q} - 1 \approx \frac{1}{2q} \gg 1\,, \tag{2.1.29}$$

given that, for a narrow resonance, $q \ll 1$. This means that, for all significant modes (i.e. the ones being produced), we have $\left(\frac{k}{a}\right)^2 \gg g^2M^2$. Since $\langle m_\chi^2(t)\rangle = g^2M^2$ is the average value of the oscillating squared mass of the χ field, we may use this quantity to define an effective mass for the χ particles, $\langle m_\chi\rangle \equiv gM$. Equation (2.1.29) then implies that the χ modes are relativistic while they are being produced, which is an important result of our model. Using the same relation, Eq. (2.1.28) becomes

$$A_k(z) \approx 2q\left(\frac{k/a}{gM}\right)^2 = \frac{M^2k^2}{a^2\dot{\phi}^2}\,, \tag{2.1.30}$$

which results in

$$A_k(z) \approx \frac{1}{2\epsilon_V}\left(\frac{k}{a(z)}\right)^2\left(\frac{M}{M_{\rm P}H}\right)^2 \tag{2.1.31a}$$

$$q = \frac{1}{4\epsilon_V}\left(\frac{gM}{H}\right)^2\left(\frac{M}{M_{\rm P}}\right)^2 . \tag{2.1.31b}$$

where we have also used the relation $\dot{\phi}^2 = 2\epsilon_V M_{\rm P}^2 H^2$, obtained using Eqs. (1.2.5) and (1.2.6).

Going back to our main discussion, Floquet's Theorem states that in the presented case (a narrow resonance, $q \ll 1$, within the first resonance band, $A_k(z) \sim 1$) the solution of the Mathieu equation evolves as $X_k(z) \propto e^{\mu_k(z)\, z}$, where $\mu_k(z)$ is the Floquet exponent and is given by

$$\mu_k(z) = \frac{1}{2}\sqrt{q^2 - [A_k(z) - 1]^2}\,. \tag{2.1.32}$$

Reverting momentarily to the time variable t, inside the first resonance band, $\mu_k(t)$ is real (and positive), such that a mode with comoving momentum k enters the band when $A_k(t_1) = 1+q$ and exits it once $A_k(t_2) = 1 - q$ (notice that $A_k(t)$ decreases as inflation progresses). As mentioned before, at the centre of this band $A_k(z) \approx 1$ (making $\mu_k = \mu_k^{\rm max} = \frac{q}{2}$), so that, using (2.1.31),

$$k_{c,\rm phys} \equiv \left(\frac{k}{a}\right)_c = \frac{\sqrt{2\epsilon_V}M_{\rm P}H}{M} = \frac{gM}{\sqrt{2q}} = \text{const.}\,, \tag{2.1.33}$$

which tells us that the modes that are at the center of the resonance band at any time t or z all share the same physical momentum $k_{c,\rm phys}$ (of course this constancy is only approximate, since q actually varies a little due to the slow-roll dynamics). Moreover, in § 2.2 we shall see that the physical momenta of *all* modes being produced at a certain time z (i.e. those that are inside the resonance band at a certain time) are in fact very close to $k_{c,\rm phys}$, which means that the momentum distribution of the χ particles being produced should be close to a Dirac delta function centered at $k_{c,\rm phys}$, thus being the same at all times. Note that it is only the physical momentum that is a constant: in principle, every comoving momentum k will be produced at some time t_c, given by

$$t_c = t_c(k) = H^{-1}\ln\frac{\sqrt{2q}\,k}{gM\,a_0}\,, \tag{2.1.34}$$

where $a_0 = a(t=0)$. We may equivalently consider that at every instant t a mode with a certain comoving momentum k_c is being produced, this momentum being given by

$$k_c = k_c(t) = \frac{gM}{\sqrt{2q}}\, a(t)\,. \tag{2.1.35}$$

It is also easy to show, using $A_k(t_1) = 1 + q$ and $A_k(t_2) = 1 - q$, that

$$\begin{cases} t_1(k) \;=\; t_c(k) - \frac{1}{2H}\,\ln(1+q) \;\approx\; t_c(k) - \frac{q}{2H} \\ t_2(k) \;=\; t_c(k) - \frac{1}{2H}\,\ln(1-q) \;\approx\; t_c(k) + \frac{q}{2H} \end{cases}, \tag{2.1.36}$$

considering that $q \ll 1$, such that the time spent inside the resonance band by each mode is simply

$$\Delta t = t_2 - t_1 = qH^{-1}\,, \tag{2.1.37}$$

or in terms of e-folds

$$N_e = H\Delta t = q\,, \tag{2.1.38}$$

which means that each mode spends a short period of time (less than one e-fold) inside the resonance band (and every mode spends roughly the same time there as well). This result validates the constant-H approximation we did in § 2.1.1: since each k mode spends much less than one e-fold in the resonance band, during that period H is in fact constant to a very good approximation, given that $H(N_e + q) \approx H(N_e)\,(1 - \epsilon_H q)$, as per Eq. (1.2.9). Surely, throughout inflation, different modes experience different values of H during their passage through the resonance band, but for each individual mode that value is essentially the same for the entire passage. Moreover, we shall see shortly that the result from Eq. (2.1.38) is an important factor to ensure that $A_k(t)$ varies adiabatically.

Looking at Eq. (2.1.34), we conclude that a mode with comoving momentum k will be inside the resonance band for a short time interval $\Delta t = qH^{-1}$ centered around $t_c(k)$, so that for these modes we may Taylor expand the scale factor $a(t)$ around $t_c(k)$ and discard second order and higher order terms

$$a(t) \;=\; a_c\, e^{H(t-t_c)} \;\approx\; a_c\,[1 + H(t - t_c)]\,. \tag{2.1.39}$$

We may do the same to the $A_k(t)$ parameter, which results in

$$A_k(t) \approx 1 - 2H[t - t_c(k)] \iff A_k(z) \approx 1 - \gamma[z - z_c(k)]\,, \tag{2.1.40}$$

where

$$\gamma = \sqrt{\frac{2}{\epsilon_V}}\frac{M}{M_{\rm P}} = 2\sqrt{2q}\frac{H}{gM}\,, \tag{2.1.41}$$

must ideally be a small quantity in order for the variation of $A_k(z)$ to be adiabatic, as was stated before; in § 3.3, we arrive at the conclusion that in fact $\gamma \ll 1$ in the interesting region of parameter space for all considered inflationary models, so that the adiabaticity is secured. Notice that, since $\epsilon_V \lesssim 1$, this condition implies that $M \ll M_{\rm P}$, which means that the mass scale of the χ particles ($\langle m_\chi \rangle = gM$) is subplanckian. With this, we may rewrite the Floquet exponent in (2.1.32) as

$$\mu_k(z) = \frac{1}{2}\sqrt{q^2 - \gamma^2[z - z_c(k)]^2}\,, \tag{2.1.42}$$

which allows us to easily calculate the values of z when a mode k enters (z_1) and leaves (z_2) the resonance band

$$\mu_k(z) = 0 \Longrightarrow \begin{cases} z_1(k) = z_c(k) - \frac{q}{\gamma} \\ z_2(k) = z_c(k) + \frac{q}{\gamma} \end{cases}\,, \tag{2.1.43}$$

with $z_c(k) = \frac{2}{\gamma}\ln\left(\frac{\gamma}{2a_0}\frac{k}{H}\right)$, which is consistent with the result from Eq. (2.1.36), and from where we conclude that $\Delta z = z_2 - z_1 = \frac{2q}{\gamma}$. It is also useful to rewrite $k_{c,\rm phys}$ in terms of q and γ, which simply becomes

$$k_{c,\rm phys} = \frac{2H}{\gamma}\,. \tag{2.1.44}$$

At this point, it is important to check if the frequency of oscillation of $m_\chi(t)$ is larger than H, which is equivalent to saying that the period of the mass oscillations is less than one Hubble time, H^{-1}. This translates into ensuring that $m_\chi(t)$ oscillates as least once within one e-fold of inflation (recall that $N_e \approx H\Delta t$), which is a necessity if we intend to have efficient particle production during inflation. From (2.1.22), we see that $m_\chi(t) = \sqrt{2}\,gM\,\sin\left(\frac{\dot\phi}{M}t\right)$, so that the frequency indeed verifies

$$\frac{|\dot\phi|}{M} = \frac{gM}{\sqrt{2q}} = k_{c,\rm phys} = \frac{2H}{\gamma} \gg H\,, \tag{2.1.45}$$

where Eqs. (2.1.26b), (2.1.33) and (2.1.44) were used, as well as $\gamma \ll 1$. Note that $k_{c,\rm phys} = \left(\frac{k}{a}\right)_c \gg H$ is precisely the condition that the k mode that is being produced at a certain

time must verify in order to be subhorizon and thus be causally connected, which is of course a necessity. Also note that the frequency at which the mass $m_\chi(t)$ oscillates is essentially equal to the frequency associated with the particles being produced, since for those particles $\omega_k(t) = \sqrt{\frac{k^2}{a^2(t)} + m_\chi^2(t)} \approx \left(\frac{k}{a}\right)_c = \frac{2H}{\gamma} = \frac{|\dot{\phi}|}{M}$; this result is in line with other common resonant systems, where the resonances arise precisely from the proximity or equality between two different frequencies, one inherent to the system and one imposed on it (ω_k and $\frac{|\dot{\phi}|}{M}$, respectively, in the case of the χ particles).

We must also ensure that the mass $m_\chi(t)$ completes at least one oscillation while each mode is inside the resonance band, which occurs during an interval $\Delta t = qH^{-1}$, cf. (2.1.37). This condition is required so that we can attain a good parametric resonance in the solutions of our Mathieu equation (2.1.25): this is easily verifiable using numerical simulations such as the ones shown later in Figure 3.2.1. This translates into

$$\frac{|\dot{\phi}|}{M}\,\Delta t \;=\; \frac{2H}{\gamma}\,qH^{-1} \;>\; 2\pi \quad\Longleftrightarrow\quad \frac{q}{\gamma} > \pi\,, \tag{2.1.46}$$

which is not straightforward to estimate. In § 3.3, however, we shall discover that this condition holds in a significant region of the allowed parameter space for all inflationary models considered in this work.

Furthermore, it is useful to establish that $\langle m_\chi \rangle > H$, this restriction being due to the fact that χ is a scalar field and therefore is subject to quantum corrections of $\mathcal{O}(H)$ that may greatly increase its mass [2, 66]: by enforcing that $\langle m_\chi \rangle > H$, we can essentially ignore this effect. Recall that the specific value of H during inflation is currently unknown, and that different inflationary models predict distinct values for this quantity, so that we may obtain various lower bounds for $\langle m_\chi \rangle$ (cf. § 3.3). Together with the subplanckian condition, $\langle m_\chi \rangle \ll M_\mathrm{P}$, we have effectively set a range for $\langle m_\chi \rangle = gM$

$$H \;<\; \langle m_\chi \rangle \;\ll\; M_\mathrm{P}\,. \tag{2.1.47}$$

2.2 Comoving particle number density

Resonant production of particles occurs while a mode is inside the resonance band. We saw in the previous section that the theory of Mathieu equations [2, 33, 36, 37] can be approximately applied to Eq. (2.1.25), so that, from Floquet's theorem, the solution to this equation can be written approximately as the product of a periodic function $P(z)$ by an exponential $e^{\mu_k(z)\,z}$, which, using $t = \frac{\gamma}{2H} z$, we can approximate as

$$X_k(z) = P(z)\, e^{\mu_k(z) z} \approx C\, e^{\pm i\omega_k \frac{\gamma}{2H} z}\, e^{\mu_k(z)\, z} \iff X_k(t) \approx C\, e^{\pm i\omega_k t}\, e^{\frac{2H}{\gamma}\mu_k(t)\, t}\,, \tag{2.2.1}$$

where, for the first resonance band ($A_k \approx 1$) and for a narrow resonance ($q \ll 1$), we have $\mu_k(t) = \frac{1}{2}\sqrt{q^2 - [A_k(t) - 1]^2}$, which takes its maximum value, $\mu_k^{\max} = \frac{q}{2}$, at $A_k = 1$.

At a time $t = t_0$, we have

$$X_k(t_0) \approx C\, e^{\left(\pm i\omega_k^0 + \frac{2H}{\gamma}\mu_k^0\right) t_0} \tag{2.2.2a}$$

$$\dot{X}_k(t_0) \approx \left(\pm i\omega_k^0 + \frac{2H}{\gamma}\mu_k^0\right) X_k(t_0)\,, \tag{2.2.2b}$$

where $\omega_k^0 = \omega_k(t_0)$ and $\mu_k^0 = \mu_k(t_0)$. For modes inside the resonance band (or close to entering or exiting it), the value of ω_k is comparable to $\frac{2H}{\gamma}$, while μ_k is of order $\frac{q}{2}$, which means that for these modes $X_k(t_0) \approx C\, e^{\pm i\omega_k^0 t_0}$ and $\dot{X}_k(t_0) \approx \pm\, i\omega_k^0\, X_k(t_0)$, comparing the absolute value of the terms inside the parentheses in (2.2.2).

We may now define the comoving energy of the k-momentum particles as [33]

$$\tilde{\rho}_k \equiv \frac{1}{2}|\dot{X}_k|^2 + \frac{1}{2}\omega_k^2\, |X_k|^2 \equiv \omega_k \left(\tilde{n}_k + \frac{1}{2}\right)\,, \tag{2.2.3}$$

where $\omega_k(t) = \sqrt{\frac{k^2}{a^2(t)} + m_\chi^2(t)}$ and $\tilde{n}_k$ is the comoving (occupation) number of k-momentum particles. If we consider that no particles have been produced at $t = t_0$ just before the mode k enters the resonance band (i.e. $\tilde{n}_k(t_0) = 0$), we may write

$$\frac{1}{2}|\dot{X}_k(t_0)|^2 + \frac{1}{2}(\omega_k^0)^2\, |X_k(t_0)|^2 = \frac{\omega_k^0}{2}\,, \tag{2.2.4}$$

so that, substituting the expressions obtained above,

$$C^2(\omega_k^0)^2 + (\omega_k^0)^2 C^2 = \omega_k^0 \implies C_k = \frac{1}{\sqrt{2\omega_k^0}}\,, \tag{2.2.5}$$

assuming $C \equiv C_k$ to be real. $X_k(z)$ is thus given by

$$X_k(z) \approx \frac{1}{\sqrt{2\omega_k^0}}\, e^{\pm i\omega_k \frac{\gamma}{2H} z}\, e^{\mu_k(z)\, z}\,, \tag{2.2.6}$$

with $\omega_k^0 \approx \frac{2H}{\gamma}$.

We can obtain the expression for $\tilde{n}_k(z)$ by inverting (2.2.3)

$$\tilde{n}_k \equiv \frac{1}{2}\left(\frac{|\dot{X}_k|^2}{\omega_k} + \omega_k\,|X_k|^2\right) - \frac{1}{2}\,, \tag{2.2.7}$$

which upon using $X_k(t) \approx \frac{1}{\sqrt{2\omega_k^0}}\, e^{\pm i\omega_k t}\, e^{\frac{2H}{\gamma}\mu_k(t)\,t}$ leads to

$$\tilde{n}_k(t) \approx \frac{1}{2}\frac{\omega_k}{\omega_k^0}\, e^{\frac{4H}{\gamma}\mu_k(t)\,t} - \frac{1}{2} \iff \tilde{n}_k(z) \approx \frac{1}{2}\frac{\omega_k}{\omega_k^0}\, e^{2\mu_k(z)\,z} - \frac{1}{2}\,, \tag{2.2.8}$$

where we assumed that $\dot{X}_k(t) \approx \pm i\omega_k X_k(t) \approx \pm\frac{i\omega_k}{\sqrt{2\omega_k^0}}\, e^{\pm i\omega_k t}\, e^{\frac{2H}{\gamma}\mu_k(t)\,t}$, due to the discussion following (2.2.2). Note that we did not do any approximations in the exponent in order to keep some form of time-dependence, which would otherwise disappear as we got rid of the leading-order term.

In particular, if a mode k is inside the resonance band, in an interval dz the function X_k in (2.2.6) will be amplified by a factor $e^{\mu_k(z)\,dz}$, so that between two instants z_s and z_e the amplification of X_k will be of a factor $e^{\mu_k z}$, where

$$\mu_k z \;\equiv\; \int_{z_s}^{z_e} \mu_k(z)\,dz \;=\; \frac{1}{2}\int_{z_s}^{z_e} \sqrt{q^2 - \gamma^2[z - z_c(k)]^2}\,dz\,, \tag{2.2.9}$$

making $X_k(z_s \to z_e) \approx \frac{1}{\sqrt{2\omega_k^0}}\, e^{\pm i\omega_k \frac{\gamma}{2H} z}\, e^{\mu_k\, z}$ [40]. Hence, from (2.2.7), the comoving number of k-momentum particles produced between z_s and z_e is simply

$$\tilde{n}_k(z_s \to z_e) \approx \frac{1}{2}\frac{\omega_k}{\omega_k^0}\, e^{2\mu_k z} - \frac{1}{2}\,. \tag{2.2.10}$$

Integrating (2.2.9) gives

$$\begin{aligned}\ln\left[\tilde{n}_k(z_s \to z_e) + \frac{1}{2}\right] \;=\; \frac{q^2}{2\gamma}\Bigg\{&\arcsin\left[\frac{\gamma}{q}(z_e - z_c)\right] + \frac{\gamma}{q}(z_e - z_c)\sqrt{1 - \left(\frac{\gamma}{q}\right)^2 (z_e - z_c)^2} \\ &- \arcsin\left[\frac{\gamma}{q}(z_s - z_c)\right] - \frac{\gamma}{q}(z_s - z_c)\sqrt{1 - \left(\frac{\gamma}{q}\right)^2 (z_s - z_c)^2}\Bigg\} + \ln\left(\frac{1}{2}\frac{\omega_k}{\omega_k^0}\right)\,,\end{aligned} \tag{2.2.11}$$

which attains its maximum value of $\frac{\pi q^2}{2\gamma} + \ln\left(\frac{1}{2}\frac{\omega_k}{\omega_k^0}\right)$ when $z_s = z_1(k)$ and $z_e = z_2(k)$, corresponding to a mode k that has been through the entire resonance band (note that if $z_s < z_1(k)$ and/or $z_e > z_2(k)$ the integral would no longer be real-valued). In § 3.2, we compare this analytical approximation with an analogue obtained by numerically solving Eq. (2.1.25).

The total comoving particle number density, $\tilde{n}_\chi(z_s \to z_e)$, is then obtained by integrating (2.2.10) for all k modes

$$\tilde{n}_\chi(z_s \to z_e) \;=\; \frac{1}{(2\pi)^3}\int \tilde{n}_k(z_s \to z_e)\, d^3k \;=\; \frac{1}{2\pi^2}\int_0^\infty k^2\, \tilde{n}_k(z_s \to z_e)\, dk\,. \tag{2.2.12}$$

It is easy to see that when the expression for $\tilde{n}_k(z_s \to z_e)$ is inserted into (2.2.12) a $\frac{1}{2}k^2$ term appears in the integrand function, which upon integration leads to an infinite value. This factor and thus this divergence are related to the energy content of the vacuum and can be dealt with through renormalisation techniques. However, given the fact that we are concerned only with the number of χ particles that are produced during inflation (and so with the energy that is added to that of the vacuum by said particles), we may neglect that part of the integral altogether, which is what we will do henceforth. The expression for the integrand function then simply becomes $\frac{1}{2}k^2\frac{\omega_k}{\omega_k^0}\, e^{2\mu_k z}$.

In order to calculate (2.2.12), we must distinguish between different regimes under which the k modes may be produced and divide the integral accordingly. If we consider the particles produced between the start of particle production at z_i (which we take to be very early in inflation, even earlier than 60 e-folds before the end of the accelerated expansion) and some posterior instant z, we have three possibilities, which are represented diagrammatically in Figure 2.2.1:

(A) modes that at the beginning of particle production were already inside the resonance band and exited it at a later instant (which we shall consider to be prior to z);

(B) modes that entered the resonance band after the beginning of particle production and exited it before z;

(C) modes that entered the resonance band after the beginning of particle production and are currently (i.e. at z) inside it.

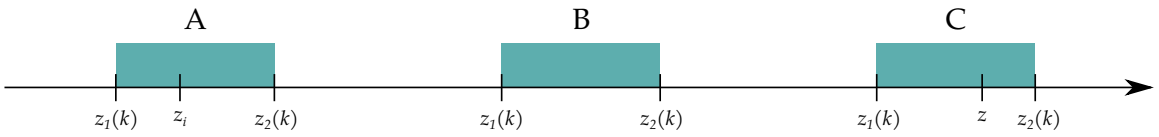

Figure 2.2.1: Diagrammatic illustration of the three regimes under which χ production may undergo. The shaded regions represent the resonance band.

We will now explore all three regimes.

2.2.1 Regime A

In this case, the modes of momentum k have entered the resonance band before the actual start of particle production at z_i, so that $z_1(k) \leqslant z_i$. We must also impose that the modes exit the resonance band *after* particle production begins, which translates to $z_2(k) \geqslant z_i$. Combining these two conditions

$$z_1(k) \leqslant z_i \leqslant z_2(k) \tag{2.2.13}$$

and using (2.1.43) we arrive at an equivalent interval for the k modes that are produced in this regime

$$k_a \leqslant k \leqslant k_b\,, \quad \text{where} \quad \begin{cases} k_a = \frac{2H}{\gamma}\, a_i\, e^{-\frac{q}{2}} = k_{\text{min}} \\ k_b = \frac{2H}{\gamma}\, a_i\, e^{\frac{q}{2}} \end{cases}\,, \tag{2.2.14}$$

and where $a_i = a(z_i) = a_0\, e^{\frac{\gamma}{2} z_i}$, which allows us to conclude that the smallest mode that is produced is $k = 0$ only if $z_i = -\infty$. Additionally, we are going to assume that $z \gg z_i$ and also that $z > z_2(k_b)$, the latter being the instant at which the last (and largest) mode produced in this regime exits the resonance band (note that the maximum value of $z_2(k_b)$ is $z_i + \frac{2q}{\gamma}$). Note that neither $k_{a,\text{phys}} = \frac{k_a}{a(z)}$ nor $k_{b,\text{phys}} = \frac{k_b}{a(z)}$ are close to $k_{c,\text{phys}} = \frac{2H}{\gamma}$ at $z \gg z_i$, as one would expect, since at that time those modes are already far from the resonance band and so are no longer being produced and their physical momenta have been redshifted away; therefore, their momentum distribution is no longer approximately a Dirac delta function centred at $k_{c,\text{phys}}$, but at $k_{c,\text{phys}} \frac{a_i}{a(z)} \ll k_{c,\text{phys}}$ (recall that the discussion from § 2.1.2 in this regard only referred to the modes *inside* the resonance band at a time z). We may estimate an approximate width for this distribution: using (2.2.14), it is simply $k_{b,\text{phys}} - k_{a,\text{phys}} = 2k_{c,\text{phys}} \frac{a_i}{a(z)} \sinh\left(\frac{q}{2}\right) \ll k_{c,\text{phys}} \frac{a_i}{a(z)}$. Moreover, for modes in this regime, $\omega_k \approx gM$, such that, for $\omega_k^0 \approx \frac{2H}{\gamma}$, we find $\frac{\omega_k}{\omega_k^0} \approx \sqrt{2q}$.

Considering all this, it is clear that for this regime the limits of integration in (2.2.11) should be $z_s = z_i$ and $z_e = z_2(k)$, resulting in

$$\tilde{n}_k^{\text{A}}(z_i \to z_2(k)) \;=\; \sqrt{\frac{q}{2}} \exp\left\{ \frac{q^2}{2\gamma} \left[\frac{\pi}{2} - \arcsin\left[\frac{\gamma}{q}(z_i - z_c)\right] - \frac{\gamma}{q}(z_i - z_c)\sqrt{1 - \left(\frac{\gamma}{q}\right)^2 (z_i - z_c)^2} \right] \right\}. \tag{2.2.15}$$

Since all calculations are done inside the resonance band, whose center at $z_c(k)$ depends on the modes being produced, we can simplify the exponent by performing a Taylor expansion in

z_i around $z_c(k)$ and keep only first-order terms, since $z_i \sim z_c(k)$ for all significant values of k, see (2.2.14). With the approximate exponent, (2.2.15) becomes

$$\tilde{n}_k^{\mathrm{A}}(z_i \to z_2(k)) \;\approx\; \sqrt{\frac{q}{2}} \exp\!\left\{ \frac{\pi q^2}{4\gamma} - q(z_i - z_c) \right\} \;=\; \sqrt{\frac{q}{2}}\, \zeta\, k^{\frac{2q}{\gamma}} \,, \tag{2.2.16}$$

with $\zeta = e^{\frac{\pi q^2}{4\gamma}} \left(\frac{\gamma}{2Ha_i}\right)^{\frac{2q}{\gamma}}$ and where we have used the expression for $z_c(k)$ defined after (2.1.43). We can now calculate the comoving number density for particles produced in this regime, $\tilde{n}_\chi^{\mathrm{A}}$, whose limits of integration must be $k_a = k_{\mathrm{min}}$ and k_b, that is

$$\tilde{n}_\chi^{\mathrm{A}} \;=\; \frac{1}{2\pi^2} \int_{k_a}^{k_b} k^2\, \tilde{n}_k^{\mathrm{A}}(z_i \to z_2(k))\, dk \;\approx\; \frac{\zeta\sqrt{q}}{2\sqrt{2}\,\pi^2 \left(3 + \frac{2q}{\gamma}\right)} \left(k_b^{3+\frac{2q}{\gamma}} - k_a^{3+\frac{2q}{\gamma}} \right) , \tag{2.2.17}$$

which, using (2.2.14) and the fact that $k_a = k_b\, e^{-q}$, we can rewrite as

$$\tilde{n}_\chi^{\mathrm{A}} \;\approx\; \frac{4\sqrt{2q}\, H^3}{\pi^2 \gamma^3}\; a_i^3\, e^{\frac{\pi q^2}{4\gamma}}\; \frac{\sinh\left[\frac{q}{2}\left(3 + \frac{2q}{\gamma}\right)\right]}{3 + \frac{2q}{\gamma}} \,, \tag{2.2.18}$$

which shows, as we would expect, that the comoving number density of particles produced in this regime is independent of z (recall that we are considering $z > z_2(k_b)$).

2.2.2 Regime B

In this regime, we will be considering the modes of momentum k that have entered the resonance band at some point after particle production began, so that $z_1(k) \geqslant z_i$, and have exited it at some point prior to z, that is $z_2(k) \leqslant z$. In other words, these modes will have been through the entirety of the resonance band by z.

Once again, we can combine these two conditions

$$z_1(k) \geqslant z_i \;\wedge\; z_2(k) \leqslant z \tag{2.2.19}$$

to find, using (2.1.43), that

$$k_b \leqslant k \leqslant k_1(z) \,, \quad \text{where} \quad \begin{cases} k_b = \frac{2H}{\gamma}\, a_i\, e^{\frac{q}{2}} \\ k_1(z) = \frac{2H}{\gamma}\, a(z)\, e^{-\frac{q}{2}} \end{cases} . \tag{2.2.20}$$

From this, we see that k_b is the smallest mode that has been through the entire resonance band, while $k_1(z)$ is the mode that has just exited the resonance band at instant z.

For the limits of integration in (2.2.11), we must then pick $z_s = z_1(k)$ and $z_e = z_2(k)$, which expectedly leads to the maximum value of the expression

$$\tilde{n}_k^{\mathrm{B}}(z_1(k) \to z_2(k)) \;=\; \frac{1}{2}\frac{\omega_k}{\omega_k^0}\, e^{\frac{\pi q^2}{2\gamma}} \;\approx\; \frac{1}{2} e^{\frac{\pi q^2}{2\gamma}}\,, \tag{2.2.21}$$

where we anticipate that the modes closer to $\frac{k_1(z)}{a(z)} \sim \frac{2H}{\gamma}$ for which $\omega_k \approx \frac{2H}{\gamma} \approx \omega_k^0$, dominate the three-momentum integration.

Calculating $\tilde{n}_\chi^{\mathrm{B}}$ is then straightforward, as (2.2.21) does not depend on k. The limits of integration for the integral are of course k_b and $k_1(z)$, such that

$$\tilde{n}_\chi^{\mathrm{B}}(z) \;=\; \frac{1}{2\pi^2}\int_{k_b}^{k_1(z)} k^2\, \tilde{n}_k^{\mathrm{B}}(z_1(k) \to z_2(k))\, dk \;=\; \frac{e^{\frac{\pi q^2}{2\gamma}}}{12\pi^2}\left(k_1^3(z) - k_b^3\right)\,, \tag{2.2.22}$$

which we can simplify using (2.2.20) and the fact that $k_b = k_1(z)\, e^q\, e^{-\frac{\gamma}{2}(z-z_i)} \ll k_1(z)$ (recall that we are considering $z \gg z_i$), leading to

$$\tilde{n}_\chi^{\mathrm{B}}(z) \;\approx\; \frac{2H^3}{3\pi^2\gamma^3}\; a^3(z)\, e^{\frac{\pi q^2}{2\gamma} - \frac{3}{2}q}\,. \tag{2.2.23}$$

2.2.3 Regime C

The modes of momentum k produced in this regime have entered the resonance band at some point after the beginning of particle production and therefore verify $z_1(k) \geqslant z_i$, as in the previous case; but, unlike in the B regime, at a time z these modes have not yet exited the band, but are still inside it, so the condition $z_2(k) \geqslant z$ must also be verified. These two conditions, however, are insufficient to define an interval in k, as they only bound this quantity from below. The missing condition is achieved by imposing $z_1(k) \leqslant z$, so that we can also guarantee to have some particle production in this regime at a time z.

Putting both conditions together,

$$z_1(k) \leqslant z \leqslant z_2(k)\,, \tag{2.2.24}$$

we readily arrive at the interval for the k values, once again by using (2.1.43),

$$k_1(z) \leqslant k \leqslant k_2(z)\,, \quad \text{where} \quad \begin{cases} k_1(z) = \frac{2H}{\gamma}\, a(z)\, e^{-\frac{q}{2}} \\ k_2(z) = \frac{2H}{\gamma}\, a(z)\, e^{\frac{q}{2}} = k_{\mathrm{max}} \end{cases}\,. \tag{2.2.25}$$

We see that the largest k mode that is produced depends on the instant z that we are considering, as one would expect. Also, we see that both $\frac{k_1(z)}{a(z)} = k_{1,\text{phys}} = k_{c,\text{phys}}\, e^{-\frac{q}{2}} \sim k_{c,\text{phys}}$ and $\frac{k_2(z)}{a(z)} = k_{2,\text{phys}} = k_{c,\text{phys}}\, e^{\frac{q}{2}} \sim k_{c,\text{phys}}$, as $q \ll 1$, so that the modes being produced at a time z, i.e. those in (2.2.25), indeed have physical momenta close to $k_{c,\text{phys}}$, just as we had stated previously in § 2.1.2; hence, the momentum distribution of the particles being produced is in fact approximately a Dirac delta function centered at $k_{c,\text{phys}}$. The rough width of the approximate Dirac peak is then simply $k_{2,\text{phys}} - k_{1,\text{phys}} = 2k_{c,\text{phys}} \sinh\left(\frac{q}{2}\right) \ll k_{c,\text{phys}}$. Notice that this distribution is severely non-thermal [67]. For modes in this regime, it is clear that $\frac{\omega_k}{\omega_k^0} \approx 1$.

The limits of integration we must use in (2.2.11) for this regime are $z_s = z_1(k)$ and $z_e = z$, which results in

$$\tilde{n}_k^{\text{C}}(z_1(k) \to z) \;=\; \frac{1}{2}\exp\left\{\frac{q^2}{2\gamma}\left[\frac{\pi}{2} + \arcsin\left[\frac{\gamma}{q}(z-z_c)\right] + \frac{\gamma}{q}(z-z_c)\sqrt{1-\left(\frac{\gamma}{q}\right)^2(z-z_c)^2}\right]\right\}. \tag{2.2.26}$$

Similarly to what we did in the A regime, we can simplify the exponent by Taylor expanding it in z around $z_c(k)$, keeping only the first-order terms, since $z \sim z_c(k)$ for all significant values of k, cf. (2.2.25). This results in

$$\tilde{n}_k^{\text{C}}(z_1(k) \to z) \;\approx\; \frac{1}{2}\exp\left\{\frac{\pi q^2}{4\gamma} + q(z-z_c)\right\} \;=\; \frac{1}{2}\,\varsigma(z)\; k^{-\frac{2q}{\gamma}}\,, \tag{2.2.27}$$

with $\varsigma(z) = e^{\frac{\pi q^2}{4\gamma}}\left(\frac{\gamma}{2Ha(z)}\right)^{-\frac{2q}{\gamma}}$, where we have used the usual expression for $z_c(k)$. We may now calculate the comoving number density for particles produced in this regime, $\tilde{n}_\chi^{\text{C}}$, by setting the limits of integration as $k_1(z)$ and $k_2(z) = k_{\max}$, making

$$\tilde{n}_\chi^{\text{C}}(z) \;=\; \frac{1}{2\pi^2}\int_{k_1(z)}^{k_2(z)} k^2\, \tilde{n}_k^{\text{C}}(z_1(k) \to z)\, dk \;\approx\; \frac{\varsigma(z)}{4\pi^2\left(3-\frac{2q}{\gamma}\right)}\left(k_2^{3-\frac{2q}{\gamma}}(z) - k_1^{3-\frac{2q}{\gamma}}(z)\right), \tag{2.2.28}$$

which can be simplified taking into account (2.2.14) and the fact that $k_2(z) = k_1(z)\, e^q$

$$\tilde{n}_\chi^{\text{C}}(z) \;\approx\; \frac{4H^3}{\pi^2\gamma^3}\; a^3(z)\, e^{\frac{\pi q^2}{4\gamma}}\; \frac{\sinh\left[\frac{q}{2}\left(3-\frac{2q}{\gamma}\right)\right]}{3-\frac{2q}{\gamma}}\,. \tag{2.2.29}$$

The total comoving number density of particles produced from z_i to z is then given by

$$\tilde{n}_\chi(z_i \to z) \equiv \tilde{n}_\chi(z) = \tilde{n}_\chi^{\mathrm{A}} + \tilde{n}_\chi^{\mathrm{B}}(z) + \tilde{n}_\chi^{\mathrm{C}}(z)\,, \tag{2.2.30}$$

but we can readily make a simplification by noting that for $z \gg z_i$, we have $a^3(z) \gg a_i^3 = a^3(z_i)$, meaning that $\tilde{n}_\chi^{\mathrm{A}} \ll \tilde{n}_\chi^{\mathrm{B}}(z)$, $\tilde{n}_\chi^{\mathrm{C}}(z)$, so that

$$\tilde{n}_\chi(z) \approx \tilde{n}_\chi^{\mathrm{B}}(z) + \tilde{n}_\chi^{\mathrm{C}}(z) \approx \frac{2H^3}{\pi^2\gamma^3}\, a^3(z) \left\{ \frac{1}{3}\, e^{\frac{\pi q^2}{2\gamma} - \frac{3}{2}q} + 2\, e^{\frac{\pi q^2}{4\gamma}}\, \frac{\sinh\left[\frac{q}{2}\left(3 - \frac{2q}{\gamma}\right)\right]}{3 - \frac{2q}{\gamma}} \right\}. \tag{2.2.31}$$

For all considered inflationary models (cf. § 3.3), it was found that in the significant regions of the parameter space (g, M) we have $\tilde{n}_\chi^{\mathrm{B}}(z) \gg \tilde{n}_\chi^{\mathrm{C}}(z)$, meaning that we may make the approximation

$$\boxed{\tilde{n}_\chi(z) \approx \frac{2H^3}{3\pi^2\gamma^3}\, a^3(z)\, e^{\frac{\pi q^2}{2\gamma} - \frac{3}{2}q}}\,, \tag{2.2.32}$$

which is the final expression for the comoving number density of particles produced since the beginning of inflation at z_i until a time $z \gg z_i$.

Notice that in Eq. (2.2.30) the full integral is from k_a to $k_2(z)$, and not strictly from 0 to ∞. This is of course due to the fact that some comoving momenta may not be produced by this mechanism. The vacuum part of the original integral, however, keeps its integration limits from 0 to ∞, as all scales should contribute to the vacuum. We could eventually integrate out the portion between k_a and $k_2(z)$, in which case Eqs. (2.2.16), (2.2.21), (2.2.27) and (2.2.32) would all get additional finite terms due to the vacuum. However, this would not be particularly useful, as at least one of the remaining integrals would still be divergent; hence, we prefer to keep the vacuum part separated as a whole and work only with the part linked to the resonant production of particles.

2.3 Physical energy density

We will now look more deeply at expression (2.1.13), while considering also the Fourier mode expansion (2.1.14), both of which we present here once again:

$$\rho_\chi = \frac{1}{2}\dot{\chi}^2 + \frac{1}{2}\frac{|\nabla\chi|^2}{a^2} + \frac{1}{2}m_\chi^2\chi^2 \tag{2.3.1}$$

and

$$\hat{\chi}(t,\mathbf{x}) = \int \frac{d^3k}{(2\pi)^3}\left[\hat{a}_{\mathbf{k}}\chi_k(t)\,e^{i\mathbf{k}\cdot\mathbf{x}} + \hat{a}^\dagger_{\mathbf{k}}\chi^*_k(t)\,e^{-i\mathbf{k}\cdot\mathbf{x}}\right], \tag{2.3.2}$$

where $\omega_k(t) = \sqrt{\frac{k^2}{a^2(t)} + m^2_\chi(t)}$. For simplicity, we shall assume that $m^2_\chi(t) = 2g^2M^2\sin^2\left(\frac{\dot{\phi}}{M}t\right) \approx \langle m^2_\chi(t)\rangle = g^2M^2 \equiv \langle m_\chi\rangle^2$, where the average is computed over a period of the oscillation.

The χ field is here interpreted as an operator $\hat{\chi}$, as we had previously seen. The value of the physical energy density can thus be obtained by calculating the vacuum expectation value of the operator $\hat{\rho}_\chi$. We again define the Bunch-Davies vacuum state [2, 7] as

$$\hat{a}_{\mathbf{k}}|0\rangle = 0\,, \tag{2.3.3}$$

so that the vacuum expectation value of $\hat{\rho}_\chi$ is given by

$$\langle\rho_\chi\rangle \equiv \langle 0|\hat{\rho}_\chi|0\rangle = \frac{1}{2}\langle 0|\,\dot{\hat{\chi}}^2\,|0\rangle + \frac{1}{2a^2}\langle 0|\,|\nabla\hat{\chi}|^2\,|0\rangle + \frac{1}{2}m^2_\chi\langle 0|\,\hat{\chi}^2\,|0\rangle\,. \tag{2.3.4}$$

Using the canonical commutation relation $[\hat{a}_{\mathbf{k}'}, \hat{a}^\dagger_{\mathbf{k}}] = (2\pi)^3\,\delta^3(\mathbf{k}-\mathbf{k}')$ and Eq. (2.3.2), it is simple to prove that

$$\langle\dot{\chi}^2\rangle \equiv \langle 0|\,\dot{\hat{\chi}}^2\,|0\rangle = \frac{1}{2\pi^2}\int_0^\infty k^2\,|\dot{\chi}_k|^2\,dk \tag{2.3.5a}$$

$$\langle|\nabla\chi|^2\rangle \equiv \langle 0|\,|\nabla\hat{\chi}|^2\,|0\rangle = \frac{1}{2\pi^2}\int_0^\infty k^4\,|\chi_k|^2\,dk \tag{2.3.5b}$$

$$\langle\chi^2\rangle \equiv \langle 0|\,\hat{\chi}^2\,|0\rangle = \frac{1}{2\pi^2}\int_0^\infty k^2\,|\chi_k|^2\,dk\,. \tag{2.3.5c}$$

Expression (2.3.4) then takes the following form

$$\langle\rho_\chi\rangle \;=\; \frac{1}{2\pi^2}\int_0^\infty k^2\left(\frac{1}{2}|\dot{\chi}_k|^2 + \frac{k^2}{2a^2}|\chi_k|^2 + \frac{1}{2}m^2_\chi|\chi_k|^2\right)dk \;\equiv\; \frac{1}{2\pi^2}\int_0^\infty k^2\rho_k\,dk\,, \tag{2.3.6}$$

where $\rho_k \equiv \frac{1}{2}|\dot{\chi}_k|^2 + \frac{k^2}{2a^2}|\chi_k|^2 + \frac{1}{2}m^2_\chi|\chi_k|^2$ is the total physical energy for each k mode. We then define the physical particle number for each mode as [2, 33]

$$\rho_k \equiv \omega_k\left(n_k + \frac{1}{2}\right) \iff n_k \equiv \frac{\rho_k}{\omega_k} - \frac{1}{2}\,, \tag{2.3.7}$$

with $\omega_k = \omega_k(t)$, such that ω_k is the physical energy per k-momentum χ particle, so that

$$\langle \rho_\chi \rangle \equiv \frac{1}{2\pi^2} \int_0^\infty k^2 \, \omega_k \left(n_k + \frac{1}{2} \right) dk \,. \tag{2.3.8}$$

We must now relate the comoving quantities calculated in the previous section to these newly defined physical quantities. It is possible to show (see Appendix C.1) that

$$n_k + \frac{1}{2} \approx \frac{1}{a^3} \left(\tilde{n}_k + \frac{1}{2} \right) , \tag{2.3.9}$$

making

$$\langle \rho_\chi \rangle \approx \frac{1}{2\pi^2 a^3} \int_0^\infty k^2 \, \omega_k \left(\tilde{n}_k + \frac{1}{2} \right) dk \,. \tag{2.3.10}$$

Recalling that $\tilde{n}_k = \frac{1}{2} \frac{\omega_k}{\omega_k^0} \, e^{2\mu_k z} - \frac{1}{2}$ (cf. Eq. (2.2.10)), we may insert it in (2.3.10), thus eliminating the $\frac{1}{2}$ factor from the integrand function, which would otherwise lead to an infinite integral. Note that both this factor and the one in the expression for $\tilde{n}_k$ have the same origin, arising from the existence of a vacuum energy, which we had already stumbled upon in (2.2.12). As before, we were able to rid ourselves of the infinity without using renormalisation techniques. The integrand function thus becomes $\frac{1}{2} k^2 \omega_k \, \frac{\omega_k}{\omega_k^0} \, e^{2\mu_k z}$. Redefining $\tilde{n}_k$ as $\tilde{n}_k \equiv \frac{1}{2} \frac{\omega_k}{\omega_k^0} \, e^{2\mu_k z}$, as it is useful notation-wise, we are left with

$$\langle \rho_\chi \rangle \approx \frac{1}{2\pi^2 a^3} \int_0^\infty k^2 \, \omega_k \, \tilde{n}_k \, dk \,, \tag{2.3.11}$$

which we must divide accordingly to what we did in §§ 2.2.1 to 2.2.3, leading to

$$\begin{aligned} \langle \rho_\chi \rangle &= \langle \rho_\chi^{\mathrm{A}} \rangle + \langle \rho_\chi^{\mathrm{B}} \rangle + \langle \rho_\chi^{\mathrm{C}} \rangle \\ &\approx \frac{1}{2\pi^2 a^3(z)} \left\{ \int_{k_a}^{k_b} k^2 \, \omega_k \, \tilde{n}_k^{\mathrm{A}} \, dk + \int_{k_b}^{k_1(z)} k^2 \, \omega_k \, \tilde{n}_k^{\mathrm{B}} \, dk + \int_{k_1(z)}^{k_2(z)} k^2 \, \omega_k \, \tilde{n}_k^{\mathrm{C}} \, dk \right\} . \end{aligned} \tag{2.3.12}$$

Note that we have been omitting the z dependence in $\tilde{n}_k$ and in $\langle \rho_\chi \rangle$ in order to simplify the notation. Let us calculate each one of the three integrals.

2.3.1 Regime A

In this case, every physical mode $\frac{k}{a(z)}$ that contributes to the integral verifies, cf. (2.2.14),

$$\frac{2H}{\gamma} \frac{a_i}{a(z)} \, e^{-\frac{q}{2}} = \frac{k_a}{a(z)} \leqslant \frac{k}{a(z)} \leqslant \frac{k_b}{a(z)} = \frac{2H}{\gamma} \frac{a_i}{a(z)} \, e^{\frac{q}{2}} , \tag{2.3.13}$$

so that for $z \gg z_i$ (and $q \ll 1$) we have $\frac{k_a}{a(z)}$, $\frac{k_b}{a(z)} \ll k_{c,\text{phys}} = \frac{2H}{\gamma}$, which means that at a time z the modes produced near the beginning of particle production have a physical momentum much smaller than when they were produced, as it was decreased by the expansion of the Universe, as expected. From (2.1.33), we have that $\frac{k_{c,\text{phys}}}{gM} = \frac{1}{\sqrt{2q}}$, so that for a narrow resonance $k_{c,\text{phys}} \gg gM = \langle m_\chi \rangle$, meaning that the modes are relativistic while they are being produced. If we take z to be sufficiently larger than z_i to make $\frac{k_a}{a(z)}$ and $\frac{k_b}{a(z)}$ small enough, we may consider $\frac{k}{a(z)} \ll \langle m_\chi \rangle$, so that $\omega_k \approx \langle m_\chi \rangle = gM$ for all significant k modes; i.e. in this regime, the modes were produced as relativistic, with physical momentum $\frac{2H}{\gamma}$, but by a time $z \gg z_i$ they have become non-relativistic.

Hence, the first integral in (2.3.12) is simply

$$\langle \rho_\chi^{\text{A}} \rangle \approx \frac{1}{2\pi^2 a^3(z)} gM \int_{k_a}^{k_b} k^2 \, \tilde{n}_k^{\text{A}} \, dk = gM \, \frac{\tilde{n}_\chi^{\text{A}}}{a^3(z)} \,, \tag{2.3.14}$$

from where, using (2.2.18),

$$\langle \rho_\chi^{\text{A}} \rangle \approx \frac{4\sqrt{2q}\, gMH^3}{\pi^2 \gamma^3} \left(\frac{a_i}{a(z)} \right)^3 e^{\frac{\pi q^2}{4\gamma}} \frac{\sinh\left[\frac{q}{2} \left(3 + \frac{2q}{\gamma} \right) \right]}{3 + \frac{2q}{\gamma}} \,, \tag{2.3.15}$$

which, as we can see, varies in time due to the expansion of the Universe (i.e. it is diluted away by the expansion).

2.3.2 Regime B

From (2.2.20), we see that $\frac{k_1(z)}{a(z)} \gg \frac{k_b}{a(z)}$ for $z \gg z_i$ (and $q \ll 1$), so that at a time $z \gg z_i$ modes closer to $k_1(z)$ should dominate the integral in this regime. The physical momentum associated with these dominating modes is of course $\frac{k_1(z)}{a(z)} = \frac{2H}{\gamma} e^{-\frac{q}{2}} \sim k_{c,\text{phys}} = \frac{2H}{\gamma} \gg gM$, which means that the modes that have just left the resonance band at a time z are relativistic, as we already knew. Hence, for the significant (dominating) k modes we can take $\omega_k(z) \approx \frac{k}{a(z)}$, making

$$\langle \rho_\chi^{\text{B}} \rangle \approx \frac{1}{2\pi^2 a^4(z)} \int_{k_b}^{k_1(z)} k^3 \, \tilde{n}_k^{\text{B}} \, dk = \frac{e^{\frac{\pi q^2}{2\gamma}}}{16\pi^2 a^4(z)} \left(k_1^4(z) - k_b^4 \right) \,, \tag{2.3.16}$$

where (2.2.21) was used. Recalling (2.2.20) and once again using the fact that $k_1(z) \gg k_b$ for $z \gg z_i$, this results in

$$\langle \rho_\chi^{\text{B}} \rangle \approx \frac{H^4}{\pi^2 \gamma^4} e^{\frac{\pi q^2}{2\gamma} - 2q} \,, \tag{2.3.17}$$

which interestingly is approximately constant (only approximately, since H, q and γ actually vary slowly due to the slow-roll dynamics, cf. § 1.2.1 and Appendix A). Note that the constancy of this quantity does not mean that no particles are being produced; it rather means that in this regime the production of the χ particles is perfectly compensated by their dilution.

2.3.3 Regime C

As we saw in the previous section, for a narrow resonance the modes near $k_1(z)$ are relativistic at all times. In § 2.2.3, we arrived at the relation $k_2(z) = k_1(z)\, e^q \sim k_1(z)$ for $q \ll 1$, so that the $k_2(z)$ modes are also relativistic at any time z. This of course means that we can write $\omega_k(z) \approx \frac{k}{a(z)}$ for all values of k such that $k_1(z) \leqslant k \leqslant k_2(z)$. The third integral in (2.3.12) is then, making use of (2.2.27),

$$\langle \rho_\chi^{\mathrm{C}} \rangle \;\approx\; \frac{1}{2\pi^2 a^4(z)} \int_{k_1(z)}^{k_2(z)} k^3\, \tilde{n}_k^{\mathrm{C}}\, dk \;\approx\; \frac{\xi(z)}{4\pi^2 a^4(z) \left(4 - \frac{2q}{\gamma}\right)} \left(k_2^{4-\frac{2q}{\gamma}}(z) - k_1^{4-\frac{2q}{\gamma}}(z) \right) , \tag{2.3.18}$$

which is easily simplifiable using (2.2.25), resulting in

$$\langle \rho_\chi^{\mathrm{C}} \rangle \;\approx\; \frac{8H^4}{\pi^2 \gamma^4}\, e^{\frac{\pi q^2}{4\gamma}}\, \frac{\sinh\left[\frac{q}{2}\left(4 - \frac{2q}{\gamma}\right)\right]}{4 - \frac{2q}{\gamma}} , \tag{2.3.19}$$

which, similarly to $\langle \rho_\chi^{\mathrm{B}} \rangle$, is an approximately constant value (again, H, q and γ are in fact time-varying quantities, albeit slowly-varying, cf. § 1.2.1 and Appendix A), meaning that the production of the χ particles in this regime is again perfectly compensated by their dilution.

The total physical energy density is now simple to calculate, but before we do so there is a useful approximation we can make. Comparing expressions (2.3.15), (2.3.17) and (2.3.19), it is clear that for $z \gg z_i$ we have $\langle \rho_\chi^{\mathrm{A}} \rangle \ll \langle \rho_\chi^{\mathrm{B}} \rangle, \langle \rho_\chi^{\mathrm{C}} \rangle$. Indeed, as time progresses, the physical energy density of the modes produced near the beginning of particle production (regime A) is diluted due to expansion, while that of the modes produced in regimes B and C (specifically, that of the modes within or just outside the resonance band) remains constant. We then have

$$\langle \rho_\chi \rangle \;\approx\; \langle \rho_\chi^{\mathrm{B}} \rangle + \langle \rho_\chi^{\mathrm{C}} \rangle \;\approx\; \frac{H^4}{\pi^2 \gamma^4} \left\{ e^{\frac{\pi q^2}{2\gamma} - 2q} + 8\, e^{\frac{\pi q^2}{4\gamma}}\, \frac{\sinh\left[\frac{q}{2}\left(4 - \frac{2q}{\gamma}\right)\right]}{4 - \frac{2q}{\gamma}} \right\} . \tag{2.3.20}$$

As in the previous section, it was found for all considered inflationary models (§ 3.3) that in the interesting regions of the parameter space (g, M) we have $\langle \rho_\chi^{\mathrm{B}} \rangle \gg \langle \rho_\chi^{\mathrm{C}} \rangle$, so that

$$\boxed{\rho_\chi \equiv \langle \rho_\chi \rangle \approx \frac{H^4}{\pi^2 \gamma^4} e^{\frac{\pi q^2}{2\gamma} - 2q}}, \tag{2.3.21}$$

which is the final expression for the physical energy density of particles produced since the beginning of particle production at z_i until a time $z \gg z_i$. Note that, building on what was stated before, the constancy of this value is due to there being a balance between the rate of χ particle production and the rate of their dilution due to the expansion of the Universe; in fact, at every time z there is always a mode k that is inside the resonance band and is thus leading to the production of χ particles, which exactly compensates the dilution of the pre-existing ones, as the total energy density of the produced particles is calculated to be proportional to a^4, while their dilution goes with a^{-4}, them being relativistic, so that the two effects essentially cancel one another. Additionally, as was seen, ρ_χ is only approximately constant; in fact it varies adiabatically due to the slow-roll dynamics, as analysed in § 3.3 and Appendix A.

Since during inflation the energy density of the Universe must be dominated by that of the inflaton field, we must ensure that the relation $\rho_\chi < \rho_\phi$ holds at least until near the end of the inflationary epoch. We will see in Chapter 3 that this is indeed true in a significant region of the parameter space (g, M) for all considered inflationary models.

Before advancing, let us note that

$$\xi \equiv \frac{\pi q^2}{2\gamma} \tag{2.3.22}$$

is a quantity that keeps showing in our expressions, appearing in particular in Eq. (2.2.21) as the argument of the exponential factor. If we recall that the expression in Eq. (2.2.21) is actually given by $\tilde{n}_k^{\mathrm{B}} \approx \frac{1}{2} e^{\xi} - \frac{1}{2}$, where we recovered the vacuum term that we had previously dropped, we see that for $\xi = 0$ no χ quanta are produced in this regime (nor in the remaining regimes[12], since a vanishing ξ implies a vanishing q). We then see that the larger ξ is, the more quanta we are able to produce, so that we may use this quantity as a measure of the efficiency of the resonance. In particular, we might expect that in order to have a very efficient production of particles we would have to require that $\tilde{n}_k^{\mathrm{B}} \gg 1$, which would be attained by imposing $e^{\xi} \gg 1$. Let us see if this is really the case. First, note that the quantities denoted by $\tilde{n}_k^{\mathrm{B}}$ need not be integers, as one might expect due to their interpretation as particle numbers; the reason for this lies in Eq. (2.3.10), where we see that these objects are defined via a vacuum expectation value, meaning that they are actually averaged quantities, and so can in principle take any real value

[12] We are focusing the discussion on the B regime, since it is the most relevant one, but these considerations remain mostly valid in the other regimes, save for a few small adaptations.

(in fact, $\tilde{n}_k^{\mathrm{B}}$ is often defined using Bogolyubov coefficients [2, 33, 68], which are complex-valued quantities; we shall make use of this alternative definition in § 2.4.1). This implies that we may only require that $\tilde{n}_k^{\mathrm{B}}$ be positive-valued, in which case $e^{\xi} \geqslant 1$, which is of course always true. Notice then that $\tilde{n}_k^{\mathrm{B}}$ can be quite small, while both $\tilde{n}_\chi$ from Eq. (2.2.32) and ρ_χ from Eq. (2.3.21) can simultaneously be quite large, in particular due to the γ^{-3} and γ^{-4} factors coming from the momentum integrations. This means that, while very few particles may be produced at each comoving momentum k, our phase space is quite big, so that we have lots of comoving momenta being produced, each contributing with some amount to the total comoving particle density and the total physical energy density. Hence, we may still have quite an efficient resonance, in spite of a small number of particles produced at each momentum k, due to phase space effects. We shall see this numerically in § 3.3, for various inflationary potentials. However, we will also find that in order to have an eventually detectable effect of the resonance, the lower bound we have just imposed is not enough, and we will need to go to higher values of ξ (and hence e^{ξ}).

2.4 Backreaction on the inflaton

It is now time to account for the backreaction of the produced χ particles on the inflaton field [33]. We shall split its effect into two parts: the backreaction on the classical, homogeneous inflaton, and the backreaction on the quantum fluctuations of the inflaton. These will be dealt with independently and so any kind of interference between the two shall be neglected as a higher-order correction. Let us start with the classical case.

2.4.1 Effect on the classical inflaton

We start by writing the full Lagrangian of our model, previously defined in (2.1.7), as

$$\begin{aligned}\mathcal{L} \;=\; & \left(D_\mu \Phi_1\right)^\dagger \left(D^\mu \Phi_1\right) + \left(D_\mu \Phi_2\right)^\dagger \left(D^\mu \Phi_2\right) + \frac{1}{2}\partial_\mu \chi\, \partial^\mu \chi - \frac{1}{4} F_{\mu\nu} F^{\mu\nu} \\ & - \mathscr{V}(|\Phi_1|, |\Phi_2|) - \frac{1}{2} g^2 |\Phi_1 - \Phi_2|^2 \chi^2 - V(\phi)\,,\end{aligned} \tag{2.4.1}$$

where, as permitted by the U(1) gauge symmetry of $\mathcal{L}$, we have now explicitly included a potential $V(\phi)$ for the inflaton, since we will now be dealing directly with effects on the dynamics of this field. Choosing the unitary gauge and excluding terms containing fields other than ϕ or χ (as in § 2.1.1), we may define the following Lagrangian

$$\mathcal{L}_{\phi\chi} \;=\; \frac{1}{2}\partial_\mu \phi\, \partial^\mu \phi + \frac{1}{2}\partial_\mu \chi\, \partial^\mu \chi - \frac{1}{2} m_\chi^2(\phi)\, \chi^2 - V(\phi)\,, \tag{2.4.2}$$

where, as before, $m_\chi^2(\phi) = 2\,g^2 M^2 \sin^2\left(\frac{\phi}{M}\right)$, allowing us to define the action functional

$$S[\phi,\chi] \;=\; \int d^4x\,\sqrt{-g}\,\mathcal{L}_{\phi\chi}\,. \tag{2.4.3}$$

In Appendix B, we show using an effective action formalism [18, 66, 69–72] that the effective EoM for the inflaton field receives two contributions: a Coleman-Weinberg (CW) term [55, 70, 73] and a term proportional to $\tilde{n}_k$ [33], which are written in Eq. (B.15) as a trace in momentum space. The CW term can be integrated and renormalised using the $\overline{\text{MS}}$ renormalisation scheme [55, 74], leading to a contribution to the effective EoM given by

$$\Delta V'_{\text{CW}}(\phi) \;\equiv\; \frac{g^4 M^3}{8\pi^2}\,\sin^2\left(\frac{\phi}{M}\right)\sin\left(\frac{2\phi}{M}\right)\ln\left(\frac{\mu^2}{m_\chi^2}\right)\,. \tag{2.4.4}$$

where μ is the $\overline{\text{MS}}$ renormalisation scale. We immediately see that if we select $\mu = m_\chi$ this contribution vanishes altogether. Nonetheless, let us compare it with the one proportional to $\tilde{n}_k$. For this, we anticipate an upcoming result (also obtained in Appendix B): that the remaining contribution to the EoM is given by

$$\Delta V'_{\text{PP}}(\phi) \;\equiv\; \frac{g^2 M}{2\pi^2}\left(\frac{H}{\gamma}\right)^2 e^{\frac{\pi g^2}{2\gamma}-q}\,\sin\left(\frac{2\phi}{M}\right)\,. \tag{2.4.5}$$

where the subscript indicates that this quantity is related to (χ) particle production. In spite of the clear suppression due to an additional g^2 factor in Eq. (2.4.4), these two contributions are not straightforward to compare using only their analytical expressions. Numerically, however, we found that for a renormalisation scale $H < \mu < M_{\text{P}}$ the CW term is subleading relative to $\Delta V'_{\text{PP}}$ for all inflationary models we considered in this work; hence, we may neglect the former in our computations and consider only the contribution coming from particle production.

In fact, this amounts to using the Hartree approximation[13] for the backreaction on the inflaton field [33, 73]. Neglecting for now the quantum fluctuations of the inflaton, such that $\phi \approx \bar{\phi} \equiv \phi$ (i.e. ϕ now refers only to the backreacted[14] classical and homogeneous inflaton, and

[13] In Ref. [33], some additional contributions are shown to be subdominant relative to the Hartree approximation. In the present work, we will not perform such an analysis and will consider exclusively this approximation, which will in principle be able to capture the main behaviour of the backreaction; however, a more rigorous study of this system is certainly of interest, as we will discuss in Chapter 4.

[14] Henceforth, we shall refer to quantities of which we consider the backreaction as *backreacted*, *corrected* or *effective*, whereas quantities without backreaction shall be referred to as *uncorrected*.

not to the full corrected field), the EoM for ϕ can be obtained simply by replacing χ^2 with its vacuum expectation value $\langle\chi^2\rangle$ in the Lagrangian (2.4.2) and varying (2.4.3) with respect to ϕ[15]

$$\Box\phi + V' + \frac{1}{2}(m_\chi^2)'\,\langle\chi^2\rangle = 0\,, \tag{2.4.6}$$

where $V \equiv V(\phi)$ and $m_\chi^2 \equiv m_\chi^2(\phi)$ and where the primes now denote derivatives with respect to ϕ. The expectation value $\langle\chi^2\rangle$ is simply given by equation (2.3.5c), which we rewrite here

$$\langle\chi^2\rangle = \int \frac{d^3k}{(2\pi)^3}\,|\chi_k|^2\,. \tag{2.4.7}$$

In order to compute the integrand in (2.4.7), we write the solution of equation (2.1.20), the EoM of $\chi_k = \chi_k(t)$, in terms of (complex) Bogoliubov coefficients $\alpha_k = \alpha_k(t)$ and $\beta_k = \beta_k(t)$ [2, 33, 68]

$$\chi_k(t) = a^{-3/2}(t)\left[\frac{\alpha_k(t)}{\sqrt{2\omega_k(t)}}\,e^{-i\int\omega_k(t)\,dt} + \frac{\beta_k(t)}{\sqrt{2\omega_k(t)}}\,e^{i\int\omega_k(t)\,dt}\right], \tag{2.4.8}$$

with the normalisation condition $|\alpha_k(t)|^2 - |\beta_k(t)|^2 = 1$ and the relation

$$\dot\alpha_k = \frac{\dot\omega_k}{2\omega_k}\,e^{2i\int\omega_k\,dt}\,\beta_k \tag{2.4.9a}$$

$$\dot\beta_k = \frac{\dot\omega_k}{2\omega_k}\,e^{-2i\int\omega_k\,dt}\,\alpha_k\,, \tag{2.4.9b}$$

which is obtained when we impose that $X_k(t) = a^{3/2}(t)\,\chi_k(t)$, with $\chi_k(t)$ given by (2.4.8), be a solution to Eq. (2.1.23).

This definition leads to

$$\begin{aligned}|\chi_k|^2 \;=\; \chi_k^*\,\chi_k \;&=\; \frac{a^{-3}}{2\omega_k}\left[|\alpha_k|^2 + |\beta_k|^2 + 2\,\mathfrak{Re}\left(\alpha_k\,\beta_k^*\,e^{-2i\int\omega_k\,dt}\right)\right] \approx \\ &\approx\; \frac{a^{-3}}{2\omega_k}\left(1 + 2\,|\beta_k|^2\right),\end{aligned} \tag{2.4.10}$$

where we dropped the high-frequency term (as it should provide a subdominant contribution [33]) and used the normalisation condition. Moreover, using Eqs. (2.2.7), (2.4.8) and (2.4.9) it can be easily shown that $|\beta_k|^2 = \tilde n_k$, so that

[15] One could equally vary (2.4.3) with respect to ϕ and then take the expectation value of the EoM, taking $\langle\phi\rangle = \phi$, as is true for a classical field.

$$\langle\chi^2\rangle \approx \frac{1}{a^3}\int \frac{d^3k}{(2\pi)^3}\,\frac{\tilde{n}_k+\frac{1}{2}}{\omega_k}\,. \tag{2.4.11}$$

Similarly to what we did in § 2.2 and § 2.3, we must divide this integral into three parts, each corresponding to a regime (A, B and C) under which the χ particles may be produced. The calculations are essentially analogous to the ones done previously. Using Eq. (2.2.10), we find that once again the B regime dominates, leaving us with

$$\langle\chi^2\rangle \approx \frac{1}{a^3}\int \frac{d^3k}{(2\pi)^3}\,\frac{e^{2\mu_k z}}{2\omega_k^0} \approx \frac{1}{2\pi^2\,a^3}\int_{k_b}^{k_1(z)} k^2\,dk\;\frac{\frac{1}{2}\,e^{\xi}}{k/a}\,, \tag{2.4.12}$$

where we used the fact that $\omega_k^0 \approx \omega_k \approx \frac{k}{a}$ for the modes of interest (i.e. the ones that dominate the integration). This leads to an effective EoM for ϕ that reads[16]

$$\Box\phi + V' + \frac{g^2 M}{2\pi^2}\left(\frac{H}{\gamma}\right)^2 e^{\frac{\pi q^2}{2\gamma}-q}\,\sin\left(\frac{2\phi}{M}\right) = 0\,, \tag{2.4.13}$$

in accordance with the result we anticipated in Eq. (2.4.5).

At this point, we note that the Hartree contribution to the backreaction may be entirely removed if instead of considering a single scalar field χ whose quanta are produced via parametric resonance we consider two scalar fields χ_1 and χ_2, whose interaction terms with the fields $\Phi_{1,2}$ are written as $-\frac{1}{2}g^2|\Phi_1-\Phi_2|^2\chi_1^2 - \frac{1}{2}g^2|\Phi_1+\Phi_2|^2\chi_2^2$, making the Lagrangian in Eq. (2.4.1) invariant under the simultaneous interchange $\Phi_1 \leftrightarrow i\Phi_2 \wedge \chi_1 \leftrightarrow \chi_2$, if furthermore $\lambda_1 = \lambda_2$ in $\mathscr{V}(|\Phi_1|,|\Phi_2|)$ [55, 57]. The effective oscillating masses for each field $\chi_{1,2}$ will then be different; in particular, $m_{\chi_1} \propto \sin\left(\frac{\phi}{M}\right)$ and $m_{\chi_2} \propto \cos\left(\frac{\phi}{M}\right)$. However, the quanta of each field $\chi_{1,2}$ are produced via the same process as described for χ, leading to variances $\langle\chi_1^2\rangle = \langle\chi_2^2\rangle = \langle\chi^2\rangle$, which means that in the Hartree approximation the contributions of each field $\chi_{1,2}$ would cancel each other, cf. Eq. (2.4.6), leaving us only with the subleading CW term (notice that this says nothing about the backreaction beyond the Hartree approximation, which may still contribute as well).

Returning to our main discussion, before we attempt to solve Eq. (2.4.13), it is useful to define an effective inflaton potential, as well as its derivatives with respect to ϕ,

[16] A similar result would be obtained if we had directly used for Eqs. (2.4.7) and (2.4.10) the approximate expression $\chi_k(z) \approx \frac{a^{-3/2}(z)}{\sqrt{2\omega_k^0}}\,e^{\pm i\omega_k(z)\frac{\gamma}{2H}z}\,e^{\mu_k z}$, with $\omega_k^0 \approx \frac{k}{a}$ for the modes of interest.

$$\mathcal{V}(\phi) = V(\tilde{\phi}) - \frac{g^2M^2}{4\pi^2}\left(\frac{H}{\gamma}\right)^2 e^{\frac{\pi q^2}{2\gamma}-q}\cos\left(\frac{2\phi}{M}\right) \tag{2.4.14a}$$

$$\mathcal{V}'(\phi) = V'(\tilde{\phi}) + \frac{g^2M}{2\pi^2}\left(\frac{H}{\gamma}\right)^2 e^{\frac{\pi q^2}{2\gamma}-q}\sin\left(\frac{2\phi}{M}\right) \tag{2.4.14b}$$

$$\mathcal{V}''(\phi) = V''(\tilde{\phi}) + \frac{g^2}{\pi^2}\left(\frac{H}{\gamma}\right)^2 e^{\frac{\pi q^2}{2\gamma}-q}\cos\left(\frac{2\phi}{M}\right) . \tag{2.4.14c}$$

Notice that we are not considering the ϕ-dependence of the oscillation amplitude when computing the derivatives, as its contribution is sub-leading when compared to the one coming from the actual oscillating part – the variation of the amplitude is due to the slow-roll dynamics of the inflaton. In particular, $H^2 \propto V(\phi)$, in the uncorrected slow-roll approximation, and so the derivative of H^2 with respect to ϕ is $(H^2)' = \sqrt{2\epsilon_V}\, H^2/M_{\rm P} \ll 2H^2/M$. Hence, in the following, we will take $\mathcal{V}(\phi)$ to be

$$\mathcal{V}(\phi) \approx V(\phi) + \Lambda^4 \cos\left(\frac{2\phi}{M}\right) , \tag{2.4.15}$$

where $\Lambda^4 \equiv -\frac{g^2M^2}{4\pi^2}\left(\frac{H}{\gamma}\right)^2 e^{\frac{\pi q^2}{2\gamma}-q}$ varies adiabatically due to slow-roll dynamics, and so is taken to be approximately constant throughout inflation (this means that, as before, time derivatives of Λ^4 will be neglected, but we will consider its time dependence when relevant, e.g. in § 3.3).

Inflationary potentials with oscillatory modulations are a well-known class of models, some of which with ties to axion monodromy in string theory [22, 23, 29, 75–79]. These modulations may arise either due to corrections of some sort, as in our case, or by construction, as in models of axion monodromy inflation [29, 76–79], and they can lead to features on the curvature power spectrum, which may be eventually be observable [23, 29, 76–78]. We may denote the correction to the n-th derivative of the potential by $\Delta V^{(n)} \equiv \mathcal{V}^{(n)} - V^{(n)}$, and in Appendix C.2 we show in particular that $\left|\frac{\Delta V}{V}\right|_{\rm max} \ll \left|\frac{\Delta V'}{V'}\right|_{\rm max} \ll \left|\frac{\Delta V''}{V''}\right|_{\rm max}$, where the subscript "max" means that we are only considering the amplitude of the oscillating term. Moreover, we anticipate that in § 3.3 we find that in general $\left|\frac{\Delta V}{V}\right| \leqslant \left|\frac{\Delta V}{V}\right|_{\rm max} \ll 1$, in accordance with the results found in Refs. [29, 76, 77] by analysis of observational data on the curvature power spectrum. In Ref. [76], for instance, the bound on $\alpha \equiv \left|\frac{\Delta V}{V}\right|_{\rm max}$ is $\alpha \lesssim 3\times 10^{-5}$, obtained for axion monodromy inflation.

We shall also define a new pair of slow-roll parameters to replace those in (1.2.6), using the potential $\mathcal{V}$ and its derivatives,

$$\epsilon_{\mathcal{V}} \equiv \frac{1}{2} M_P^2 \left(\frac{\mathcal{V}'(\phi)}{\mathcal{V}(\phi)} \right)^2 \tag{2.4.16a}$$

$$\eta_{\mathcal{V}} \equiv M_{\rm P}^2 \, \frac{\mathcal{V}''(\phi)}{\mathcal{V}(\phi)} \,, \tag{2.4.16b}$$

as well as new Hubble slow-roll parameters as in Eq. (1.2.7), using the effective Hubble parameter $\mathcal{H}$, defined by the Friedmann equation $\mathcal{V}(\phi) \equiv 3 M_{\rm P}^2 \mathcal{H}^2$

$$\epsilon_{\mathcal{H}} \equiv -\frac{\dot{\mathcal{H}}}{\mathcal{H}^2} \tag{2.4.17a}$$

$$\eta_{\mathcal{H}} \equiv 2\,\epsilon_{\mathcal{H}} - \frac{1}{2}\,\frac{\dot{\epsilon}_{\mathcal{H}}}{\epsilon_{\mathcal{H}}\,\mathcal{H}} \,. \tag{2.4.17b}$$

We may now try to find an analytical solution to Eq. (2.4.13), now rewritten as $\Box\phi + \mathcal{V}'(\phi) = 0$, with $\mathcal{V}(\phi)$ given by Eq. (2.4.15) and where the d'Alembertian is now defined using $\mathcal{H}$, rather than H. This allows us to follow Ref. [23] somewhat closely.[17] As such, we start by expanding the field as

$$\tilde{\phi} = \phi_0 + \phi_1 + \cdots \,, \tag{2.4.18}$$

where ϕ_0 is simply the uncorrected, homogeneous inflaton, and ϕ_1 is the first-order correction (linear in Λ^4) due to the backreaction of χ. Hence, the EoM for ϕ_0 is just Eq. (1.2.4), which during slow-roll can be approximated as Eq. (1.2.5b); combined with the Friedmann equation (1.2.5a), it leads to

$$\dot{\phi}_0 = -M_{\rm P}\,\frac{V_{,\phi_0}(\phi_0)}{\sqrt{3\,V(\phi_0)}} \,, \tag{2.4.19}$$

which can of course be solved independently of ϕ_1.

With this, we need only find an EoM for ϕ_1 alone. We thus expand $\mathcal{V}(\phi)$ as a function of ϕ_1

$$\begin{aligned} \mathcal{V}(\phi) &= \mathcal{V}(\phi_0 + \phi_1 + \cdots) \\ &= \mathcal{V}(\phi_0) \,+\, \mathcal{V}_{,\phi_0}(\phi_0)\,\phi_1 \,+\, \frac{1}{2}\,\mathcal{V}_{,\phi_0\phi_0}(\phi_0)\,\phi_1^2 \,+\, \cdots \,, \end{aligned} \tag{2.4.20}$$

[17] Accounting for the time-dependence of Λ^4 in these calculations would require a more complicated treatment, which we will not consider here. We will, however, consider the adiabatic variation of this and other quantities when working out the numerical treatment of our model in § 3.3.

and we do the same with $\mathcal{H}(\phi)$

$$\begin{aligned}\mathcal{H}(\phi) &= \mathcal{H}(\phi_0+\phi_1+\cdots) = \sqrt{\frac{\mathcal{V}(\phi_0+\phi_1+\cdots)}{3\,M_{\rm P}^2}} \\ &\approx \underbrace{\sqrt{\frac{V(\phi_0)}{3\,M_{\rm P}^2}}}_{H\equiv H_0}\left[1+\frac{1}{2}\frac{\Lambda^4}{V(\phi_0)}\cos\left(\frac{2\phi_0}{M}\right)+\frac{1}{2}\frac{\mathcal{V}_{,\phi_0}(\phi_0)}{V(\phi_0)}\,\phi_1+\cdots\right] \\ &\equiv H_0+H_1+\cdots,\end{aligned} \tag{2.4.21}$$

where we performed a Taylor expansion of the square root, taking into account that $\left|\frac{\Lambda^4}{V(\phi_0)}\right| \ll 1$ and $\left|\frac{\mathcal{V}_{,\phi_0}(\phi_0)}{V(\phi_0)}\,\phi_1\right| \ll 1$, the latter being shown in Appendix C.2.

We then substitute (2.4.18), (2.4.20) and (2.4.21) in $\Box\phi+\mathcal{V}'(\phi)=0$, where now $\mathcal{V}'(\phi) \equiv \mathcal{V}_{,\phi_1}(\phi_1)$, leading to

$$\ddot{\phi}_1+3\,(H_0+H_1)\,\dot{\phi}_1+3H_1\dot{\phi}_0+\mathcal{V}_{,\phi_0\phi_0}(\phi_0)\,\phi_1=\frac{2}{M}\,\Lambda^4\sin\left(\frac{2\phi_0}{M}\right), \tag{2.4.22}$$

where we used Eq. (1.2.4) once again. It is useful to convert the cosmic time derivatives of ϕ_1 into derivatives with respect to ϕ_0; this can be achieved using $\dot{\phi}_1=\frac{d\phi_1}{d\phi_0}\,\dot{\phi}_0$ and Eq. (2.4.19). Assuming that $|\phi_1| \ll \frac{M}{2}$ (which we shall see is the case), and given that $|\Lambda^4| \ll \left|\frac{M}{2}\,V_{,\phi_0}(\phi_0)\right|$ (cf. Appendix § C.2), we arrive, after some algebra and keeping only terms linear in ϕ_1, at the following equation

$$\phi_1''-\frac{3}{M_{\rm P}}\frac{1}{\sqrt{2\epsilon_{V_0}}}\,\phi_1'+\frac{3}{2M_{\rm P}^2}\left(\frac{\eta_{V_0}}{\epsilon_{V_0}}-1\right)\phi_1=\frac{3\,\Lambda^4}{\epsilon_{V_0}V_0M}\sin\left(\frac{2\phi_0}{M}\right), \tag{2.4.23}$$

where the primes now denote derivatives with respect to ϕ_0, and where ϵ_{V_0} and η_{V_0} are given by (1.2.6), using the potential $V(\phi_0)\equiv V_0$.

In order to solve Eq. (2.4.23), we need to make a further approximation: following [23], we shall replace ϕ_0 by a pivot value ϕ_* (taken to be the value of ϕ_0 at the CMB pivot scale k_*) everywhere except in the argument of the sine on the right-hand side of the equation. This step basically assumes that the dynamics of ϕ_1 are predominantly described by the oscillatory part of the equation, such that the coefficients of every term may be taken to be constant. Thus, the equation becomes

$$\phi_1''-\frac{3}{M_{\rm P}}\frac{1}{\sqrt{2\epsilon_{V_*}}}\,\phi_1'+\frac{3}{2M_{\rm P}^2}\left(\frac{\eta_{V_*}}{\epsilon_{V_*}}-1\right)\phi_1=\frac{3\,\Lambda^4}{\epsilon_{V_*}V_*M}\sin\left(\frac{2\,\phi_0(t)}{M}\right), \tag{2.4.24}$$

where we have made explicit the time-dependence of ϕ_0, which is given by Eq. (2.4.19). Setting $A = -\frac{3}{M_{\rm P}}\frac{1}{\sqrt{2\epsilon_{V_*}}}$, $B = \frac{3}{2M_{\rm P}^2}\left(\frac{\eta_{V_*}}{\epsilon_{V_*}} - 1\right)$ and $C = \frac{3\,\Lambda^4}{\epsilon_{V_*} V_* M}$, this equation has a general solution

$$\begin{aligned}\phi_1(t) \;=\; & \alpha_1\, e^{\frac{1}{2}\left(-A-\sqrt{A^2-4B}\right)\phi_0(t)} \;+\; \alpha_2\, e^{\frac{1}{2}\left(-A+\sqrt{A^2-4B}\right)\phi_0(t)} \\ & - \frac{CM^2\left[\sin\left(\frac{2\,\phi_0(t)}{M}\right) + A\,\frac{M}{2}\cos\left(\frac{2\,\phi_0(t)}{M}\right) - B\,\frac{M^2}{4}\sin\left(\frac{2\,\phi_0(t)}{M}\right)\right]}{\left[2+\frac{M^2}{4}\left(A^2-2B+A\sqrt{A^2-4B}\right)\right]\left[2+\frac{M^2}{4}\left(A^2-2B-A\sqrt{A^2-4B}\right)\right]}\,.\end{aligned} \tag{2.4.25}$$

Since ϕ_1 must vanish if $\Lambda^4 = 0$ (and so $C = 0$), we readily conclude that $\alpha_1 = \alpha_2 = 0$, meaning that only the particular solution to the equation is important (the exponentials being solutions to the homogeneous equation). Moreover, it can be shown that $|A\,\frac{M}{2}| \ll 1$, $|B\,\frac{M^2}{4}| \ll 1$ and $A^2 \gg |B|$ (cf. Appendix C.2), and so this solution is well approximated by

$$\phi_1(t) \;\approx\; -C\,\frac{M^2}{4}\sin\left(\frac{2\,\phi_0(t)}{M}\right) \;=\; -\frac{3\,\Lambda^4 M}{4\,\epsilon_{V_*} V_*}\sin\left(\frac{2\,\phi_0(t)}{M}\right)\,, \tag{2.4.26}$$

at which point we may notice that this amounts to integrating Eq. (2.4.24) with vanishing coefficients for ϕ_1' and ϕ_1. The full analytical solution for the backreacted field ϕ is then

$$\phi(t) \;=\; \phi_0(t) \;-\; \frac{3\,\Lambda^4 M}{4\,\epsilon_{V_*} V_*}\sin\left(\frac{2\,\phi_0(t)}{M}\right)\,. \tag{2.4.27}$$

The amplitude of the sine term is found to generally be quite small compared to ϕ_0, which is typically $\mathcal{O}(M_{\rm P})$ at CMB scales, while $\frac{\Lambda^4}{\epsilon_{V_*} V_*} \ll 1$ (cf. § 3.3), which furthermore shows that indeed $|\phi_1| \ll \frac{M}{2}$. In fact, plotting this solution against the uncorrected one for various families of potentials would reveal that the two follow each other exceedingly closely.[18] However, if we plug this solution into either (2.4.16) or (2.4.17) and we plot the resulting expression for the same potentials, we find that the slow-roll parameters have large oscillation amplitudes (see § 3.3). We could then be led to conclude that it should be impossible to a attain slow-roll evolution. Oddly, this is not what we observe in the numerical solution (see § 3.3), which retains its slow-roll behaviour even if including backreaction. This may be attributed to the very large frequency of the oscillation ($f \sim \frac{2H_0}{\gamma}$), such that only the average value of each slow-roll parameter has any impact on the field dynamics. This type of behaviour has also been encountered in Ref. [58]. If

[18] Both the analytical and the numerical solutions for the backreacted field follow the uncorrected full solution (i.e. without the slow-roll approximation) during the entirety of inflation, and these three solutions start to deviate from the uncorrected slow-roll one only in the last few e-folds.

we solve Eq. (2.4.13) numerically and use that solution to determine the slow-roll parameters, the results are exactly the same. It appears that having an inflationary potential with a sinusoidal modulation does not have a great impact in the slow-roll dynamics – we will see in § 3.3 that in some situations this is not entirely true.

We may then follow a similar procedure to that in Ref. [58] and compute the average values of $\epsilon_{\mathcal{H}}$ and $\eta_{\mathcal{H}}$ within an oscillation (in principle, it would be equally valid to use $\epsilon_{\mathcal{V}}$ and $\eta_{\mathcal{V}}$). For this, we will not be using the expansion of Eq. (2.4.21) to compute $\dot{\mathcal{H}}$, but rather

$$\begin{aligned} \dot{\mathcal{H}}(\phi) \;&=\; \frac{d}{dt}\left(\sqrt{\frac{\mathcal{V}(\phi)}{3\,M_{\rm P}^2}}\right) \;=\; \frac{\mathcal{V}^{-1/2}(\phi)}{2\sqrt{3\,M_{\rm P}^2}}\,\mathcal{V}_{,\phi}(\phi)\,\dot{\phi} \\ &\approx\; \frac{V^{-1/2}(\phi)}{2\sqrt{3\,M_{\rm P}^2}}\left(V_{,\phi_0}(\phi_0)+\Delta V_{,\phi_0}(\phi_0)\right)\left(\dot{\phi}_0+\dot{\phi}_1\right)\,, \end{aligned} \tag{2.4.28}$$

where we have taken $\mathcal{V}^{-1/2}(\phi)\approx V^{-1/2}(\phi)$ and $\mathcal{V}_{,\phi}(\phi)\approx\mathcal{V}_{,\phi_0}(\phi_0)$, since $\Lambda^4\ll V(\phi_0)$ and $\phi\approx\phi_0$. We shall also replace ϵ_* and V_* in (2.4.27) by ϵ_{V_0} and $V_0=V(\phi_0)$, respectively, to a good approximation (these quantities are slow-varying), which will allow us to simplify the calculation. After some algebra, the resulting expression for $\epsilon_{\mathcal{H}}$ is found to be

$$\epsilon_{\mathcal{H}} \;=\; \epsilon_{H_0} \,+\, \frac{\mathrm{sgn}(\dot{\phi}_0)\,\Lambda^4}{2\,V(\phi_0)}\left[\frac{4}{\gamma}\,\sin\left(\frac{2\phi_0}{M}\right) \,+\, 3\,\cos\left(\frac{2\phi_0}{M}\right) \,-\, \frac{3\,\Lambda^4}{\epsilon_{V_0}V(\phi_0)\,\gamma}\,\sin\left(\frac{4\phi_0}{M}\right)\right]\,, \tag{2.4.29}$$

where we have used $\dot{\phi}_0=\mathrm{sgn}(\dot{\phi}_0)\,\sqrt{2\epsilon_{V_0}}\,M_{\rm P}H_0$ and where $\gamma=\sqrt{\frac{2}{\epsilon_{V_0}}}\,\frac{M}{M_{\rm P}}$. Moreover, the potential $V(\phi_0)$ is equal to $3\,M_{\rm P}^2H_0^2$, as given by the uncorrected Friedmann equation. The first term inside the square brackets probably provides the dominant contribution, but we will keep all three terms and compute the average value of each of them separately. Considering the first term, let us define the quantity

$$\left|\langle\Delta\epsilon^{(1)}_{H_0}\rangle_T\right| \;\equiv\; \left|\left\langle\frac{2\,\Lambda^4}{V(\phi_0)\,\gamma}\,\sin\left(\frac{2\phi_0(t)}{M}\right)\right\rangle_T\right|\,, \tag{2.4.30}$$

where we may approximate $\phi_0(t)\approx\phi_0(t_i)+\dot{\phi}_0(t_i)\,(t-t_i)\equiv\phi_0+\dot{\phi}_0\,(t-t_i)$, making $T=\frac{2\pi}{2|\dot{\phi}_0|/M}=\frac{\pi\gamma}{2H_0}$ the oscillation period (the quantities in this definition are to be evaluated at t_i). Notice that this approximation for the field is indeed valid for $t\in\left[t_i-\frac{T}{2},\,t_i+\frac{T}{2}\right]$, given that $T\ll H_0^{-1}$. Using the expression for Λ^4, we find

$$\left|\langle\Delta\epsilon^{(1)}_{H_0}\rangle_T\right| \;=\; \frac{1}{6}\left(\frac{gM}{\pi M_{\rm P}}\right)^2\left|\left\langle\frac{e^{\,\xi-q}}{\gamma^3}\,\sin\left(\frac{4H_0}{\gamma}\,t+\alpha\right)\right\rangle_T\right|\,, \tag{2.4.31}$$

where again the quantities in the argument of the sine are to be evaluated at t_i, while the ones outside remain functions of t. Defining $E_1(t) \equiv \frac{1}{6}\left(\frac{gM}{\pi M_{\rm P}}\right)^2 \frac{e^{\,\xi-q}}{\gamma^3} \approx E_1(t_i) + \dot{E}_1(t_i)\,(t-t_i)$, the average can be computed as

$$\begin{aligned}
\left|\langle \Delta\epsilon^{(1)}_{H_0}\rangle_T\right|_{\rm max} &\approx \left|\frac{1}{T}\int_{t_i-\frac{T}{2}}^{t_i+\frac{T}{2}} \left[E_1(t_i) + \dot{E}_1(t_i)\,(t-t_i)\,\sin\left(\frac{4H_0}{\gamma}\,t+\alpha\right)\right] dt\right|_{\rm max} \\
&= \left|\frac{\dot{E}_1(t_i)}{T}\int_{t_i-\frac{T}{2}}^{t_i+\frac{T}{2}} t\,\sin\left(\frac{4H_0}{\gamma}\,t+\alpha\right) dt\right|_{\rm max} \\
&= \frac{\gamma}{4H_0}\,|\dot{E}_1(t_i)| \\
&= \frac{1}{24}\left(\frac{gM}{\pi M_{\rm P}}\right)^2 \frac{e^{\,\xi-q}}{\gamma^2}\left|\xi\,(3\,\eta_{V_0}-2\,\epsilon_{V_0}) - 2q\,(\eta_{V_0}-\epsilon_{V_0}) - 3\,(\eta_{V_0}-2\,\epsilon_{V_0})\right|,
\end{aligned} \tag{2.4.32}$$

where the last line was obtained by computing the time derivative using the expressions from Appendix A, and where the subscript "max" is included so that we may drop a cosine factor associated with a phase. Once again, all quantities are to be evaluated at t_i. A similar procedure can be followed for the two remaining terms, leading to[19]

$$\left|\langle \Delta\epsilon^{(2)}_{H_0}\rangle_T\right|_{\rm max} \approx \frac{1}{32}\left(\frac{gM}{\pi M_{\rm P}}\right)^2 \frac{e^{\,\xi-q}}{\gamma^2}\left|\xi\,(3\,\eta_{V_0}-2\,\epsilon_{V_0}) - 2q\,(\eta_{V_0}-\epsilon_{V_0}) - 2\,(\eta_{V_0}-2\,\epsilon_{V_0})\right| \tag{2.4.33}$$

$$\left|\langle \Delta\epsilon^{(3)}_{H_0}\rangle_T\right|_{\rm max} \approx \frac{1}{768}\left(\frac{g^2M}{\pi^2 M_{\rm P}}\right)^2 \frac{e^{\,2(\xi-q)}}{\gamma^2}\left|2\xi\,(3\,\eta_{V_0}-2\,\epsilon_{V_0}) - 4q\,(\eta_{V_0}-\epsilon_{V_0}) - 3\,(\eta_{V_0}-2\,\epsilon_{V_0})\right|. \tag{2.4.34}$$

Each of these terms can be plotted as a function of t_i (or equivalently as a function of the corresponding N_e), in which case we discover that their values are generally smaller than ϵ_{H_0} for whatever instant we centre our average on, cf. § 3.3; that is, when we take averages, the large oscillations of $\epsilon_{\mathcal{H}}$ become quite suppressed, such that their effective effect on the field dynamics is negligible. We can define a maximum average correction to ϵ_{H_0} as

$$|\langle \Delta\epsilon_{H_0}\rangle_T|_{\rm max} \equiv \sum_{i=1}^{3}\left|\langle \Delta\epsilon^{(i)}_{H_0}\rangle_T\right|_{\rm max}, \tag{2.4.35}$$

which is generally smaller than ϵ_{H_0}. Also in § 3.3, we show that using the condition $\epsilon_{H_0} + |\langle \Delta\epsilon_{H_0}\rangle_T|_{\rm max} \sim 1$ as a replacement for $\epsilon_{H_0} \sim 1$ to determine when inflation ends when including backreaction only very slightly anticipates that event.

[19] Notice that we may use the same period $T = \frac{\pi\gamma}{2H_0}$ for the two remaining calculations, despite the third term inside the brackets in Eq. (2.4.29) having twice the frequency and so half the period of the other ones.

Now turning to $\eta_{\mathcal{H}}$, we start by using Eq. (2.4.29) to define $\Delta\epsilon_{H_0} \equiv \epsilon_{\mathcal{H}} - \epsilon_{H_0}$, where $\Delta\epsilon_{H_0}$ is taken to be smaller than ϵ_H. In this case, we find

$$\begin{aligned}
\eta_{\mathcal{H}} &= 2\,(\epsilon_{H_0} + \Delta\epsilon_{H_0}) - \frac{\epsilon'_{H_0} + \Delta\epsilon'_{H_0}}{2\,(\epsilon_{H_0} + \Delta\epsilon_{H_0})} \\
&\approx 2\,(\epsilon_{H_0} + \Delta\epsilon_{H_0}) - \frac{\epsilon'_{H_0} + \Delta\epsilon'_{H_0}}{2\,\epsilon_{H_0}}\left(1 - \frac{\Delta\epsilon_{H_0}}{\epsilon_{H_0}}\right) \\
&\approx \eta_{H_0} + \underbrace{\left(4 - \frac{\eta_{H_0}}{\epsilon_{H_0}}\right)\Delta\epsilon_{H_0} - \frac{\Delta\epsilon'_{H_0}}{2\,\epsilon_{H_0}}}_{\equiv\Delta\eta_{H_0}},
\end{aligned} \tag{2.4.36}$$

where the primes now denote derivatives with respect to N_e (we are once again considering $\mathcal{H} \approx H_0$, which as we have seen is a good approximation), and where we discarded a term of $\mathcal{O}(\Delta\epsilon^2_{H_0})$ in order to get the last line. The quantity $\Delta\epsilon'_{H_0}$ is readily computed as

$$\begin{aligned}
\Delta\epsilon'_{H_0} &= \frac{\mathrm{sgn}(\dot\phi_0)\,\Lambda^4}{V(\phi_0)\,M}\,\phi'_0\left[\frac{4}{\gamma}\cos\left(\frac{2\phi_0}{M}\right) - 3\sin\left(\frac{2\phi_0}{M}\right) - \frac{6\,\Lambda^4}{\epsilon_{V_0}V(\phi_0)\,\gamma}\cos\left(\frac{4\phi_0}{M}\right)\right] \\
&= \frac{2\,\Lambda^4}{V(\phi_0)\,\gamma}\left[\frac{4}{\gamma}\cos\left(\frac{2\phi_0}{M}\right) - 3\sin\left(\frac{2\phi_0}{M}\right) - \frac{6\,\Lambda^4}{\epsilon_{V_0}V(\phi_0)\,\gamma}\cos\left(\frac{4\phi_0}{M}\right)\right],
\end{aligned} \tag{2.4.37}$$

where we only considered the derivatives of the oscillatory functions (which provide the dominant contribution). We also used the fact that $\mathrm{sgn}(\dot\phi_0)\,\phi'_0 = H_0^{-1}\,|\dot\phi_0| = H_0^{-1}\,\frac{|\dot\phi_0|}{M}\,M = \frac{2M}{\gamma}$. This means that we must compute six averages: three due to the $\Delta\epsilon_{H_0}$ term, which have been mostly obtained already, and three due to the $\Delta\epsilon'_{H_0}$ term, which can be obtained in a similar way. The resulting expressions are

$$\left|\langle\Delta\eta^{(1)}_{H_0}\rangle_T\right|_{\mathrm{max}} \approx \frac{1}{24}\left|4 - \frac{\eta_{H_0}}{\epsilon_{H_0}}\right|\left(\frac{gM}{\pi M_{\mathrm{P}}}\right)^2\frac{e^{\,\xi-q}}{\gamma^2}\left|\xi\,(3\,\eta_{V_0} - 2\,\epsilon_{V_0}) - 2q\,(\eta_{V_0} - \epsilon_{V_0}) - 3\,(\eta_{V_0} - 2\,\epsilon_{V_0})\right| \tag{2.4.38}$$

$$\left|\langle\Delta\eta^{(2)}_{H_0}\rangle_T\right|_{\mathrm{max}} \approx \frac{1}{32}\left|4 - \frac{\eta_{H_0}}{\epsilon_{H_0}}\right|\left(\frac{gM}{\pi M_{\mathrm{P}}}\right)^2\frac{e^{\,\xi-q}}{\gamma^2}\left|\xi\,(3\,\eta_{V_0} - 2\,\epsilon_{V_0}) - 2q\,(\eta_{V_0} - \epsilon_{V_0}) - 2\,(\eta_{V_0} - 2\,\epsilon_{V_0})\right| \tag{2.4.39}$$

$$\left|\langle\Delta\eta^{(3)}_{H_0}\rangle_T\right|_{\mathrm{max}} \approx \frac{1}{768}\left|4 - \frac{\eta_{H_0}}{\epsilon_{H_0}}\right|\left(\frac{g^2M}{\pi^2 M_{\mathrm{P}}}\right)^2\frac{e^{\,2(\xi-q)}}{\gamma^2}\left|2\xi\,(3\,\eta_{V_0} - 2\,\epsilon_{V_0}) - 4q\,(\eta_{V_0} - \epsilon_{V_0}) - 3\,(\eta_{V_0} - 2\,\epsilon_{V_0})\right| \tag{2.4.40}$$

$$\left|\langle\Delta\eta^{(4)}_{H_0}\rangle_T\right|_{\mathrm{max}} \approx \frac{1}{12\,\epsilon_{H_0}}\left(\frac{gM}{\pi M_{\mathrm{P}}}\right)^2\frac{e^{\,\xi-q}}{\gamma^3}\left|\xi\,(3\,\eta_{V_0} - 2\,\epsilon_{V_0}) - 2q\,(\eta_{V_0} - \epsilon_{V_0}) - 4\,(\eta_{V_0} - 2\,\epsilon_{V_0})\right| \tag{2.4.41}$$

$$\left|\langle\Delta\eta^{(5)}_{H_0}\rangle_T\right|_{\rm max} \approx \frac{1}{16\,\epsilon_{H_0}}\left(\frac{gM}{\pi M_{\rm P}}\right)^2 \frac{e^{\,\xi-q}}{\gamma^2}\left|\xi\,(3\,\eta_{V_0}-2\,\epsilon_{V_0})-2q\,(\eta_{V_0}-\epsilon_{V_0})-3\,(\eta_{V_0}-2\,\epsilon_{V_0})\right| \quad (2.4.42)$$

$$\left|\langle\Delta\eta^{(6)}_{H_0}\rangle_T\right|_{\rm max} \approx \frac{1}{384\,\epsilon_{H_0}}\left(\frac{g^2M}{\pi^2 M_{\rm P}}\right)^2 \frac{e^{\,2(\xi-q)}}{\gamma^3}\left|2\xi\,(3\,\eta_{V_0}-2\,\epsilon_{V_0})-4q\,(\eta_{V_0}-\epsilon_{V_0})-4\,(\eta_{V_0}-2\,\epsilon_{V_0})\right|, \quad (2.4.43)$$

where the first three are related to each term of $\Delta\epsilon_{H_0}$ (in order), and the last three are related to each term of $\Delta\epsilon'_{H_0}$ (also in order). Defining

$$|\langle\Delta\eta_{H_0}\rangle_T|_{\rm max} \equiv \sum_{i=1}^{6}\left|\langle\Delta\eta^{(i)}_{H_0}\rangle_T\right|_{\rm max}\,, \quad (2.4.44)$$

we find in § 3.3 that the condition $|\eta_{H_0}|+|\langle\Delta\eta_{H_0}\rangle_T|_{\rm max}\sim 1$ is generally also a suitable replacement for $\eta_{H_0}\sim 1$ in the scenario including backreaction.

2.4.2 Effect on inflaton fluctuations

We may now turn to the effect of the backreaction in the quantum fluctuations of the inflaton field. Recovering the Lagrangian (2.4.2), we write the full backreacted inflaton field as $\phi=\bar\phi+\varphi$, where the behaviour of $\bar\phi$ has been determined in § 2.4.1 to be given by Eq. (2.4.27), and where φ describes the fluctuations of the inflaton including backreaction. In this section, however, we will ignore the backreaction on the classical field in order to focus on the leading order effect of χ on the inflaton fluctuations alone. The Lagrangian then becomes (expanding $m^2_\chi(\bar\phi)$ and $V(\bar\phi)$ to second order in φ)

$$\begin{aligned}\mathcal{L}_{\phi\chi} \;=\; & \frac{1}{2}\,\partial_\mu\bar\phi\,\partial^\mu\bar\phi \;+\; \frac{1}{2}\partial_\mu\varphi\,\partial^\mu\varphi \;+\; \partial_\mu\bar\phi\,\partial^\mu\varphi \;+\; \frac{1}{2}\partial_\mu\chi\,\partial^\mu\chi \\ & -\frac{1}{2}\left[m^2_\chi(\bar\phi) \;+\; (m^2_\chi)_{,\bar\phi}(\bar\phi)\,\varphi \;+\; \frac{1}{2}\,(m^2_\chi)_{,\bar\phi\bar\phi}(\bar\phi)\,\varphi^2\right]\chi^2 \\ & -\left[V(\bar\phi) \;+\; V_{,\bar\phi}(\bar\phi)\,\varphi \;+\; \frac{1}{2}\,V_{,\bar\phi\bar\phi}(\bar\phi)\,\varphi^2\right],\end{aligned} \quad (2.4.45)$$

Inserting this into the action (2.4.3) and replacing χ^2 by $\langle\chi^2\rangle$, in accordance with the Hartree approximation [33, 73], we may vary $S_{\phi\chi}$ with respect to φ and use Eq. (2.4.6) to find the EoM

$$\Box\varphi \;+\; V_{,\bar\phi\bar\phi}(\bar\phi)\,\varphi \;+\; \frac{1}{2}\,(m^2_\chi)_{,\bar\phi\bar\phi}(\bar\phi)\,\langle\chi^2\rangle\,\varphi \;=\; 0\,, \quad (2.4.46)$$

which can effectively be rewritten as

$$\Box\,\varphi = -\mathcal{V}_{,\bar{\phi}\bar{\phi}}(\bar{\phi})\;\varphi\,, \tag{2.4.47}$$

which is of course very reminiscent of Eq. (1.2.11).

Expanding the fluctuations in Fourier modes

$$\hat{\varphi}(t,\mathbf{x}) = \int \frac{d^3k}{(2\pi)^3}\,\left[\hat{a}_{\mathbf{k}}\,\varphi_k(t)\,e^{i\mathbf{k}\cdot\mathbf{x}} \;+\; \hat{a}^{\dagger}_{\mathbf{k}}\,\varphi^{*}_k(t)\,e^{-i\mathbf{k}\cdot\mathbf{x}}\right]\,, \tag{2.4.48}$$

where the operator $\hat{a}_{\mathbf{k}}$ annihilates the Bunch-Davis vacuum $|0\rangle$ [2, 7], we find that each mode function $u_k(t) = a^{3/2}(t)\,\varphi_k(t)$ satisfies an equation of motion

$$\ddot{u}_k \;+\; \left[\frac{k^2}{a^2} \;-\; \frac{9}{4}\,H^2 \;+\; \mathcal{V}_{,\bar{\phi}\bar{\phi}}(\bar{\phi})\right]\,u_k \;=\; 0\,, \tag{2.4.49}$$

which, changing the time variable to $z = \frac{|\dot{\bar{\phi}}|}{M}\,t = \frac{2H}{\gamma}\,t$, becomes

$$u_k'' \;+\; \left[A_k(z) \;-\; 2\,q_{\varphi}\cos(2z)\right]\,u_k \;=\; 0\,, \tag{2.4.50}$$

where the primes denote derivatives with respect to z and where

$$A_k(z) = \left(\frac{\gamma}{2H}\right)^2\left[\frac{k^2}{a^2(z)} - \frac{9}{4}H^2 + V_{,\bar{\phi}\bar{\phi}}(\bar{\phi})\right] \approx \left(\frac{k/a}{2H/\gamma}\right)^2 \tag{2.4.51a}$$

$$q_{\varphi} = \frac{g^2}{8\pi^2}\,e^{\frac{\pi g^2}{2\gamma}-q} \;=\; \frac{g^2}{8\pi^2}\,e^{\,\xi-q}\,. \tag{2.4.51b}$$

We recognize Eq. (2.4.50) as being a Mathieu-like equation, with parameters given by (2.4.51). In particular, we identify the parameter $A_k(z)$ from (2.4.51a) as being equal (in the approximation regime we are considering) to the corresponding parameter (2.1.31a) from the Mathieu equation for the χ mode functions, whereas the parameter q_{φ} depends exponentially on both ξ and q. It is then clear that resonant production of quanta of the inflaton field (i.e. inflatons) can be a consequence of the backreaction. In order to obtain Eq. (2.4.51), we have taken into account that the inflaton is a light field ($V_{,\bar{\phi}\bar{\phi}}(\bar{\phi}) \sim m^2_{\bar{\phi}} \ll H^2$) and that the produced u_k modes must be subhorizon ($\frac{k}{a} > H$) while inside the resonance band, as noted in §§ 1.2.1 and 2.1.2, respectively, resulting in $\left(\frac{k}{a}\right)_c \gg m_{\bar{\phi}}$ (i.e. the inflaton particles are relativistic while they are being produced); moreover, we have dropped a minus sign in the definition of q_{φ}, as it can be absorbed as a phase on the cosine which we eliminate via a change of variable.

Due to these similarities, the ensuing discussion is entirely analogous to the one in §§ 2.1.2 and 2.2. We shall once again consider a narrow resonance ($q_\varphi \ll 1$), which we shall see in § 3.3 is not difficult to ensure, in spite of the exponential factor in the definition, and focus on the first resonance band ($A_k(z) \sim 1$), in which case we need only replace q by q_φ in the expression for the Floquet exponent (2.1.32), which becomes

$$\mu_k^{q_\varphi}(z) = \frac{1}{2}\sqrt{q_\varphi^2 - [A_k(z) - 1]^2}\,, \tag{2.4.52}$$

as well as in subsequent quantities (e.g. $\Delta t = q_\varphi H^{-1}$). Notice, however, that we need not replace q in quantities like $k_{c,\mathrm{phys}}$ or $z_c(k)$, since these depend only on $A_k(z)$, which remains the same – in fact, these quantities can be written entirely in terms of γ (the adiabatic coefficient in the expansion of $A_k(z)$), which does not explicitly depend on q. Using this, we rewrite the Floquet exponent as

$$\mu_k^{q_\varphi}(z) = \frac{1}{2}\sqrt{q_\varphi^2 - \gamma^2[z - z_c(k)]^2}\,, \tag{2.4.53}$$

from where it follows that we can recycle the results previously obtained for the χ field. In particular, from Floquet's theorem, the solutions to Eq. (2.4.50) are the mode functions

$$u_k(z) \approx \frac{1}{\sqrt{2\omega_k^0}}\, e^{\pm i\omega_k(z)\frac{\gamma}{2H}z}\, e^{\mu_k^{q_\varphi}(z)\,z}\,, \tag{2.4.54}$$

where $\omega_k^0 \equiv \sqrt{\frac{k^2}{a^2(z_0)} + m_{\tilde{\phi}}^2} \approx \frac{k}{a(z_0)} \equiv k_{0,\mathrm{phys}}$ is now the frequency of the inflaton fluctuations at a time z_0 just before the mode k enters the resonance band (note that z_0 need not be $z = 0$ and so $a(z_0)$ need not be $a(z = 0)$). Notice that the mode functions are essentially plane waves with an additional exponential factor accounting for the parametric resonance. In fact, just like in § 2.2, if a mode k is inside the resonance band between two instants z_s and z_e, the corresponding mode function is amplified as

$$u_k(z) \approx \frac{1}{\sqrt{2\omega_k^0}}\, e^{\pm i k_{\mathrm{phys}}(z)\frac{\gamma}{2H}z}\, e^{\mu_k^{q_\varphi}z}\,, \tag{2.4.55}$$

where $\mu_k^{q_\varphi} z \equiv \int_{z_s}^{z_e} \mu_k^{q_\varphi}(z)\, dz$ accounts for the cumulative effect of the resonance.

One could now compute the comoving number density of the produced inflatons $\tilde{n}_\varphi$, as well as their contribution ρ_φ to the total physical energy density of the inflaton field ρ_ϕ, in a similar fashion to what was done in §§ 2.2 and 2.3. However, these contributions should be subdominant,

as they are generated by a secondary resonance, of which the q_φ parameter is suppressed by a factor of g^2. In fact, we shall see in § 3.3 that despite the exponential factor in the definition of q_φ a narrow resonance regime for χ typically implies a narrower resonance for φ, at least in the regions of the parameter space (g, M) we are concerned with. Since the energy density of χ should be subdominant relative to that of the inflaton field (which we shall see also in § 3.3 is indeed the case), the contribution of φ to the inflaton energy density should be even less relevant. As such, we refrain from performing these computations here and simply assume that their effect is negligible. In any case, we may concern ourselves with a deeper analysis of this in future work.

We are, however, interested in the effect of this secondary resonance on the variance of the inflaton field, previously computed in Eq. (1.2.15). Now, using Eq. (2.4.48) and Eq. (2.4.55), we find

$$\begin{aligned} \langle 0|\hat{\varphi}^2(z,0)|0\rangle &= \frac{1}{a^3(z)}\int \frac{d^3k}{(2\pi)^3}\,|u_k(z)|^2 = \frac{1}{a^3(z)}\int \frac{d^3k}{(2\pi)^3}\,\frac{e^{2\mu_k^{q_\varphi} z}}{2\omega_k^0} \\ &\equiv \int \frac{d^3k}{(2\pi)^3}\,\tilde{\mathcal{P}}_\varphi(k)\,, \end{aligned} \tag{2.4.56}$$

where $\tilde{\mathcal{P}}_\varphi(k)$ is the backreacted power spectrum of inflaton fluctuations (as indicated by the tilde[20]). As in §§ 2.2, 2.3 and 2.4.1, we may consider three regimes (A, B and C) under which the resonance occurs, depending on when each mode k enters the resonance band. However, since we will ultimately be concerned with quantities at horizon-crossing, when $k = aH$, and modes cross the resonance band when $k \sim \frac{2H}{\gamma}\,a \gg aH$, we expect the second regime (B), which corresponds to modes that at a certain instant have already crossed the entirety of the resonance band, to be the one of interest. The modes from regime C are still a long way from crossing the horizon and so are not interesting at this stage, whereas the modes from regime A, despite having already exited the horizon, have physical momenta that have been severely redshifted by the expansion of the Universe, making them inaccessible by observations (we are assuming that $z \gg z_i$, with z_i again marking the start of particle production, early in inflation).

We may nonetheless compute the power spectrum for all three regimes and then select the most suitable one. For this, we start by recognising, following arguments similar to those in § 2.2, that $\frac{1}{2\omega_k^0}\,e^{2\mu_k^{q_\varphi} z} = \frac{1}{\omega_k(z)}\left(\tilde{n}_k^\varphi(z) + \frac{1}{2}\right)$, where $\tilde{n}_k^\varphi$ is the comoving number of produced inflatons

[20] Henceforth, backreacted quantities (mainly observables) are denoted using a tilde, while quantities without backreaction maintain their usual symbols. We must not confuse this notation with the one used for comoving quantities, which also employs a tilde; in any case, the latter is used only for occupation numbers, number densities, energies and energy densities, for which we do not consider a backreaction.

with comoving momentum k and $\omega_k(z) \approx \frac{k}{a(z)}$. Taking our previous expressions for the comoving number of particles in each regime, Eqs. (2.2.16), (2.2.21) and (2.2.27), we find (omitting the z dependence in the argument of the power spectrum)

$$\begin{aligned}\tilde{\mathcal{P}}_\varphi(k) &= \frac{a^{-2}(z)}{2k}\left(2\,\tilde{n}_k^\varphi(z)+1\right) \\ &= \frac{a^{-2}(z)}{2k}\times\begin{cases}\sqrt{2q}\,e^{\frac{\pi q_\varphi^2}{4\gamma}}\left(\frac{k/a(z_i)}{2H/\gamma}\right)^{\frac{2q_\varphi}{\gamma}}, & k_a^\varphi < k < k_b^\varphi \\ e^{\frac{\pi q_\varphi^2}{2\gamma}} \qquad\qquad\qquad\quad , & k_b^\varphi < k < k_1^\varphi(z) \\ e^{\frac{\pi q_\varphi^2}{4\gamma}}\left(\frac{k/a(z)}{2H/\gamma}\right)^{-\frac{2q_\varphi}{\gamma}} , & k_1^\varphi(z) < k < k_2^\varphi(z)\end{cases}\end{aligned} \tag{2.4.57}$$

where k_a^φ, k_b^φ, $k_1^\varphi(z)$ and $k_2^\varphi(z)$ are obtained by replacing q by q_φ in Eqs. (2.2.14), (2.2.20) and (2.2.25), respectively. We readily conclude that at horizon-crossing ($a(z) = \frac{k}{H}$) the only suitable modes are those contained between k_b^φ and $k_1^\varphi(z)$, since the ones contained between $k_1^\varphi(z)$ and $k_2^\varphi(z)$ verify $\frac{k}{a} \sim \frac{2H}{\gamma}$, and those between k_a^φ and k_b^φ indeed have too small physical momenta to be observationally relevant. Hence, at horizon-crossing, the power spectrum becomes simply

$$\tilde{\mathcal{P}}_\varphi(k) = \frac{H^2}{2k^3}\,e^{\frac{\pi q_\varphi^2}{2\gamma}} \equiv \frac{H^2}{2k^3}\,e^{\xi_\varphi}\,, \tag{2.4.58}$$

which we recognise as the spectrum obtained in (1.2.15) multiplied by a factor coming from the resonance, whose effect is then simply an exponential amplification of the amplitude (as we have stated before, this is only approximately true, since there is also some additional k-dependence due to the temporal variation of ξ_φ.

2.4.3 Effect on CMB observables

As we have alluded to in § 1.2.1, currently the best experimental probe for the inflationary epoch is the CMB radiation. The effect of the backreaction on CMB observables can be split into two contributions: those coming from the corrections to the classical inflaton (§ 2.4.1), and those coming from the corrections to the inflaton quantum fluctuations (§ 2.4.2). As in those subsections, we shall deal with each contribution separately and treat any interference between the two as a higher-order effect, which we will neglect. We shall focus on the backreaction on the dimensionless curvature power spectrum $\Delta^2_{\mathcal{R}}(k)$ and related quantities, namely the scalar spectral index n_s and the tensor-to-scalar ratio r. Note that the power spectrum of tensor perturbations is not altered due to the backreaction of the inflaton, but may receive contributions

from χ directly via gravitational wave generation [25, 26, 47], which is an effect we will not consider in this work (but intend to compute and analyse in the future).

Classical contribution to $\Delta^2_{\mathcal{R}}(k)$

Let us focus on the classical contribution first, ignoring the correction on the fluctuations. We shall use the notation employed in § 2.4.1. In order to determine this effect, Ref. [23] can be followed once more, in which case $\tilde{\Delta}^2_{\mathcal{R}}(k)$ is obtained by solving the Mukhanov-Sasaki equation [8, 27, 28] for the mode functions of the backreacted (gauge-invariant) comoving curvature perturbation $\tilde{\mathcal{R}}$, whose uncorrected version we defined in § 1.2.1, Eq. (1.2.21). This derivation, however, is too lengthy to include here and moreover it is well detailed in Ref. [23], so we merely quote the final result, which is

$$\tilde{\Delta}^2_{\mathcal{R}}(k) = \Delta^2_{\mathcal{R}}(k) \left[1 + \frac{3\,\Lambda^4}{\epsilon_{V_*} V_*} \sqrt{\frac{2\pi}{\gamma_*}} \cos\left(\frac{2\,\phi_0(k)}{M}\right)\right], \tag{2.4.59}$$

where $\Delta^2_{\mathcal{R}}(k) = \Delta^2_{\mathcal{R}}(k_*) \left(\frac{k}{k_*}\right)^{n_s - 1}$, with $\Delta^2_{\mathcal{R}}(k_*) = \left(\frac{H_*}{\dot{\phi}_*}\right)^2 \left(\frac{H_*}{2\pi}\right)^2$ during inflation, is the usual power law from Eq. (1.2.23), $\phi_0(k)$ is the value of the uncorrected inflaton field when the mode with comoving momentum k exits the causal horizon and $\gamma_* = \sqrt{\frac{2}{\epsilon_{V_*}}} \frac{M}{M_{\mathrm{P}}}$. Thus, the effect of the "classical backreaction" on the curvature power spectrum is the introduction of features [29, 80], in particular a fixed-amplitude sinusoidal oscillation.[21] It has been shown [29, 76, 77] that in order for a correction of this type to be compatible with current CMB data for the curvature power spectrum, the amplitude $\delta n_s \equiv \frac{3\,\Lambda^4}{\epsilon_{V_*} V_*} \sqrt{\frac{2\pi}{\gamma_*}}$ (following the notation used in the literature) must verify $|\delta n_s| \lesssim 10^{-1}$ for axion monodromy inflation (see in particular Ref. [29]). In § 3.3, we shall see that this condition is possible to attain in our case for all considered inflationary potentials, roughly corresponding to the alternative condition $\left|\frac{\Lambda^4}{V_*}\right| \lesssim 10^{-5}$, which in general requires that the resonances be not too efficient at the start of inflation, although we have encountered some cases (namely, hilltop potentials [22, 81–83]) that seem to allow both an initially efficient resonance for χ (and to some extent for φ) and an agreement with observational data for all the CMB observables we considered (see § 3.3.2).

One might wonder whether we could simply have taken the uncorrected expression of the curvature power spectrum and substituted H_0 and $\dot{\phi}_0$ by the first order expansions of $\mathcal{H}$ and $\dot{\phi}$, respectively; following this less rigorous procedure would lead to a result similar to Eq. (2.4.59),

[21] Recall that in deriving Eq. (2.4.59) we took Λ^4 to be constant, which is of course an approximation. For a more general treatment taking into account the time-dependence of Λ^4, which we will not consider in this work, one could follow Ref. [79].

but without the factor $\sqrt{\frac{2\pi}{\gamma_*}}$. This is because the Mukhanov-Sasaki equation itself is altered by the presence of the sinusoidal modulation of the potential, in particular via the slow-roll parameters, as can be understood from Ref. [23].

Furthermore, it is pertinent to find whether the scalar spectral index suffers any alteration due to this contribution. Using Eq. (1.2.24) as the definition of $\tilde{n}_s$, we find that

$$\begin{aligned}
\tilde{n}_s - 1 &\equiv \frac{d\ln\tilde{\Delta}^2_{\mathcal{R}}(k)}{d\ln k} \\
&= (n_s - 1) - \frac{\dot{\phi}_0}{H_0}\frac{\frac{2}{M}\sin\left(\frac{2\,\phi_0(k)}{M}\right)}{\frac{\epsilon_{V_*}V_*}{3\,\Lambda^4}\sqrt{\frac{\gamma_*}{2\pi}} + \cos\left(\frac{2\,\phi_0(k)}{M}\right)} \\
&= (n_s - 1) - \frac{\frac{4}{\gamma}\sin\left(\frac{2\,\phi_0(k)}{M}\right)}{\frac{\epsilon_{V_*}V_*}{3\,\Lambda^4}\sqrt{\frac{\gamma_*}{2\pi}} + \cos\left(\frac{2\,\phi_0(k)}{M}\right)} \\
&\approx (n_s - 1) - \frac{4\,\delta n_s}{\gamma_*}\sin\left(\frac{2\,\phi_0(k)}{M}\right),
\end{aligned} \tag{2.4.60}$$

where n_s is the uncorrected scalar spectral index and where we have used the fact that during inflation and at horizon-crossing $\frac{d}{d\ln k} = (a_0 H_0)\frac{d}{d(a_0 H_0)} \approx a_0\frac{d}{da_0} = \frac{1}{H_0}\frac{d}{dt} = \frac{\dot{\phi}_0}{H_0}\frac{d}{d\phi_0}$, with $a_0 \propto e^{H_0 t}$. We have also set $\gamma = \sqrt{\frac{2}{\epsilon_{V_0}}}\frac{M}{M_{\rm P}}$ as before (notice that we absorbed a factor $\mathrm{sgn}(\dot{\phi}_0)$ as a phase in the sine, which we readily discarded). In the last equality we used the fact that $\frac{3\,\Lambda^4}{\epsilon_{V_*}V_*}\sqrt{\frac{2\pi}{\gamma_*}} \equiv \delta n_s \lessapprox 10^{-1}$ and we approximated $\gamma \approx \gamma_*$, since all the quantities in Eq. (2.4.60) are to be evaluated near the CMB pivot scale k_*. We clearly see that the scalar spectral index acquires a sinusoidal modulation around its uncorrected value. The amplitude of this oscillation is approximately constant and can be quite large (due to the γ_*^{-1} factor). However, due to the large frequency of the oscillation, it is likely that only the average value of $\tilde{n}_s - 1$ is relevant, similarly to what we concluded in § 2.4.1 regarding the backreacted slow-roll parameters, where we followed Ref. [58]. Proceeding similarly, we obtain (for a positive index), using the triangle inequality,

$$\tilde{n}_s = |\tilde{n}_s| \lessapprox n_s + \frac{g^2}{2\,(2\pi)^{3/2}}\frac{e^{\xi-q}}{\gamma^{3/2}}\left|\xi\,(3\eta_V - 2\epsilon_V) - 2q\,(\eta_V - \epsilon_V) - \frac{3}{2}\,(\eta_V - 2\epsilon_V)\right|, \tag{2.4.61}$$

where all quantities are to be evaluated at some time t_i near the CMB scale. This expression is not straightforward to evaluate, but it is clear that the average effect of the "classical back-reaction" on the scalar spectral index, and thus on the tilt of the curvature power spectrum, can still be non-negligible. We can also follow an alternative numerical approach where we plot the natural logarithm of Eq. (2.4.59) as a function of N_e, sample a sufficient number of points

and perform a linear fit, the slope of which we may take to be $\tilde{n}_s - 1$. The results of this procedure can be shown to be consistent with the ones obtained via the analytical approach leading to Eq. (2.4.61) for several choices of potential $V(\phi_0)$. It can also be shown that in some situations (i.e. for some potentials $V(\phi_0)$ and some values of the free parameters g and M) the effect of this backreaction can indeed significantly alter the uncorrected value of n_s, which may, for instance, cause problems in inflationary models for which this value is already compatible with observations. However, we shall see in § 3.3 that the effect of the "quantum backreaction" computed in the following subsection can compensate the one derived here and lead to some interesting results.

Moreover, one could try to analyse the impact of the "classical backreaction" on the running of n_s, but we have not considered this this in the present work. We will also not concern ourselves with the impact of this backreaction on the tensor-to-scalar ratio r, although this would also be interesting to analyse. In principle, the tensor-to-scalar ratio $\tilde{r}$ could eventually remain essentially unaltered and thus equal to r, since it only depends on the amplitudes of the power spectra at horizon-crossing: in the case of $\tilde{\Delta}^2_{\mathcal{R}}$, we may take the amplitude to be approximately given by an average of Eq. (2.4.59) over a period of the oscillation, similarly to what we did for the effective slow-roll parameters in § 2.4.1, which we found leads to a suppressed effect of the backreaction. Sure enough, a more rigorous treatment of this would be required.

Quantum contribution to $\Delta^2_{\mathcal{R}}(k)$

We may now study how the backreaction on the inflaton fluctuations affects the curvature power spectrum. For this, we shall ignore the backreaction on the classical inflaton field $\bar{\phi}$ (in keeping with the notation used in § 2.4.2). In the backreacted case, the relation between the power spectra of curvature perturbations and of inflaton fluctuations at horizon-crossing is again given by $\tilde{\mathcal{P}}_{\mathcal{R}}(k) = \left(\frac{H}{\dot{\bar{\phi}}}\right)^2 \tilde{\mathcal{P}}_{\varphi}(k)$, which leads to

$$\tilde{\Delta}^2_{\mathcal{R}}(k) \equiv \frac{k^3}{2\pi^2}\,\tilde{\mathcal{P}}_{\mathcal{R}}(k) = \left(\frac{H}{\dot{\bar{\phi}}}\right)^2 \left(\frac{H}{2\pi}\right)^2 e^{\,\xi_{\varphi}} = \Delta^2_{\mathcal{R}}(k)\, e^{\,\xi_{\varphi}}\,, \tag{2.4.62}$$

where $\Delta^2_{\mathcal{R}}(k)$ contains the observed power law behaviour. Thus, we have found that the backreaction only introduces an exponential factor on the amplitude of the power spectrum.

The scalar spectral index is also affected by the backreaction on the fluctuations. Using the same definition for n_s as before, we readily find

$$\begin{aligned}\tilde{n}_s - 1 \;&\equiv\; \frac{d\ln\tilde{\Delta}^2_{\mathcal{R}}(k)}{d\ln k} \\ &=\; (n_s - 1) \;+\; \frac{d\xi_\varphi}{dN_e} \\ &=\; (n_s - 1) \;+\; \xi_\varphi\left[2\xi\left(3\eta_V - 2\epsilon_V\right) - 4q\left(\eta_V - \epsilon_V\right) - \left(\eta_V - 2\epsilon_V\right)\right] ,\end{aligned} \tag{2.4.63}$$

where we used $\frac{d}{d\ln k} \approx \frac{1}{H}\frac{d}{dt} = \frac{d}{dN_e}$ (at horizon-crossing), as well as the results from Appendix A. Like Eq. (2.4.61), this expression is not straightforward to evaluate, and in principle it allows both an increase and a decrease of the scalar spectral index. A numerical approach analogous to the one described in the previous subsection may be followed as well, leading to a result for $\tilde{n}_s$ compatible with the one obtained in Eq. (2.4.63), but we will not present it in this work. If we take Eq. (2.4.63) and use for n_s the "classically corrected" value that can be obtained numerically, we are able to define a "globally corrected" scalar spectral index: this is done in § 3.3 for several potentials $V(\bar{\phi})$, where it is shown that this quantity is compatible with the measured value of this index [29]. We shall not concern ourselves with the impact of the "quantum backreaction" either on the running of n_s.

We may now briefly evaluate the effect of this backreaction on the tensor-to-scalar ratio, which is a rather straightforward computation. Since the power spectrum of tensor perturbations suffers no alteration due to either backcreation on ϕ, we immediately conclude from Eq. (2.4.62) that the tensor-to-scalar ratio acquires an exponential suppression due to the "quantum backreaction"

$$\tilde{r} \;\equiv\; \frac{\Delta^2_t(k_*)}{\tilde{\Delta}^2_{\mathcal{R}}(k_*)} \;=\; \frac{\Delta^2_t(k_*)}{\Delta^2_{\mathcal{R}}(k_*)}\, e^{-\xi_\varphi} \;=\; r\, e^{-\xi_\varphi} , \tag{2.4.64}$$

with r as defined in Eq. (1.2.33), and where we considered that the exponential factor integrates the amplitude of the corrected curvature power spectrum. Moreover, recall that this result was obtained after ignoring the "classical backreaction" on the tensor-to-scalar ratio, meaning that this quantity could be further altered by effects linked to the former. As was mentioned previously, we will not concern ourselves with that computation, but such a study would certainly be of interest.

For completeness, the full backreaction on the curvature power spectrum is thus obtained by combining Eqs. (2.4.59) and (2.4.62), resulting in

$$\tilde{\Delta}^2_{\mathcal{R}}(k) = \Delta^2_{\mathcal{R}}(k)\left[1 \;+\; \frac{3\,\Lambda^4}{\epsilon_{V_*} V_*}\sqrt{\frac{2\pi}{\gamma_*}}\,\cos\left(\frac{2\,\phi_0(k)}{M}\right)\right] e^{\,\xi_\varphi} , \tag{2.4.65}$$

where $\Delta^2_{\mathcal{R}}(k) = \Delta^2_{\mathcal{R}}(k_*)\left(\frac{k}{k_*}\right)^{n_s-1}$, with $\Delta^2_{\mathcal{R}}(k_*) = \left(\frac{H_*}{\dot{\phi}_*}\right)^2\left(\frac{H_*}{2\pi}\right)^2$ during inflation. In § 3.3, we plot this expression and its natural logarithm as functions of N_e for various uncorrected potentials and do a linear fit of the latter, thus finding a numerical "globally corrected" value of $\tilde{n}_s$. For some of the inflationary models considered, this value is found to be consistent with the semi-analytical one mentioned earlier in this subsection, and with the measured value of the scalar spectral index [29].

3 Numerical Results and Simulations

This chapter is concerned with the numerical study of our model. In it, we shall test its theoretical results for a selection of common inflationary models and compare them with observational data, primarily from the Planck Collaboration [4, 29]. All numerical computations were done using the software Wolfram Mathematica 12.0 [84].

3.1 General considerations

Before advancing into this study, however, we should note that during the construction and exploration of our mechanism, we imposed a few conditions on some quantities. We shall now list and review those conditions, so that we can figure out what restrictions they impose on our model's free parameters, g and M. Whenever possible, we will use experimental results to limit our parameter space; otherwise, we will employ theoretical predictions from each inflationary model we test, with the caveat that they may not be entirely consistent with observations.

The first condition we imposed was that of a narrow resonance on the EoM for $X_k(z)$ modes, i.e. $q < 1$ (cf. § 2.1.2). Since $q = \frac{1}{4\epsilon_V}\left(\frac{gM}{H}\right)^2\left(\frac{M}{M_\mathrm{P}}\right)^2$, we may write

$$\sqrt{g}\,M \;<\; \epsilon_V^{\frac{1}{4}}\sqrt{2\,M_\mathrm{P}H} \;\approx\; \sqrt{\frac{\pi}{2\sqrt{2}}\,r\sqrt{\Delta^2_{\mathcal{R}}(k_*)}}\;M_\mathrm{P}\,, \tag{3.1.1}$$

where we used $r \approx 16\,\epsilon_V$ and $r = \frac{2}{\pi^2}\frac{H^2}{M_\mathrm{P}^2}\frac{1}{\Delta^2_{\mathcal{R}}(k_*)}$, as obtained for single-field inflation (cf. Eqs. (1.2.30), (1.2.33) and (1.2.39)). Computing $\Delta^2_{\mathcal{R}}(k_* = 0.002\,\mathrm{Mpc}^{-1})$ via Eqs. (1.2.23) and (1.2.25), and using the current upper bound on the tensor-to-scalar ratio, $r_{0.002} < 0.044$, we obtain

$$\sqrt{g}\,M \;\lessapprox\; 10^{15}\,\mathrm{GeV}\,, \tag{3.1.2}$$

which is compatible with the condition (2.1.47) on $\langle m_\chi\rangle = gM$. We shall take these two conditions into account when selecting ranges or specific values for g and M in order to obtain our plots.

Later on, in the same subsection, we assumed an adiabatic behaviour for the Mathieu parameter $A_k(z)$, leading to the condition $\gamma \ll 1$, which, using $\gamma = \sqrt{\frac{2}{\epsilon_V}}\frac{M}{M_{\rm P}}$, we may rewrite as

$$M \ll \sqrt{\frac{\epsilon_V}{2}} M_{\rm P} \approx 2^{-\frac{5}{2}} \sqrt{r}\, M_{\rm P} \lessapprox 10^{16}\,\text{GeV}\,, \tag{3.1.3}$$

where we used $r \approx 16\,\epsilon_V$ and $r_{0.002} < 0.044$ again. We see that this condition can be easily verified if the condition for a narrow resonance, Eq. (3.1.2), is imposed.

We then imposed that these two quantities, q and γ, should be related by the inequality $\frac{q}{\gamma} > \pi$, in order to ensure that the mass $m_\chi(t)$ completes at least one oscillation inside the resonance band. This condition is easily shown to be equivalent to

$$g^{\frac{2}{3}} M > 2^{\frac{13}{6}} \pi \sqrt{\epsilon_V}\, (\Delta^2_{\mathcal{R}}(k_*))^{\frac{1}{3}}\, M_{\rm P}\,, \tag{3.1.4}$$

which is difficult to evaluate, since we only have an upper bound for $r \approx 16\,\epsilon_V$. Thus, we will postpone this evaluation to the sections where we deal with specific inflationary potentials (§§ 3.3.1 and 3.3.2), so we can directly use the values for ϵ_V predicted by each model and with those determine in which regions of our parameter space (g, M) the above condition holds. Notice that these regions are not be static, as ϵ_V varies throughout inflation.

Lastly, in § 2.4.1, we imposed the condition $|\phi_1| \ll \frac{M}{2}$, establishing our expectation that the scale of the backreaction on the field solution be small compared to the scale of the oscillation frequency of the modulation. This condition can be rewritten using the analytical solution for ϕ_1, given by Eq. (2.4.26), and the definition $\Lambda^4 \equiv -\frac{g^2 M^2}{4\pi^2}\left(\frac{H}{\gamma}\right)^2 e^{\,\xi - q}$ (where we evaluate all quantities at the CMB pivot scale), leading to

$$e^{\,\xi - q} \ll \frac{16\pi^2}{g^2}\,, \tag{3.1.5}$$

which sets an upper limit on the strength of our resonance, in particular on the number of χ particles that are produced via our mechanism, as per the discussion at the end of § 2.3, where we had already examined the lower bound on $e^{\,\xi}$ in order to have efficient χ production and/or detectable signs of its existence. Notice that the value on the right-hand side of the inequality can be rather large, as we are taking $g < 1$. However, in §§ 3.3.1 and 3.3.2, it can be seen that the above relation is generally true for all considered inflationary potentials. Moreover, we note that an almost identical condition would be attained by imposing that the Floquet solutions for the φ modes undergo a narrow resonance, i.e. $q_\varphi = \frac{g^2}{8\pi^2}\, e^{\,\xi - q} \ll 1$.

Apart from these conditions, there are a few approximations that must be checked, namely that the B regime dominates $\tilde{n}_\chi$, ρ_χ and $\langle\chi^2\rangle$, as stated in §§ 2.2, 2.3 and 2.4.1, respectively. Moreover, we must verify whether the energy density of the Universe is dominated by ρ_ϕ until the end of inflation, i.e. whether the condition $\rho_\phi > \rho_\chi$ holds during the entire inflationary epoch (or at least until near its end). Since these relations depend on the inflationary model we select, we need also defer their testing to §§ 3.3.1 and 3.3.2. There, we find that our parameter space (g, M) becomes restricted to smaller values of both g and M when we impose $\rho_\phi > \rho_\chi$, and conclude that the B regime indeed dominates the three aforementioned quantities in the acceptable region of the parameter space.

Furthermore, given that all quantities vary due to slow-roll dynamics, we should ensure that the conditions we have set remain valid during the entire inflationary period. However, since the variation due to slow-roll is quite limited (cf. Appendix A), this will generally not be a problem. For instance, taking the narrow resonance condition for the χ modes as an example, one may produce plots similar to those in §§ 3.3.1 and 3.3.2 to see that even for inflaton models in which q grows, in the majority of the interesting regions of parameter space the value of q remains smaller than unity throughout inflation.

Now that we have established most conditions on our free parameters, we can start dealing with the actual numerical computations.

3.2 Numerical solution of the Mathieu equation

We may compare our analytical expression in Eq. (2.2.11) with an equivalent expression obtained by numerically solving the Mathieu equation from (2.1.25). This procedure produces a numerical solution $X_k(z)$ that can be used to calculate a numerical version of $\ln\left[2\tilde{n}_k(z)+1\right]$, through

$$\ln\left[2\tilde{n}_k(z)+1\right] \equiv \ln\left[\frac{k_{c,\mathrm{phys}}^2}{\omega_k}\left|X_k'(z)\right|^2 + \omega_k\left|X_k(z)\right|^2\right], \tag{3.2.1}$$

where the primes denote differentiation with respect to $z = \frac{2H}{\gamma}t$, and where we used Eq. (2.2.7) and the fact that $\dot{X}_k = \frac{2H}{\gamma}X_k' = k_{c,\mathrm{phys}}\,X_k'$. In fact, inside the resonance band the modes are relativistic and $\omega_k \approx \frac{2H}{\gamma}$, but we will not make this approximation in the present numerical treatment.

For the analytical approximation, we shall consider the case where $z_s = z_1(k)$ and $z_e = z$, so that (2.2.11) becomes

$$\ln\left[2\tilde{n}_k(z)+1\right] \;=\; \frac{q^2}{2\gamma}\left[\frac{\pi}{2}+\arcsin\left[\frac{\gamma}{q}(z-z_c)\right]+\frac{\gamma}{q}(z-z_c)\sqrt{1-\left(\frac{\gamma}{q}\right)^2(z-z_c)^2}\right], \qquad (3.2.2)$$

where in this case we have indeed set the factor $\frac{\omega_k}{\omega_k^0}$ to unity, since this expression describes k modes that have entered the resonance band at $z_1(k)$ and will exit it at $z_2(k)$, between which instants $\omega_k \approx \omega_k^0 = \frac{2H}{\gamma}$ and the right-hand side of (3.2.2) is real.

The plot in Figure 3.2.1 was obtained for a mode with $k = 10^{22}$ GeV and having considered a quartic hilltop inflationary potential with $\phi_i = 7\,M_{\rm P}$ and $\kappa = 10^{-4}$ (see § 3.3.2 for details). We considered $\epsilon_V \approx 0.0007$, which is the value of this parameter at the start of inflation under the specified conditions. Moreover, we chose $g = 0.25$ and $M = 1.3 \times 10^{15}$ GeV, so that we consider this case to represent an efficient resonance (cf. § 3.3.2, in particular Figure 3.3.18a). Similar plots can be obtained for other values of these quantities, but we show this particular case since the resonance attained here was quite marked. The initial values of X_k and X_k' are given by Eq. (2.2.2), resulting in $X_k(z = z_1(k)) = \frac{1}{\sqrt{2k_{c,\rm phys}}}$ and $X_k'(z = z_1(k)) = -\frac{i}{\sqrt{2k_{c,\rm phys}}}$, with $k_{c,\rm phys} = \frac{2H}{\gamma}$, if we employ the approximations suggested in that appendix.

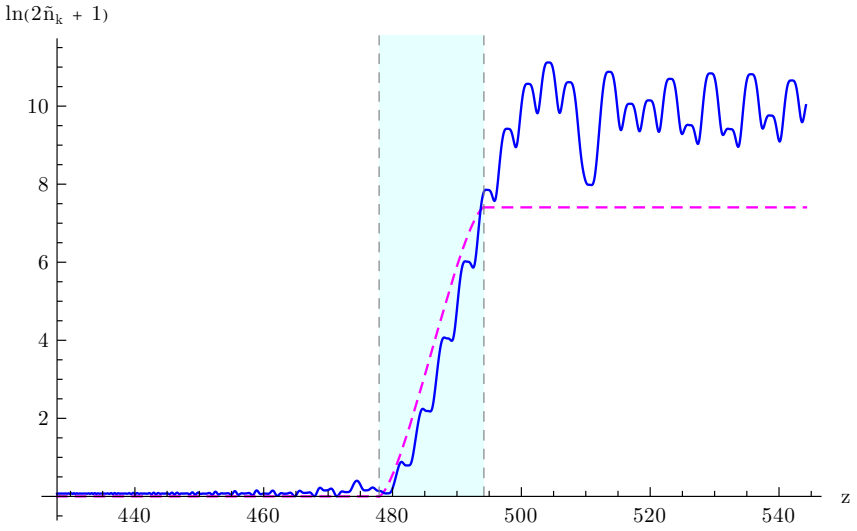

Figure 3.2.1: Graphical representation of the numerical (solid blue line) and approximate analytical (dashed magenta line) solutions to the Mathieu equation (2.1.25) for a mode with comoving momentum $k = 10^{22}$ GeV, considering an efficient resonance, i.e. for $g = 0.25$ and $M = 1.3\times10^{15}$ GeV. The shaded region represents the period this mode is inside the first resonance band, with the vertical dashed lines being placed at $z_1(k)$ and $z_2(k)$.

Analysing the plot from Figure 3.2.1, we can see the evolution of the comoving particle number $\tilde{n}_k(z)$ for a certain mode k as it crosses the entire first resonance band. Before entering the band, the comoving particle number obtained numerically oscillates near $\tilde{n}_k = 0$, since

no χ particles have been produced by the resonance by then; notice that in the analytical approximation the oscillation is absent, as $X_k(z)$ assumes a simple plane wave solution during that time. When the mode enters the resonance band at $z_1(k)$, the solution for $X_k(z)$ acquires a non-oscillating exponential factor, due to the Floquet exponent from Eq. (2.1.32) becoming real-valued. Thus, from $z_1(k)$ to $z_2(k)$, the comoving particle number grows rapidly from $\tilde{n}_k = 0$ to some non-zero value, where it stabilises as the mode exits the resonance band and the Floquet exponent becomes imaginary again, causing the regular oscillatory behaviour of $X_k(z)$ to resume (the oscillation being again absent in the analytical case).

Moreover, it appears that the approximate analytical expression is consistent with the one resulting from the numerical solution of the Mathieu equation while the mode is inside the resonance band, although the analytical approximation slightly overestimates the solution obtained numerically. Once the mode exits the band, however, our analytical estimate becomes less accurate and leads to a more significant underestimation of the numerical solution, although the difference between the two (in terms of their orders of magnitude) is still not very large. We may thus consider the analytical approximation to be successful in describing the main behaviour of the true solution. This was attained for a specific inflationary model, but proceeding similarly for other models (in particular, the ones considered in § 3.3) produced equally reasonable results.

We could follow a similar procedure for the backreacted quantum fluctuations of the inflaton field, which also obey a Mathieu equation, as we derived in § 2.4.2. In general, a less pronounced resonance should be attained for the same sets of parameters used for the χ case, since, as we shall see in § 3.3, the resonance for φ tends to be narrower.

3.3 Probing specific inflationary potentials

In order to further illustrate and explore the dynamics of our model, we will now consider specific inflaton models to work with. We shall see that different choices for $V(\phi)$ will produce distinct effects and signals. We will focus on two of the simplest families of potentials (monomial potentials and hilltop potentials), but many other selections are also possible (see e.g. [22, 85]). The majority of the following is dedicated to numerical computations, whose results are compared to their analytical counterparts whenever possible, but some model-specific theoretical computations are also included. In this study, two types of plots were used: region plots of our parameter space (g, M), and plots displaying the time evolution of physical quantities during inflation.

The region plots were produced by imposing some of the conditions listed in § 3.1, and while

the range for g is always taken to be $[0,1]$, the chosen range for M will not be the same for all families of potentials (as can be understood from Eq. (2.1.47)). Moreover, we compute these plots in two distinct times, in order to capture how they change throughout inflation.

In order to determine how the relevant physical quantities evolve in time for each choice of potential, we numerically solved Eqs. (2.4.13) and (1.2.4) for the dynamics of the inflaton field with and without backreaction, respectively; in both cases, we performed a change of variable from t to N_e and considered the full inflaton (and so time) dependence of all participating quantities, namely $H = H(\phi)$ and $\Lambda^4 = \Lambda^4(\phi)$. The solutions to these two equations were then plugged into the ϕ-dependent expressions for each relevant quantity, which were then plotted against N_e. With this procedure, we were able to account for and analyse the adiabatic variation of quantities like H, q, ξ and Λ^4, among others, which up to this point had for the most part been considered constant when doing calculations. Although we do not show it here explicitly, the solutions obtained analytically for these equations (most importantly the solution of Eq. (2.4.27)) very closely match the ones computed numerically, which further proves that the adiabatic approximations we considered for some quantities are perfectly valid.

In the following, the subscripts i and f refer to quantities evaluated at the beginning and at the end of inflation, respectively (in our numerical computations, we set inflation to begin at $N_e = 0$). Moreover, note that we use the same initial conditions for both the uncorrected and the backreacted EoM. Since we are dealing with second-order ordinary differential equations, we require two initial conditions per equation. In particular, the initial condition on the field derivatives depends on the selected inflationary model and can be expressed using the uncorrected Klein-Gordon equation in the slow-roll approximation, Eq. (1.2.5b), here re-derived in terms of N_e

$$\phi_i' \equiv \phi'(N_e = 0) = -M_{\rm P}^2 \frac{V_{,\phi}(\phi_i)}{V(\phi_i)}\,, \tag{3.3.1}$$

where the prime denotes differentiation with respect to N_e and $\phi_i \equiv \phi(N_e = 0)$ is set by the initial condition on the fields, which is chosen to produce the required number of e-folds of accelerated expansion in the case without backreaction.

3.3.1 Monomial potentials (large-field models)

Let us then consider the class of one-parameter, large-field models defined by potentials of the form [22]

$$V(\phi) = \lambda\phi^n\,, \tag{3.3.2}$$

which are the canonical example of the *chaotic inflation* paradigm [3, 13, 16, 22]. Note that even though we refer to these potentials as monomials, we may not restrict ourselves to integer values of n. It is possible to show [22] that in this scenario we have

$$\epsilon_V = \frac{n^2}{2}\left(\frac{M_\mathrm{P}}{\phi}\right)^2 \tag{3.3.3a}$$

$$\eta_V = n(n-1)\left(\frac{M_\mathrm{P}}{\phi}\right)^2 \tag{3.3.3b}$$

and

$$N_e \approx \frac{1}{2n}\left[\left(\frac{\phi_i}{M_\mathrm{P}}\right)^2 - \left(\frac{\phi_f}{M_\mathrm{P}}\right)^2\right] \tag{3.3.4a}$$

$$\frac{\phi_f}{M_\mathrm{P}} = \frac{n}{\sqrt{2}}\,, \tag{3.3.4b}$$

where Eq. (3.3.4a) is the duration of inflation in e-folds, computed using Eq. (1.2.8), and Eq. (3.3.4b) is the solution to $\epsilon_V = 1$.

Applying Eq. (3.3.3) to the results of Appendix A, we find

$$\frac{q'}{q} = n(n-2)\left(\frac{M_\mathrm{P}}{\phi}\right)^2 \tag{3.3.5a}$$

$$\frac{\gamma'}{\gamma} = -n\left(\frac{M_\mathrm{P}}{\phi}\right)^2 \tag{3.3.5b}$$

$$\frac{\xi'}{\xi} = 2n(n-\frac{3}{2})\left(\frac{M_\mathrm{P}}{\phi}\right)^2\,. \tag{3.3.5c}$$

We see that, for all non-negative values of n, γ decreases during inflation, ensuring that the variation of $A_k(z)$ stays adiabatic. However, only when $n \leqslant 2$ does q decrease or remain constant during inflation (assuming n to be positive), the equality being achieved for the quadratic potential; this means that for some monomial potentials (for $n > 2$) the value of q increases throughout inflation, possibly leading to a broad resonance regime, in which case our analysis ceases to be valid. For ξ, we must ensure that $n \geqslant \frac{3}{2}$ for it to increase or remain constant during inflation, thus maintaining the effectiveness of the resonance. Nonetheless, the values of the three quantities in Eq. (3.3.5) are small, meaning that q, γ and ξ vary little during inflation.

Accordingly, even if q does increase in that time, we may not necessarily enter a broad resonance regime, invalidating our results. Likewise, even if ξ does decrease during inflation, this may not inevitably lead to a regime of inefficient resonance and therefore negligible particle production (recall the discussion at the end of § 2.3). Thus, these seemingly counterproductive cases may not be troublesome for our model in the end.

As we saw in § 1.2.1, the CMB observables n_s and r acquire simple approximate expressions in terms of the potential slow-roll parameters ϵ_V and η_V evaluated at the beginning of inflation, near the CMB pivot scale, cf. Eqs. (1.2.27) and (1.2.37b). In this class of models, using Eq. (3.3.3), we may obtain alternative expressions, now in terms of the number of e-folds from Eq. (3.3.4a)

$$n_s - 1 \approx -\frac{2+n}{2\,N_e} \tag{3.3.6a}$$

$$r \approx \frac{4n}{N_e}\,, \tag{3.3.6b}$$

which immediately allows us to conclude that the predicted values for r are at least $\mathcal{O}(10^{-1})$, and so are too large to be compatible with observations [29]. This overestimation of the value of r is a common feature of this class of models, and is the main reason why these have been mostly abandoned as potential choices for $V(\phi)$. In spite of this, and given the historical importance of this family of potentials, we shall explore the results of our theory for a few values of n, primarily as instructive examples. In particular, we will focus on the two cases of greatest importance, the quadratic potential ($n = 2$) and the quartic potential ($n = 4$)[22].

In the ensuing numerical treatment, the value of the coupling λ is set by the measured amplitude of the curvature power spectrum $\Delta^2_{\mathcal{R}}(k_*)$ (we will consider $k_* = 0.05$ Mpc^{-1} and use the value for the power spectrum quoted in Ref. [29] for this pivot scale (see also Eq. (1.2.25a)), $\Delta^2_{\mathcal{R}}(k_* = 0.05\ \text{Mpc}^{-1}) = 2.099 \times 10^{-9}$), which is related to the value of the inflaton field at k_* (cf. Eq. (1.2.26)), which we take to be ϕ_i; the resulting expression for λ is then

$$\lambda = 12n^2\pi^2\,\Delta^2_{\mathcal{R}}(k_*)\,\frac{M_{\rm P}^6}{\phi_i^{n+2}}\,. \tag{3.3.7}$$

[22]The limiting case for which ξ is constant, the potential with $n = \frac{3}{2}$, would also be interesting to explore, but since it produces similar results we refrain from including it here.

Quadratic monomial potential $(n = 2)$

Since its introduction as a candidate for $V(\phi)$ within the single-field inflation paradigm [22, 86], the quadratic potential was able to remain somewhat undisturbed in the spotlight of inflationary research, both due to its naturalness and simplicity (surely, it corresponds to a simple scalar mass term), and to its ability to align with CMB data for the scalar spectral index n_s, for which it predicts a range of values perfectly consistent with observations [29]. However, its failure in predicting the value of the tensor-to-scalar ratio r, greatly overestimating its magnitude, like all monomial potentials, has driven physicists away from it. Its remaining hope would be to somehow reduce the weight of tensor perturbations, or equivalently increase the weight of scalar perturbations, leading to a smaller value for r. If we take a look at Eq. (2.4.64), we see that with our model we might be able to attain this desired behaviour, and thus bring quadratic monomial inflation back to the table, as long as the φ resonance parameter ξ_φ is large enough to allow this. However, since a GW spectrum is also expected to be generated by the χ particles [25, 26, 47], the weight of tensor perturbations and consequently the predicted value of r should increase even more. Moreover, while the "classical backreaction" on r, which we did not account for, could eventually improve this prediction, it is unlikely that it will be sufficient for the quadratic model to match observations. In any case, we shall test our theoretical results using this potential choice.

For this model, considering $\phi_i = 15\, M_\mathrm{P}$, the region plots were computed in the range $0 < g < 1$ and 10^{15} GeV $< M < 10^{16}$ GeV at two different times, corresponding to two distinct values of the slow-roll parameter ϵ_V, which were taken to be $\epsilon_V \approx 0.009$ (which is the initial value of this parameter for $\phi_i = 15\, M_\mathrm{P}$) and $\epsilon_V = 0.5$ (which is attained at a later stage of slow-roll evolution). The obtained plots can be found in Figure 3.3.1.

The shaded areas correspond to regions of parameter space that were excluded due to satisfying either of the conditions $\frac{q}{\gamma} < \pi$ or $\rho_\chi > \rho_\phi$. The condition $\gamma > 1$ was found to be non-restrictive, in accordance with Eq. (3.1.3), while $q > 1$ coincides almost perfectly with $\rho_\chi > \rho_\phi$ and so was not plotted. Contour lines for the χ resonance parameter ξ are also drawn (for $0 \leqslant \xi \leqslant 15$). We thus see that there exists a significant region of parameter space where all the required conditions are met. Moreover, it was found (but is not included here) that in roughly the entirety of this acceptable region, the B regime dominates $\tilde{n}_\chi$, ρ_χ and $\langle\chi^2\rangle$, meaning that the approximations done in §§ 2.2, 2.3 and 2.4.1 are valid[23]. We also note that from $\epsilon_V \approx 0.009$ to $\epsilon_V = 0.5$ the acceptable region slightly shifted towards smaller values of g and

[23] Even in the regions of parameter space where the B regime does not dominate, its contributions are comparable to those of regime C, so that the error we incur on is negligible.

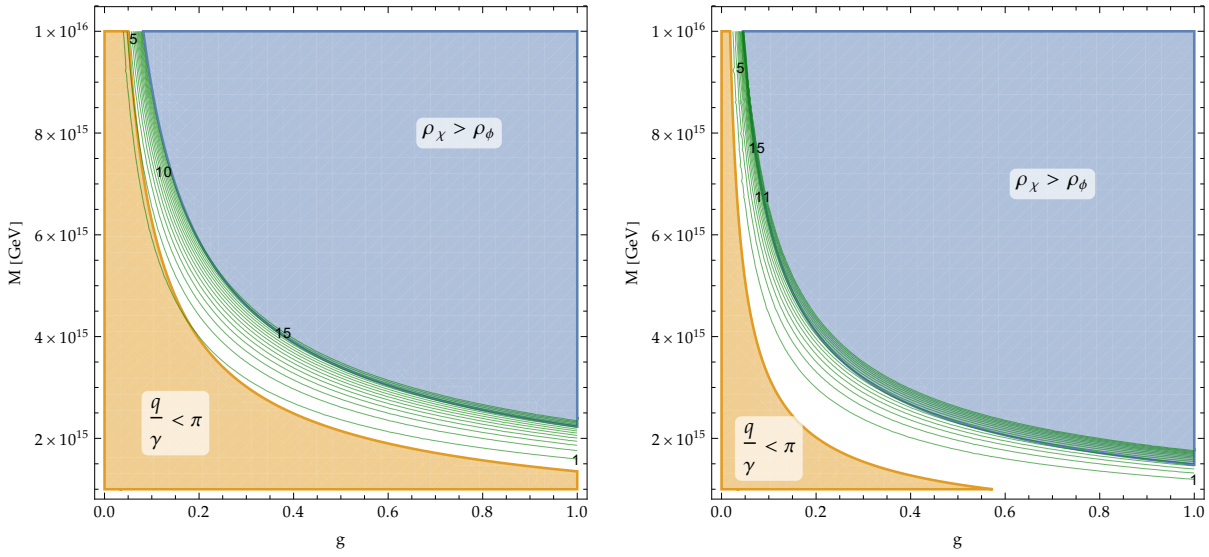

(a) (b)

Figure 3.3.1: Parameter space (g, M) for the quadratic monomial potential with $\phi_i = 15\,M_{\mathrm{P}}$, for two values of the slow-roll parameter ϵ_V: (a) $\epsilon_V \approx 0.009$ and (b) $\epsilon_V = 0.5$. The acceptable region not excluded by the conditions $\frac{q}{\gamma} < \pi$ (orange) and $\rho_\chi > \rho_\phi$ (blue) is shown in white. Contour lines (as well as some values) for the resonance parameter ξ (for $0 \leqslant \xi \leqslant 15$) are shown in green.

M, meaning that we must be careful when picking values for these parameters, so as to avoid entering excluded regions as inflation progresses: for instance, if we start inflation within the acceptable region, eventually the condition $\rho_\chi < \rho_\phi$ might cease to be verified, as we enter the region where $\rho_\chi > \rho_\phi$ (which is not necessarily problematic if it occurs sufficiently late in the slow-roll regime, as we shall discover).

We may now proceed to the time evolution plots. We again take $\phi_i = 15\,M_{\mathrm{P}}$, allowing us to get about 56 e-folds of uncorrected inflation, leading to $n_s \approx 0.9643$ and $r \approx 0.143$, the former being compatible with CMB data, see Eqs. (1.2.25b) and (1.2.34a), and Ref. [29]. We also choose the values $g = 0.33$ and $M = 3 \times 10^{15}$ GeV for our free parameters, which, as we can see in Figure 3.3.1a, are acceptable at the start of inflation.

In Figure 3.3.2, we show how the quantities q, γ and ξ evolve throughout inflation, as well as the energy densities of ϕ and χ (the latter being given by Eq. (2.3.21)).

As per Eq. (3.3.5a), q assumes a constant value and verifies the narrow resonance condition. Moreover, the γ parameter indeed decreases and is much smaller than unity throughout inflation, thus verifying the adiabaticity condition, while the ξ parameter is large enough to ensure a rather efficient resonance, in fact increasing during inflation, as expected. The energy density of the inflaton strictly decreases as inflation develops, while that of the χ field strictly increases,

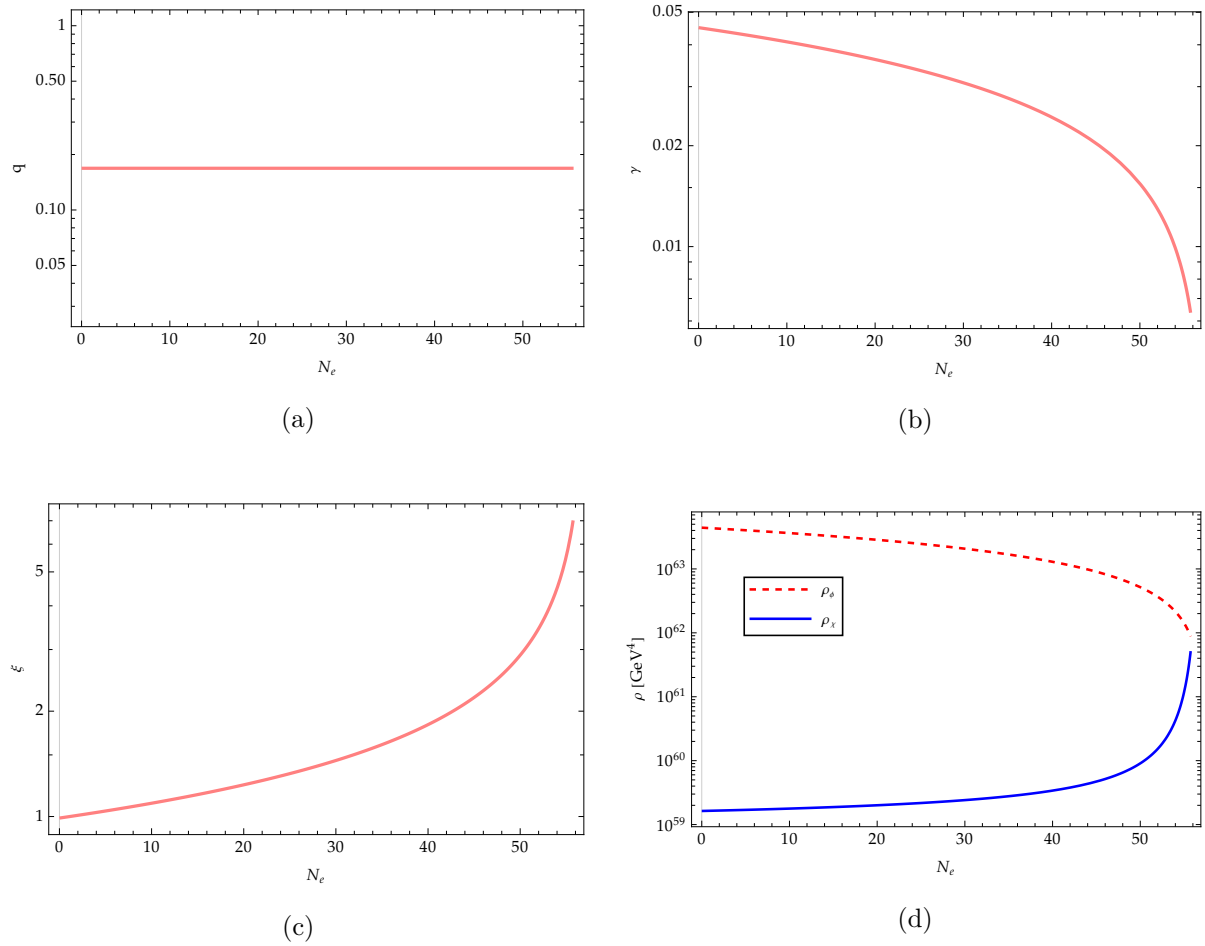

Figure 3.3.2: Evolution of the parameters (a) q, (b) γ and (c) ξ, and of (d) the energy densities ρ_χ and ρ_ϕ for the quadratic monomial potential with $\phi_i = 15\, M_{\rm P}$ and model parameters $g = 0.33$ and $M = 3 \times 10^{15}$ GeV.

becoming comparable to ρ_ϕ by the end of inflation. This points to a possible graceful exit from inflation, where the accelerated expansion is terminated naturally as the energy density is overtaken by another field, in this case χ, also a scalar.

In Figure 3.3.3a, we plot the classical inflaton field solution in the uncorrected and in the backreacted case. We immediately see that the backreacted field solution appears to perfectly follow the uncorrected solution, as we expected from Eq. (2.4.27). Moreover, in Figure 3.3.3b, we display the effective inflaton potential as a function of the field solution, as defined in Eq. (2.4.14a). As inflation progresses and the inflaton field takes smaller and smaller values, it rolls down its potential curve, eventually reaching the region where the oscillations become non-negligible. Additionally, in Figure 3.3.3c we plot the ratios $\left|\frac{\Delta V}{V}\right|_{\rm max}$, $\left|\frac{\Delta V'}{V'}\right|_{\rm max}$ and $\left|\frac{\Delta V''}{V''}\right|_{\rm max}$ as functions of the number of e-folds, whereby we conclude that the relation derived in Appendix C.2 is indeed verified numerically. Moreover, the bounds on $\left|\frac{\Delta V}{V}\right|_{\rm max}$ from Refs. [29, 76, 77]

are indeed verified at horizon-crossing of CMB scales, in particular the most constraining one, $\left|\frac{\Delta V}{V}\right|_{\max} \lesssim 3 \times 10^{-5}$, from Ref. [76].

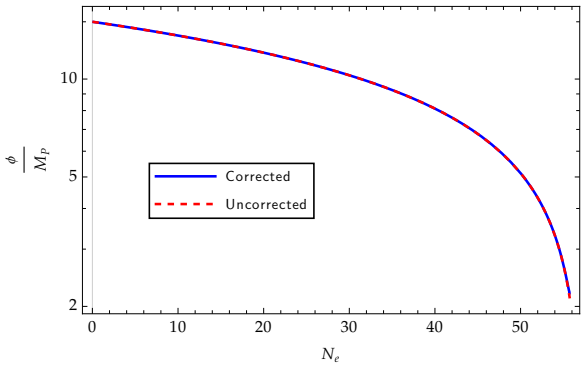

(a)

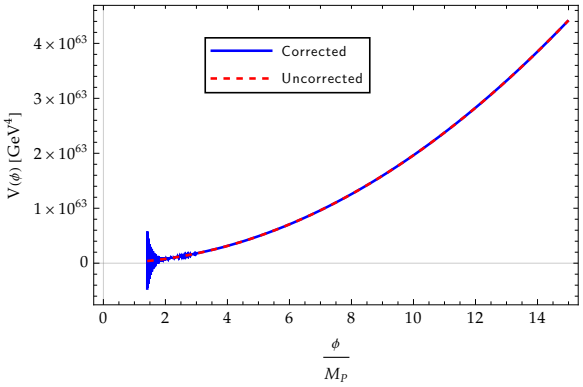

(b)

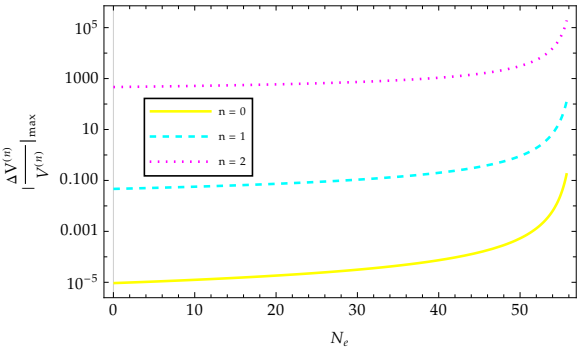

(c)

Figure 3.3.3: Evolution of (a) the corrected and uncorrected ϕ field solutions and of (c) the ratios $\left|\frac{\Delta V^{(n)}}{V^{(n)}}\right|_{\max}$, as well as (b) the corrected and uncorrected potentials plotted as functions of ϕ, for the quadratic monomial potential with $\phi_i = 15\, M_{\rm P}$ and model parameters $g = 0.33$ and $M = 3 \times 10^{15}$ GeV.

Let us now see what happens to the slow-roll parameters, in particular to ϵ_H and $|\eta_H|$ (which, as we know, are equal to ϵ_V and η_V during slow-roll). In Figures 3.3.4a and 3.3.4b, we simultaneously show the uncorrected and the effective Hubble slow-roll parameters, while in Figures 3.3.4c and 3.3.4d we display the average effect of the correction on those parameters, computed using Eqs. (2.4.35) and (2.4.44).

We observe that the backreaction introduces large-amplitude oscillations on both slow-roll parameters, which, as we mentioned before, clashes with the unchanged behaviour of the backreacted inflaton seen in Figure 3.3.3a. However, as seen in the plots above, the average behaviour of the correction on the slow-roll parameters, in particular on ϵ_H, is quite suppressed, thus explaining the minimal alteration observed on the field solution. Furthermore, the analysis of

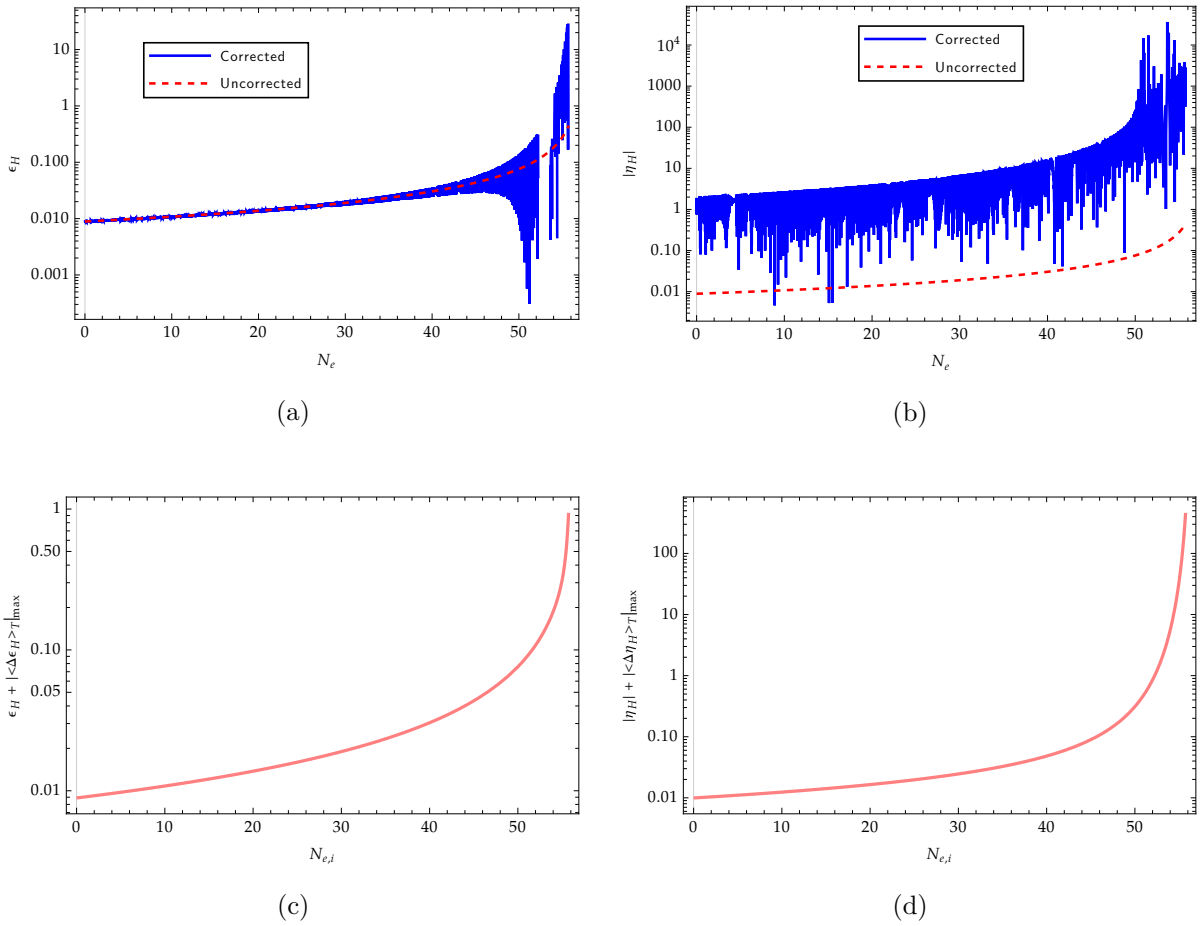

Figure 3.3.4: Evolution of the corrected and uncorrected Hubble slow-roll parameters (a) ϵ_H and (b) $|\eta_H| = \eta_H$, as well as their average corrections (c) $\epsilon_H + |\langle\Delta\epsilon_H\rangle_T|_{\max}$ and (d) $|\eta_H| + |\langle\Delta\eta_H\rangle_T|_{\max}$ plotted as functions of the average centre $N_{e,i}$, for the quadratic monomial potential with $\phi_i = 15\,M_{\rm P}$ and model parameters $g = 0.33$ and $M = 3 \times 10^{15}$ GeV.

these plots allows us to conclude that, for the chosen values of g, M and ϕ_i, we get roughly the same 56 e-folds of inflation in the case with backreaction (i.e. the backreaction does not seem to lead to a premature ending of inflation; there is, of course, a slight anticipation, since the average correction added to either slow-roll parameter is non-zero).

In Figure 3.3.5, we show the temporal evolution of the φ resonance parameters q_φ and ξ_φ, where we see that they are clearly suppressed relative to their analogues q and ξ (notice that this may not always be the case, as q_φ depends exponentially on the value of ξ).

Moreover, in Figure 3.3.6a, we plot the curvature power spectra defined by Eqs. (1.2.22b) and (2.4.59), respectively the uncorrected spectrum and the fully corrected spectrum (the plots are over the first 10 e-folds of inflation, which is roughly the interval of relevance for CMB observables). The amplitude of the oscillating part is consistent with the bounds from Refs. [29, 76, 77], imposed on $\left|\frac{\Delta V}{V}\right|_{\max}$. Since the definition of the scalar spectral index assumes a

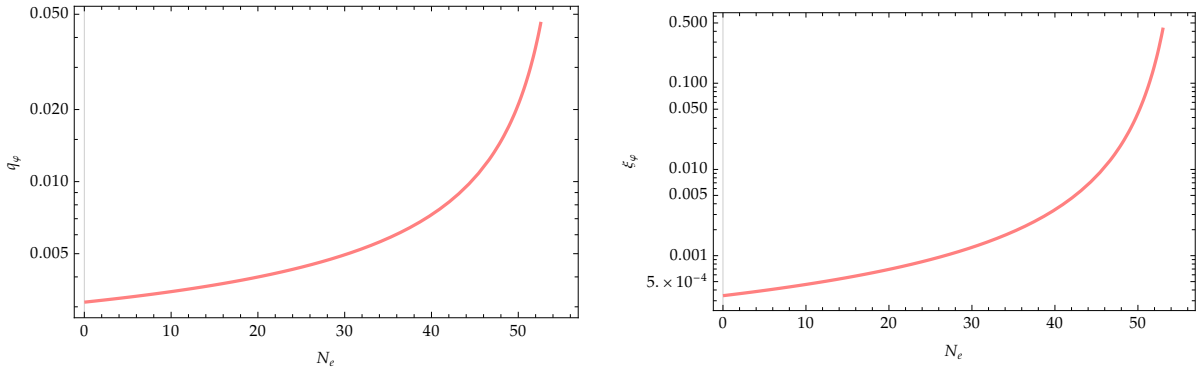

(a) (b)

Figure 3.3.5: Evolution of the φ resonance parameters (a) q_φ and (b) ξ_φ for the quadratic monomial potential with $\phi_i = 15\, M_{\rm P}$ and model parameters $g = 0.33$ and $M = 3 \times 10^{15}$ GeV.

power law behaviour for the power spectrum, we may determine its value by performing a linear fit to the natural logarithm of the power spectrum and retrieving the resulting slope, as shown in Figure 3.3.6b.

This procedure results in a value for the backreacted scalar spectral index, $\tilde{n}_s \approx 0.9612$, that is also consistent with observations, see Eq. (1.2.25b) and Ref. [29]; in fact, this value is quite close to the uncorrected n_s, meaning that the overall backreaction produces little effect on this observable (in particular, both the χ and the φ resonance parameters are quite small), which can bee seen in Figure 3.3.6b by the fact that the linear fit and the uncorrected spectrum coincide almost perfectly. Other values for ϕ_i, g and M produce equally good predictions for the scalar spectral index. As for the tensor-to-scalar ratio, in Figure 3.3.6c we plot (also over the first 10 e-folds of inflation) the "quantum-backreacted" version $\tilde{r}$ from Eq. (2.4.64) against the uncorrected version r, given by Eq. (1.2.33), and confirm that the two are essentially equal and so incompatible with observations (cf. Eq. (1.2.34a)), as expected from the smallness of the φ resonance parameters; thus, the effect of the χ particles appears to be insufficient to make the quadratic model's prediction for the tensor-to scalar ratio align with experimental data. We may try to increase the values of ϕ_i, g and M so as to get a larger number of e-folds of inflation (making r decrease) and a smaller exponential $e^{-\xi_\varphi}$ suppressing $\tilde{r}$. However, we find that for some larger values of g and M the backreacted inflaton field solution becomes constant a certain number of e-folds before N_e (given by Eq. (3.3.4a)), that number growing with the magnitudes of g and M; this can be seen in the plots from Figures 3.3.7a and 3.3.7b, which were computed using $g = 0.4$ and $g = 0.45$, while keeping all other parameters the same, and were plotted until the condition $\epsilon_H + |\langle \Delta\epsilon_H \rangle_T|_{\rm max} = 1$ was verified in each case.

This unexpected behaviour can be understood by looking at Figures 3.3.7c and 3.3.7d, which

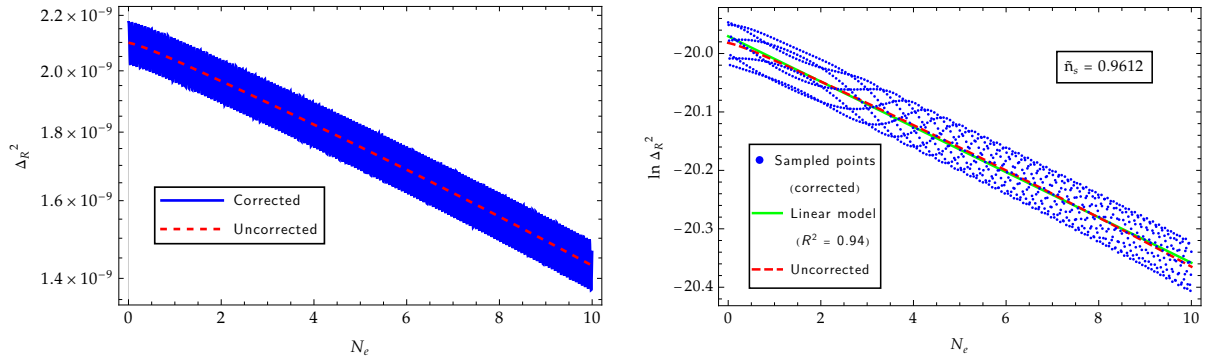

(a)

(b)

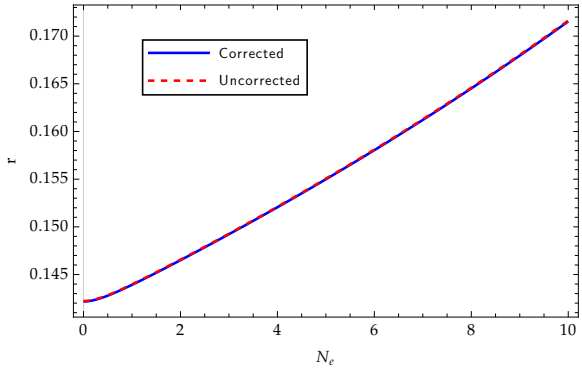

(c)

Figure 3.3.6: Evolution (over the initial 10 e-folds of inflation) of the CMB observables (a) $\Delta^2_{\mathcal{R}}$ and (c) r (both their corrected and uncorrected versions) for the quadratic monomial potential with $\phi_i = 15\,M_{\rm P}$ and model parameters $g = 0.33$ and $M = 3\times10^{15}$ GeV. In (b) we perform a linear fit to $\ln\Delta^2_{\mathcal{R}}$ and display the obtained R^2 coefficient, as well as the obtained value for $\tilde{n}_s$.

show the effective potential as a function of ϕ for the two alternative parameter values, $g = 0.4$ and $g = 0.45$. We see that the field rolls down its potential, driving accelerated expansion, until it reaches a region where the oscillations become non-negligible. If the oscillations are small enough to allow the inflaton to climb the potential wall they induce, then inflation is able to continue; if, instead, the oscillations are too large ($\sim \mathcal{O}(\dot{\phi}^2)$), the inflaton's kinetic energy may be insufficient to overcome the potential wall and the field gets stuck in a local minimum, assuming a constant value. We must be wary of this result, however: as the inflaton gets stuck and its value stops changing, the ϕ-dependent mass of the χ field, $m_\chi(t) \propto \sin\left(\frac{\phi(t)}{M}\right)$, stops oscillating and so the parametric resonance driving χ production terminates. Since this resonant phenomenon is what originates the correction to the inflaton potential, which would then be absent, and since this correction is responsible for the apparent constancy of ϕ, we must conclude that this behaviour is fictitious and does not have any physical significance; that is, our model breaks down and

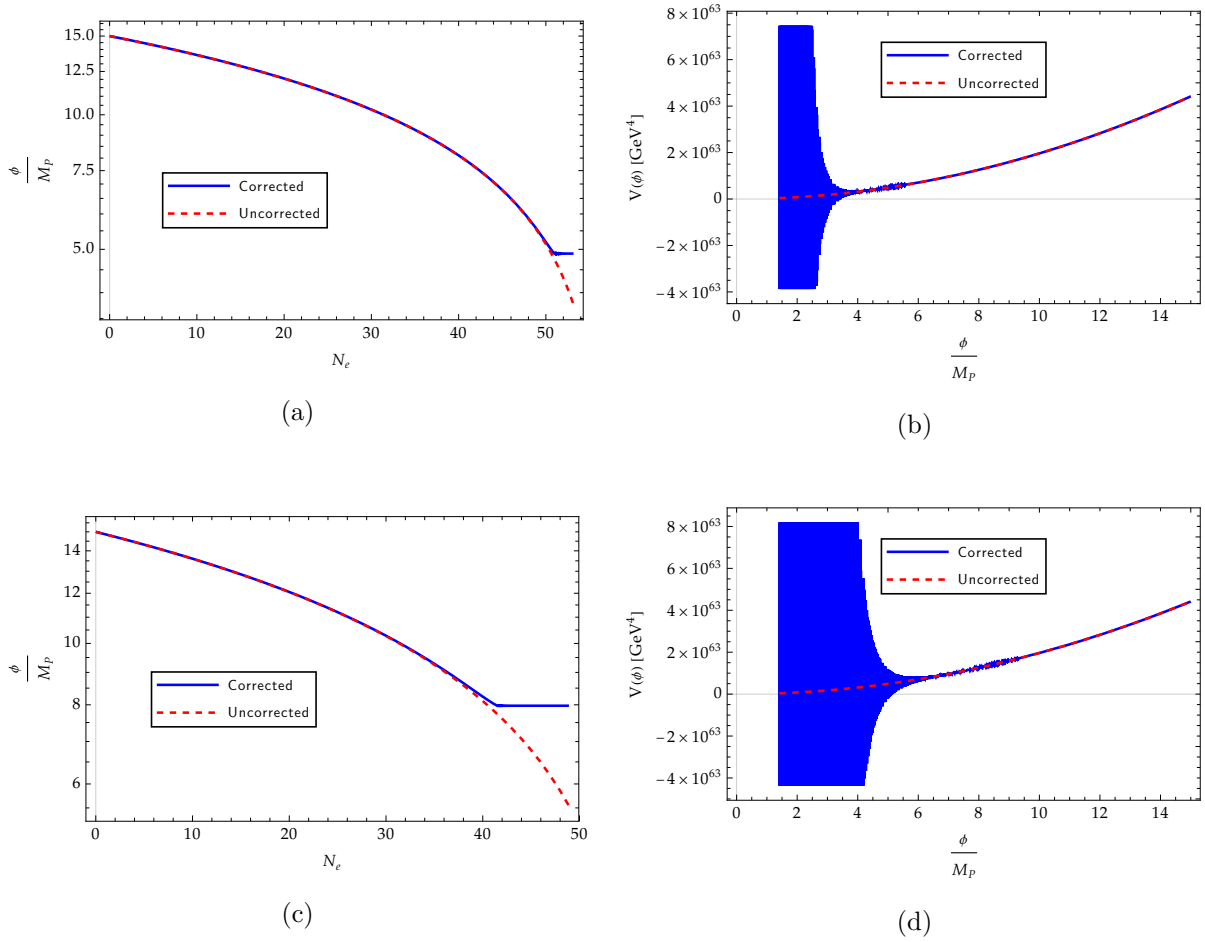

Figure 3.3.7: Evolution (until $\epsilon_H + |\langle \Delta\epsilon_H \rangle_T|_{\max} = 1$) of the corrected and uncorrected ϕ field solutions for (a) $g = 0.4$ and (c) $g = 0.45$, as well as the corresponding corrected and uncorrected potentials as functions of the field value ϕ, respectively (b) and (d). Obtained for the quadratic monomial potential with $\phi_i = 15\, M_{\rm P}$ and model parameter $M = 3 \times 10^{15}$ GeV.

loses its validity before the end of inflation.[24] Perhaps some kind of modification could alleviate this effect, but we have yet to research this matter. Furthermore, note that this effect does not arise when the approximate analytical expression for ϕ, Eq. (2.4.27), is plotted, in which case the uncorrected solution is closely followed for the entirety of inflation. However, this result is of course unphysical, since by conservation of energy the field should not be able to reach the region where the oscillations become $\sim \mathcal{O}(\dot{\phi}^2)$. Clearly, this means that the average corrections on the slow-roll parameters, computed using Eq. (2.4.27), also cease to be valid after the field gets stuck.

As it is, we have found that no combination of values for g, M and ϕ_i that avoids ϕ getting stuck produces a pair $(\tilde{n}_s, \tilde{r})$ consistent with observational data, meaning that the quadratic

[24] Notice that this may also render invalid the correction to $|\eta_H|$ attained by the end of inflation in Figure 3.3.4d, which was in fact still quite substantial.

monomial potential should remain excluded.

Quartic monomial potential $(n = 4)$

The quartic monomial has also been extensively studied as an inflationary potential, corresponding to a common interaction term used in QFT [18, 66]. Unlike in the quadratic model, the predicted values for n_s are too small to be compatible with CMB data, while r is too large as well. These aspects have also made it an inadequate candidate for $V(\phi)$. A large enough backreaction on the curvature power spectrum would thus be required to potentially increase the value of n_s, as well as decrease the value of the tensor-to-scalar ratio r.

For this potential, taking $\phi_i = 22\,M_{\rm P}$, the region plots were also computed in the range $0 < g < 1$ and 10^{15} GeV $< M < 10^{16}$ GeV at two different moments: $\epsilon_V \approx 0.017$ (corresponding to the value of this parameter at $\phi_i = 22\,M_{\rm P}$) and $\epsilon_V = 0.2$ (attained later in slow-roll). The results are displayed in Figure 3.3.8.

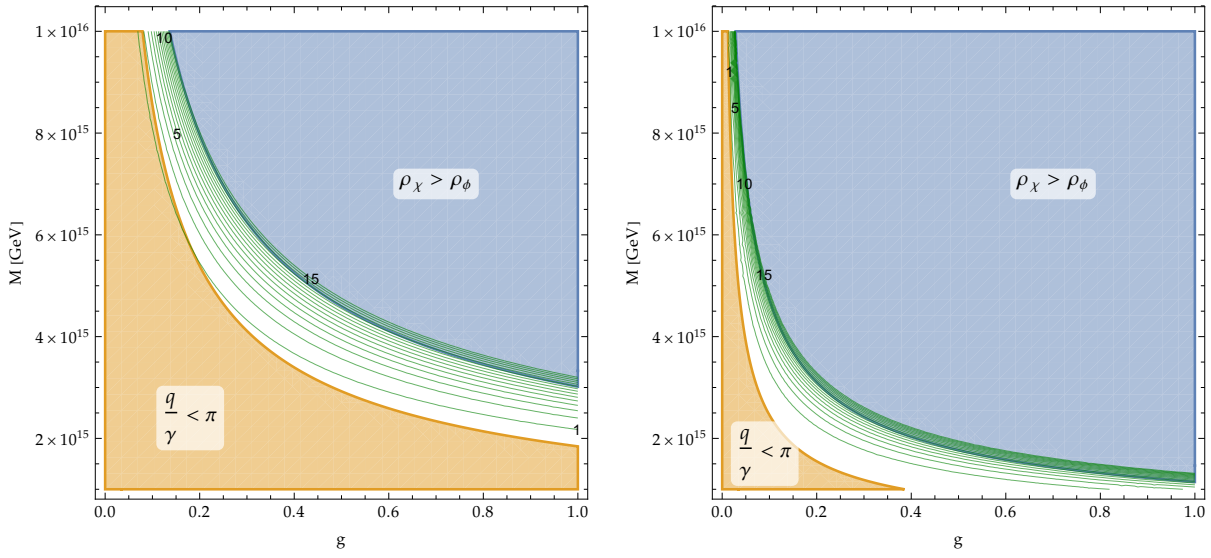

(a) (b)

Figure 3.3.8: Parameter space (g, M) for the quartic monomial potential with $\phi_i = 22\,M_{\rm P}$, for two values of the slow-roll parameter ϵ_V: (a) $\epsilon_V \approx 0.017$ and (b) $\epsilon_V = 0.2$. The acceptable region not excluded by the conditions $\frac{q}{\gamma} < \pi$ (orange) and $\rho_\chi > \rho_\phi$ (blue) is shown in white. Contour lines (as well as some values) for the resonance parameter ξ (for $0 \leqslant \xi \leqslant 15$) are shown in green.

Once again, the shaded areas correspond to regions of parameter space that were excluded due to satisfying either $\frac{q}{\gamma} < \pi$ or $\rho_\chi > \rho_\phi$, while the conditions $\gamma > 1$ and $q > 1$ are not plotted for the same reasons as in the quadratic potential. Contour lines for the χ resonance

parameter ξ are shown (for $0 \leqslant \xi \leqslant 15$). As before, we see that there exists a significant region of parameter space where all the required conditions are met and in roughly the entirety of this region, the B regime again dominates $\tilde{n}_\chi$, ρ_χ and $\langle\chi^2\rangle$. We clearly see that from $\epsilon_V \approx 0.017$ to $\epsilon_V = 0.2$ the shift of the acceptable region towards smaller values of g and M is much more drastic than in the previous case, which means that, for some initially acceptable pair (g, M), we may eventually enter the excluded region where $\rho_\chi > \rho_\phi$ quite early in inflation (which can in fact be problematic).

For the time evolution plots, we also take $\phi_i = 22\, M_{\mathrm{P}}$, leading to around 60 e-folds of accelerated expansion in the uncorrected regime, resulting in $n_s \approx 0.9497$ and $r \approx 0.268$ (compare with Eqs. (1.2.25b) and (1.2.34a)). We also pick $g = 0.7$ and $M = 2 \times 10^{15}$ GeV. Notice that these values do not verify the condition $\frac{q}{\gamma} > \pi$ in the first few e-folds of inflation, as can be seen in Figure 3.3.8a; we shall understand the reason for this choice soon. The time evolution of q, γ and ξ is shown in Figure 3.3.9, together with the evolution of the energy densities ρ_χ and ρ_ϕ. There, we see that q is no longer constant, but increases during inflation, while the remaining quantities maintain their behaviour. However, we readily notice that ξ grows much quicker than in the quadratic case, due to the also-increasing q^2 in its definition, Eq. (2.3.22).

This fast growth of ξ is problematic, as it causes ϕ to get stuck in a local minimum of $\mathcal{V}(\phi)$ rather early in inflation, even when we start with small values of ξ. This can be seen in Figure 3.3.10a, displaying the inflaton field solutions as functions of the number of e-folds, and Figure 3.3.10b, displaying the effective inflaton potential $\mathcal{V}(\phi)$ as a function of ϕ. Like in the quadratic case, the field rolls down its potential until it reaches the region where the amplitude of the oscillations becomes large enough to prevent it from climbing the induced potential wall, causing the field to get stuck, only this occurs faster than for the quadratic monomial, due to the faster-growing ξ. Had we picked smaller values for g and/or M, this behaviour would be attenuated and the field would not get stuck, but simultaneously we would be delving deeper into the region of parameter space where the condition $\frac{q}{\gamma} > \pi$ is not realised, leading to a meagre resonance, which is also undesirable. On the other hand, selecting larger values for g and/or M would cause the field to get stuck too early in inflation, causing our model to lose physical significance.

The results for the remaining plots are quite similar to those obtained in the previous section. We include only in Figure 3.3.11 the plot for the "globally corrected" curvature power spectrum from Eq. (2.4.65), containing also the numerically-obtained scalar spectral index, $\tilde{n}_s \approx 0.9462$, as well as the plot for the "quantum-backreacted" tensor-to-scalar ratio from Eq. (2.4.64). Although we do not show the plot for the ratios $\left|\frac{\Delta V^{(n)}}{V^{(n)}}\right|_{\max}$, the results obtained here are also compatible

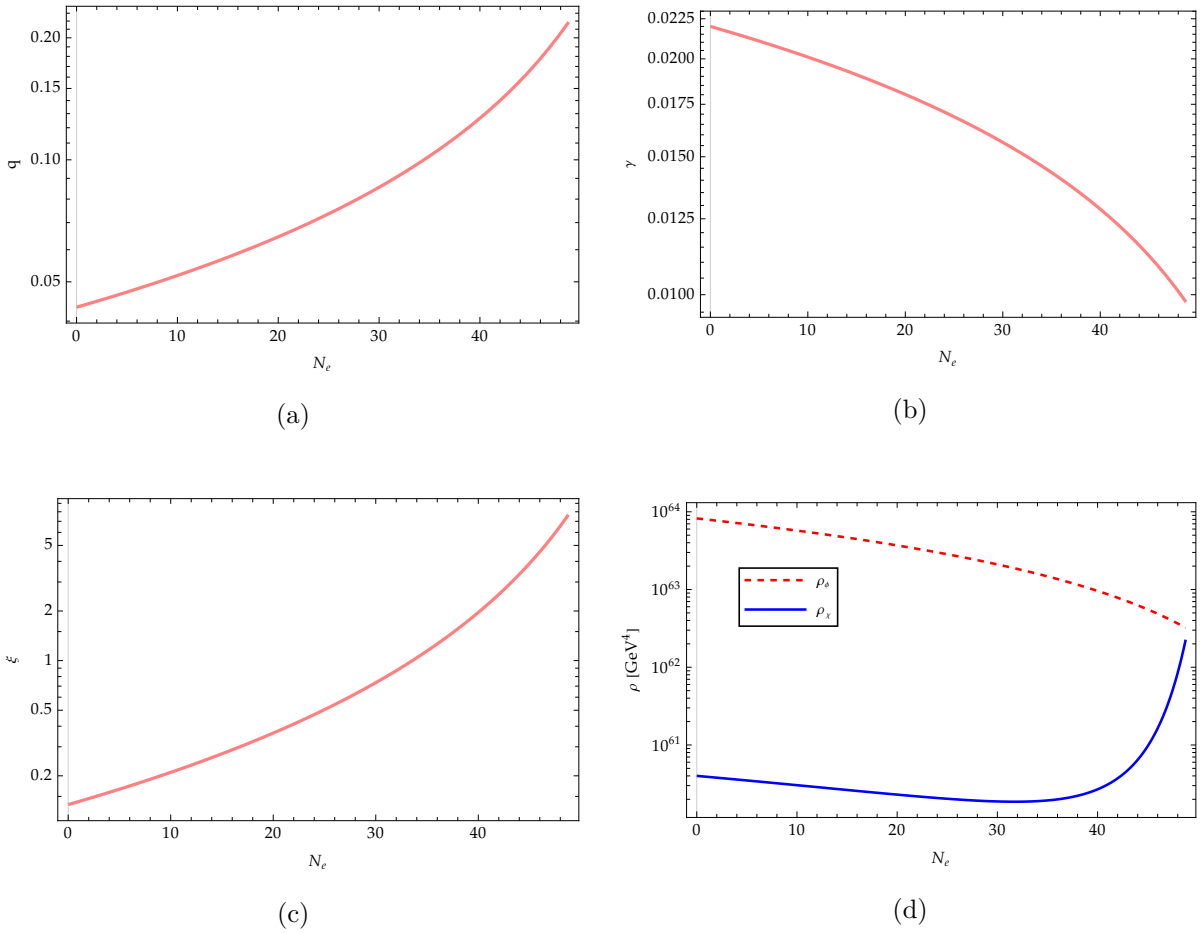

Figure 3.3.9: Evolution of the parameters (a) q, (b) γ and (c) ξ, and of (d) the energy densities ρ_χ and ρ_ϕ for the quartic monomial potential with $\phi_i = 22\,M_{\rm P}$ and model parameters $g = 0.7$ and $M = 2 \times 10^{15}$ GeV.

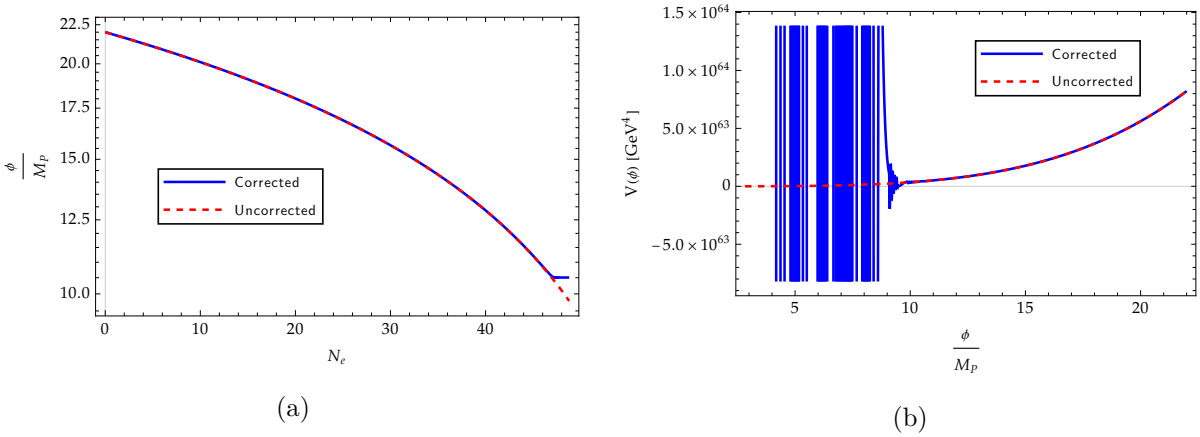

Figure 3.3.10: Evolution of (a) the corrected and uncorrected ϕ field solutions in e-folds and of (b) the corrected and uncorrected potentials plotted as functions of ϕ, for the quartic monomial potential with $\phi_i = 22\,M_{\rm P}$ and model parameters $g = 0.7$ and $M = 2 \times 10^{15}$ GeV.

with the bounds on $\left|\frac{\Delta V}{V}\right|_{\max}$ from Refs. [29, 76, 77]. However, we see that the values obtained for $\tilde{n}_s$ and $\tilde{r}$ are incompatible with observations [29], as expected from the small values of the resonance parameters at the start of inflation (once again, the linear fit to $\ln \tilde{\Delta}^2_{\mathcal{R}}$ follows the uncorrected curve exceedingly close). If we try to increase the magnitudes of either g or M so as to get larger initial values for q, ξ, q_φ and ξ_φ and thus an appropriate pair $(\tilde{n}_s, \tilde{r})$, we find that the only combinations which could achieve that cause ϕ to get stuck too early in inflation, rendering our model useless. Hence, we conclude that our mechanism is unable to modify the predictions of the quartic potential in a way to make them agree with experimental data.

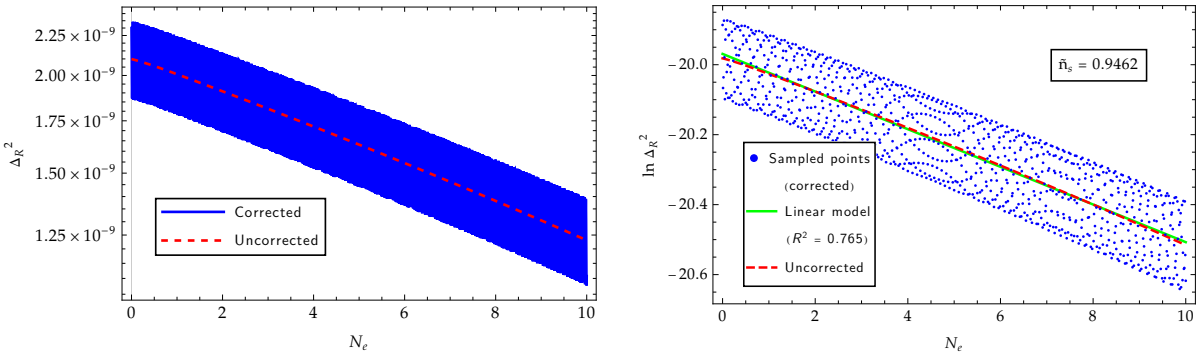

(a)

(b)

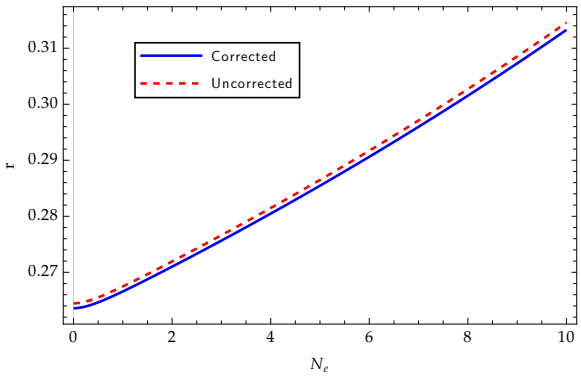

(c)

Figure 3.3.11: Evolution (over the initial 10 e-folds of inflation) of the CMB observables (a) $\Delta^2_{\mathcal{R}}$ and (c) r (both their corrected and uncorrected versions) for the quartic monomial potential with $\phi_i = 22\, M_{\rm P}$ and model parameters $g = 0.7$ and $M = 2 \times 10^{15}$ GeV. In (b) we perform a linear fit to $\ln \Delta^2_{\mathcal{R}}$ and display the obtained R^2 coefficient, as well as the obtained value for $\tilde{n}_s$.

3.3.2 Hilltop potentials (small-field models)

We may now consider another class of potentials, in this case that of two-parameter, small-field models [22, 81–83], which we can generally write as

$$V(\phi) = V_0 \left[1 - \frac{\kappa}{n}\left(\frac{\phi}{M_\mathrm{P}}\right)^n\right]^m , \tag{3.3.8}$$

with $n \geqslant 2$ and $x^n \equiv \frac{\kappa}{n}\left(\frac{\phi_i}{M_\mathrm{P}}\right)^n \ll 1$, making the second term in the brackets subdominant (we will consider $\kappa \ll 1$ in order to attain this). Moreover, henceforth we shall always consider $m = 1$. These typically arise in the study of spontaneous symmetry breaking, in particular in the Abelian Higgs model [18, 66, 74]. Using the definitions of the potential slow-roll parameters, Eq. (1.2.6), one can show that [22, 81–83]

$$\epsilon_V = \frac{\kappa^2}{2}\frac{\left(\frac{\phi}{M_\mathrm{P}}\right)^{2(n-1)}}{\left[1 - \frac{\kappa}{n}\left(\frac{\phi}{M_\mathrm{P}}\right)^n\right]^2} \tag{3.3.9a}$$

$$\eta_V = -\kappa(n-1)\frac{\left(\frac{\phi}{M_\mathrm{P}}\right)^{n-2}}{1 - \frac{\kappa}{n}\left(\frac{\phi}{M_\mathrm{P}}\right)^n} . \tag{3.3.9b}$$

Since $\epsilon_V > 0$ and $\eta_V < 0$ for all accepted values of n, it is easy to see from (A.5), (A.7) and (A.8) that all three quantities $\frac{q'}{q}$, $\frac{\gamma'}{\gamma}$ and $\frac{\xi'}{\xi}$ are negative, meaning that q, γ and ξ all decrease during inflation. This is not inherently problematic and does not immediately force us to conclude that an appreciable resonance cannot be attained. For instance, this behaviour still allows for a resonance that is rather strong at the start of inflation but gets gradually less efficient as slow-roll develops. In fact, we will see that it is precisely this behaviour that leads to some very interesting results for our model.

The duration of inflation in e-folds and the field value at $\epsilon_V = 1$ are given by [81]

$$N_e \approx \begin{cases} \frac{1}{\kappa}\ln\left(\frac{\phi_f}{\phi_i}\right) + \frac{1}{4}\left[\left(\frac{\phi_i}{M_\mathrm{P}}\right)^2 - \left(\frac{\phi_f}{M_\mathrm{P}}\right)^2\right] , & n = 2 \\ \frac{1}{2n}\left[\left(\frac{\phi_i}{M_\mathrm{P}}\right)^2 - \left(\frac{\phi_f}{M_\mathrm{P}}\right)^2\right] + \frac{1}{\kappa(n-2)}\left[\left(\frac{\phi_i}{M_\mathrm{P}}\right)^{2-n} - \left(\frac{\phi_f}{M_\mathrm{P}}\right)^{2-n}\right] , & n > 2 \end{cases} \tag{3.3.10a}$$

$$\frac{\phi_f}{M_\mathrm{P}}\Big|_{n=2} = \sqrt{1 + \frac{2}{\kappa} + \frac{2}{\sqrt{\kappa}} + \frac{\sqrt{\kappa}}{4}} \approx \sqrt{\frac{2}{\kappa}} , \tag{3.3.10b}$$

where Eq. (3.3.10b) was obtained using the full expression for ϵ_V. The value of $\frac{\phi_f}{M_\mathrm{P}}$ for the remaining choices for n must be obtained by solving $\epsilon_V = 1$ numerically.

As for the CMB observables, one can obtain [81]

$$n_s - 1 \;\approx\; -n^{1-\frac{2}{n}}\,\kappa^{\frac{2}{n}}\,\frac{2(n-1)+(n+2)\,x_i^n}{\left(x_i^n-1\right)^2}\,x_i^{n-2} \tag{3.3.11a}$$

$$r \;\approx\; 8n^{2\left(1-\frac{1}{n}\right)}\,\kappa^{\frac{2}{n}}\,\frac{x_i^{2\left(1-\frac{1}{n}\right)}}{\left(1-x_i^n\right)^2}\,, \tag{3.3.11b}$$

where $x_i^n \equiv \frac{\kappa}{n}\left(\frac{\phi_i}{M_{\rm P}}\right)^n$. Some of these expressions are not straightforward to evaluate, and so we cannot easily determine whether the hilltop models predict values for these quantities that are compatible with observations [29]. We shall obtain numerical values for them in the following portion of this work. We will be focusing our upcoming analysis and discussion on the two cases that are arguably the best motivated in terms of spontaneous symmetry breaking and the Abelian Higgs mechanism [18, 66, 74]: the quadratic hilltop potential ($n = 2$) and the quartic hilltop potential ($n = 4$).

As mentioned before, the hilltop family of potentials is defined by two parameters, V_0 and κ. In the following, the former is set by the measured amplitude of the curvature power spectrum $\Delta^2_{\mathcal{R}}(k_*)$, which we will again consider to be $\Delta^2_{\mathcal{R}}(k_* = 0.05\ \text{Mpc}^{-1}) = 2.099 \times 10^{-9}$ (cf. Eq. (1.2.25a) and Ref. [29]), leading to (cf. Eq. (1.2.26))

$$V_0 \;=\; 12\pi^2\,\Delta^2_{\mathcal{R}}(k_*)\,M_{\rm P}^4\,\kappa^2\,\frac{\left(\frac{\phi_i}{M_{\rm P}}\right)^{2(n-1)}}{\left[1-\frac{\kappa}{n}\left(\frac{\phi_i}{M_{\rm P}}\right)^n\right]^3} \tag{3.3.12}$$

On the other hand, κ is a free parameter for this class of potentials, whose value we must choose in order to get ϕ_f, as well as an adequate duration for inflation, cf. Eq. (3.3.10); there will exist, of course, an interplay between κ and ϕ_i in order to attain a proper value for N_e.

Quadratic hilltop potential ($n = 2$)

The first particular realisation of the hilltop potential we will test is the quadratic case, which corresponds to the mass term in the Abelian Higgs potential [18, 66, 74], which is the dominant contribution, considering $x^2 \equiv \frac{\kappa}{2}\left(\frac{\phi}{M_{\rm P}}\right)^2 \ll 1$. The uncorrected version of this potential is already able to produce values for the CMB observables n_s and r that agree with measurements [29]. Surely, we would like to avoid losing this, and we shall see that for an appreciable range of values for the pair (g, M) this agreement can indeed be maintained even with non-negligible resonances for χ and φ.

For this model, setting $\phi_i = 5\,M_{\rm P}$ and $\kappa = 10^{-2}$, we computed the region plots in the range $0 < g < 1$ and $10^{14}\ \text{GeV} < M < 6 \times 10^{15}\ \text{GeV}$ (the upper limit of M was chosen to improve

visibility for the analysis, but we could have gone up to $M < 10^{16}$ GeV) again at two different stages of inflation: $\epsilon_V \approx 0.002$ (corresponding to the initial value of this parameter for $\phi_i = 5\,M_{\rm P}$ and $\kappa = 10^{-2}$) and $\epsilon_V = 0.5$ (attained later). In Figure 3.3.12, we display the resulting plots.

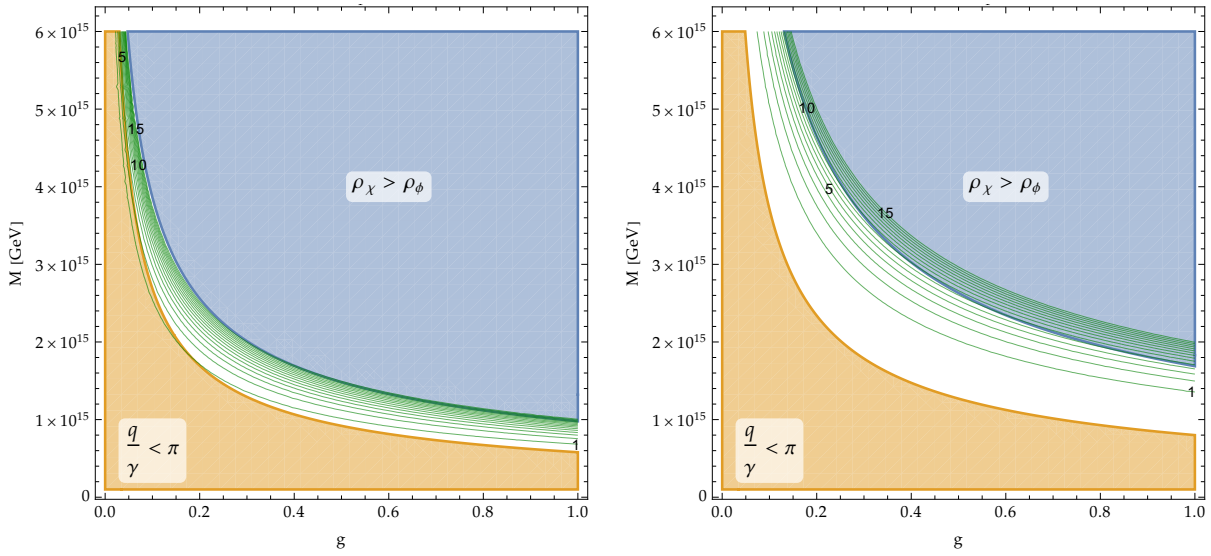

Figure 3.3.12: Parameter space (g, M) for the quadratic hilltop potential with $\phi_i = 5\,M_{\rm P}$ and $\kappa = 10^{-2}$, for two values of the slow-roll parameter ϵ_V: (a) $\epsilon_V \approx 0.002$ and (b) $\epsilon_V = 0.5$. The acceptable region not excluded by the conditions $\frac{q}{\gamma} < \pi$ (orange) and $\rho_\chi > \rho_\phi$ (blue) is shown in white. Contour lines (as well as some values) for the resonance parameter ξ (for $0 \leqslant \xi \leqslant 15$) are shown in green.

The shaded areas again correspond to regions excluded due to the conditions $\frac{q}{\gamma} < \pi$ or $\rho_\chi > \rho_\phi$ being verified there, and the conditions $\gamma > 1$ and $q > 1$ are not plotted since they are non-restrictive and redundant, respectively. In Figure 3.3.12b, we also do not show an additional region where $\rho_\chi > \rho_\phi$, as it is fully contained in the region $\frac{q}{\gamma} < \pi$, which is already excluded. The contour lines for $0 \leqslant \xi \leqslant 15$ are also drawn. We observe that there exists a significant region of parameter space where all the required conditions are met, in this case that region being in fact larger than the one obtained for the two monomial cases we studied. Furthermore, we found that in this region the B regime dominates $\tilde{n}_\chi$, ρ_χ and $\langle\chi^2\rangle$, again ensuring the validity of the approximations used in §§ 2.2, 2.3 and 2.4.1. We note that for this model, from $\epsilon_V \approx 0.002$ to $\epsilon_V = 0.5$, the acceptable region became broader and shifted slightly upwards, allowing larger values of g and M. Thus, if we start inflation within the acceptable region, we might eventually enter the region where $\frac{q}{\gamma} < \pi$, which is somewhat expected, since the resonance does become less efficient as inflation progresses, as we concluded earlier; note, however, that this is not necessarily troublesome if it happens towards the end of inflation, which is found to generally

be the case.

Let us now analyse the time evolution plots. As before, we take $\phi_i = 5\,M_\mathrm{P}$ and $\kappa = 10^{-2}$, which allows us to get about 62 e-folds of inflation neglecting backreaction. This yields a scalar spectral index $n_s \approx 0.9673$ and a tensor-to-scalar ratio $r \approx 0.026$, both compatible with *Planck* data, cf. Eqs. (1.2.25b) and (1.2.34a), and Ref. [29]. Additionally, considering the results from Figure 3.3.12a, we choose $g = 0.2$ and $M = 2 \times 10^{15}$ GeV for our free parameters.

In Figure 3.3.13, we show the time evolution of the quantities q, γ and ξ throughout inflation, as well as the energy densities of ϕ and χ.

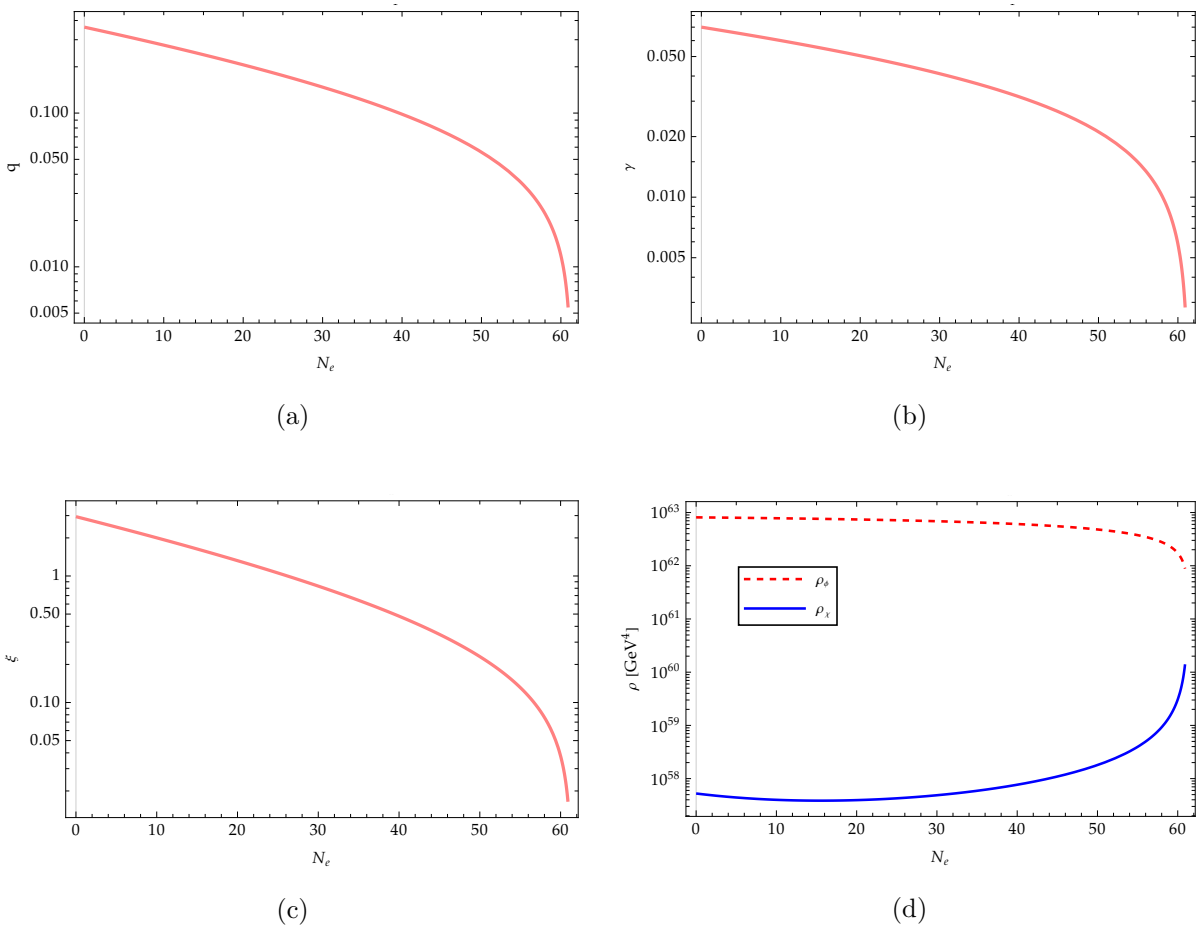

Figure 3.3.13: Evolution of the parameters (a) q, (b) γ and (c) ξ, and of (d) the energy densities ρ_χ and ρ_ϕ for the quadratic hilltop potential with $\phi_i = 5\,M_\mathrm{P}$ and $\kappa = 10^{-2}$, and model parameters $g = 0.2$ and $M = 2 \times 10^{15}$ GeV.

We see that q, γ and ξ indeed behave as we had predicted based on Appendix A and Eq. (3.3.9), i.e. they all decrease during inflation, and q and γ indeed verify the narrow resonance and the adiabaticity conditions, respectively. Looking at Figure 3.3.13c in particular, we find that the resonance is quite large at the beginning of inflation, since $\xi \gtrsim 1$, and gradually becomes less and less efficient as time goes on. However, considering now Figure 3.3.13d, this does not

make the energy density of χ decrease throughout inflation, which might seem slightly counter-intuitive. The explanation lies in the phase space effects we described at the end of § 2.3. In spite of the decreasing value of ξ and it becoming sub-unity, leading to a small number of particles being produced *at each comoving momentum* k, a large interval of comoving momenta provide contributions to ρ_χ; since the comoving momentum of the χ modes being produced grows as inflation develops ($k_c(t) \propto a(t)$, cf. Eq. (2.1.35)), so does their respective phase space contribution, making ρ_χ increase, as per Eq. (2.3.11). Since the energy density of the inflaton strictly decreases as inflation develops, we see in this particular case that ρ_χ becomes less than two orders of magnitude smaller than ρ_ϕ by the end of inflation, which may also point to a graceful exit from inflation, although in this situation the final energy density of the χ field is not sufficient to completely overtake that of the inflaton.

In Figure 3.3.14, we plot the inflaton field solution in the uncorrected and in the backreacted case, the effective and the uncorrected potentials as functions of ϕ, as defined in Eq. (2.4.14a), and the ratios $\left|\frac{\Delta V^{(n)}}{V^{(n)}}\right|_{\max}$ as functions of N_e.

Like for the monomial potentials, the backreacted field solution perfectly follows the uncorrected solution; however, in the present case, the effective potential also appears to follow the uncorrected curve, since the oscillatory correction to the potential is quite small compared to $V(\phi)$, as we can see in Figure 3.3.14c, which shows in particular that indeed $\left|\frac{\Delta V}{V}\right|_{\max} \lesssim 3\times10^{-5}$, in accordance with the bounds obtained in Refs. [29, 76, 77].

Considering now the Hubble slow-roll parameters, we show in Figures 3.3.15a and 3.3.15b their uncorrected and effective versions, while in Figures 3.3.15c and 3.3.15d we display the average effect of the correction. The results are similar to those obtained for the monomial family: the backreaction again introduces large-amplitude oscillations on both slow-roll parameters, despite the field solution appearing unaltered, which is explained by the average effect of the backreaction on ϵ_H and $|\eta_H|$ being quite suppressed. Additionally, this allows us to get roughly 61 e-folds of inflation in the quantum-corrected scenario, which then manifests a slight anticipation of the ending of inflation relative to the uncorrected case, due to a non-zero average correction on ϵ_H.

The time evolution of the φ resonance parameters q_φ and ξ_φ is shown in Figures 3.3.16a and 3.3.16b, where we find that their orders of magnitude are smaller than those of q and ξ, respectively. However, both parameters still assume large enough values to generate a somewhat efficient resonance for φ, leading to some interesting observational effects.

These effects can be seen in Figure 3.3.17a, where we plot the curvature power spectra defined by Eqs. (1.2.22b) and (2.4.59), respectively the uncorrected spectrum and the fully

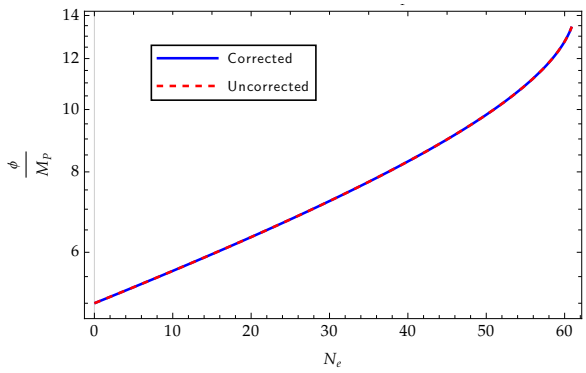

(a)

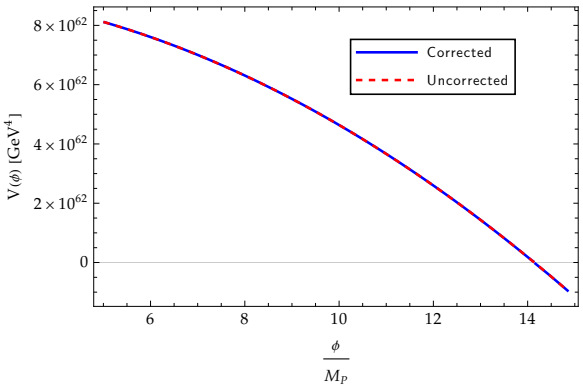

(b)

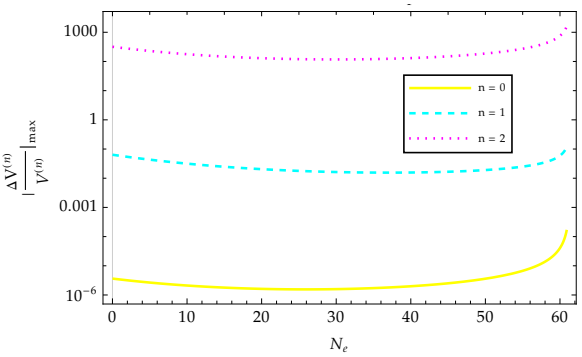

(c)

Figure 3.3.14: Evolution of (a) the corrected and uncorrected ϕ field solutions and of (c) the ratios $\left|\frac{\Delta V^{(n)}}{V^{(n)}}\right|_{\max}$, as well as (b) the corrected and uncorrected potentials plotted as functions of ϕ, for the quadratic hilltop potential with $\phi_i = 5\,M_{\rm P}$ and $\kappa = 10^{-2}$, and model parameters $g = 0.2$ and $M = 2 \times 10^{15}$ GeV.

corrected spectrum. We again determine the value of $\tilde{n}_s$ by performing a linear fit to the natural logarithm of the corrected power spectrum and taking the resulting slope as $\tilde{n}_s - 1$, as is shown in Figure 3.3.17b. For the selected values of the parameters, the value we obtain for the backreacted scalar spectral index, $\tilde{n}_s \approx 0.9658$ is also consistent with observations, cf. Eq. (1.2.25b) and Ref. [29], and moreover it is remarkably close to the uncorrected one (as is the linear model to the uncorrected curve), in spite of the substantial values of the resonance parameters, both for χ and φ. Like we had hinted at before, the effects of the "quantum" and the "classical backreactions" have compensated each other, leaving us with an almost unaltered scalar spectral index. In fact, had we taken only one of these backreaction effects into account, we would have obtained quite different predictions for $\tilde{n}_s$ due to each of them, with the "classical" one being above the measured value and the "quantum" one being below. Other values for ϕ_i, κ and for the pair (g, M) produce equally good predictions for the scalar spectral index. Furthermore, the results

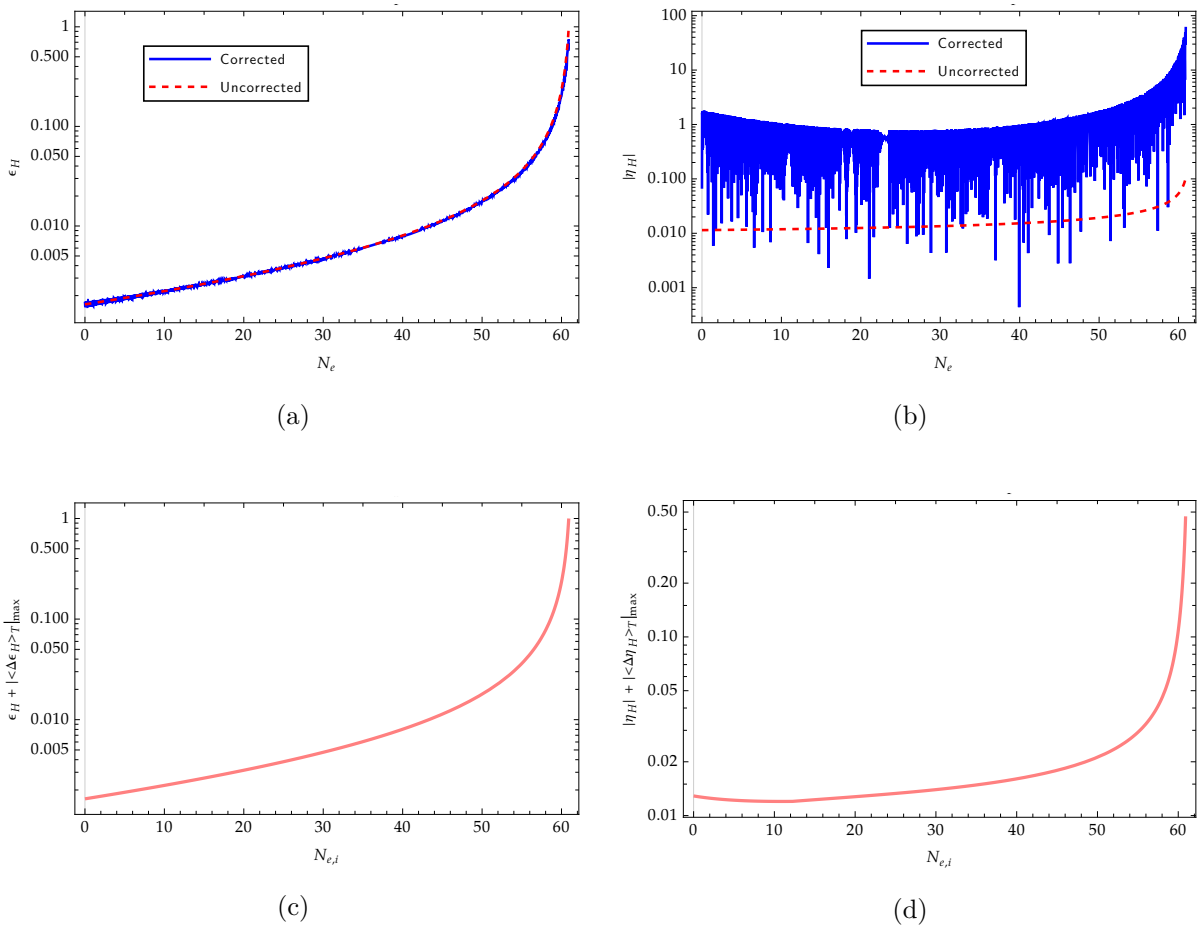

Figure 3.3.15: Evolution of the corrected and uncorrected Hubble slow-roll parameters (a) ϵ_H and (b) $|\eta_H|$, as well as their average corrections (c) $\epsilon_H + |\langle\Delta\epsilon_H\rangle_T|_{\max}$ and (d) $|\eta_H| + |\langle\Delta\eta_H\rangle_T|_{\max}$ plotted as functions of the average centre $N_{e,i}$, for the quadratic hilltop potential with $\phi_i = 5\,M_{\rm P}$ and $\kappa = 10^{-2}$, and model parameters $g = 0.2$ and $M = 2 \times 10^{15}$ GeV.

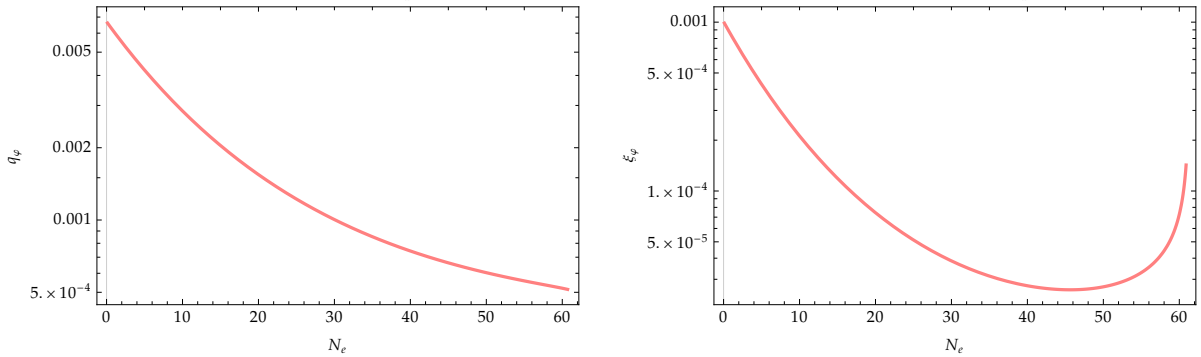

Figure 3.3.16: Evolution of the φ resonance parameters (a) q_φ and (b) ξ_φ (the tildes are omitted in the plots) for the quadratic hilltop potential with $\phi_i = 5\,M_{\rm P}$ and $\kappa = 10^{-2}$, and model parameters $g = 0.2$ and $M = 2 \times 10^{15}$ GeV.

for the tensor-to-scalar ratio are plotted in Figure 3.3.17c, where we see that the already-small value predicted by the uncorrected model suffers almost no alteration due to the "quantum backreaction" described by Eq. (2.4.64), and so remains within the acceptable range from Ref. [29], quoted in Eq. (1.2.34a). This behaviour was verified also for other values of the parameters ϕ_i, κ and (g, M).

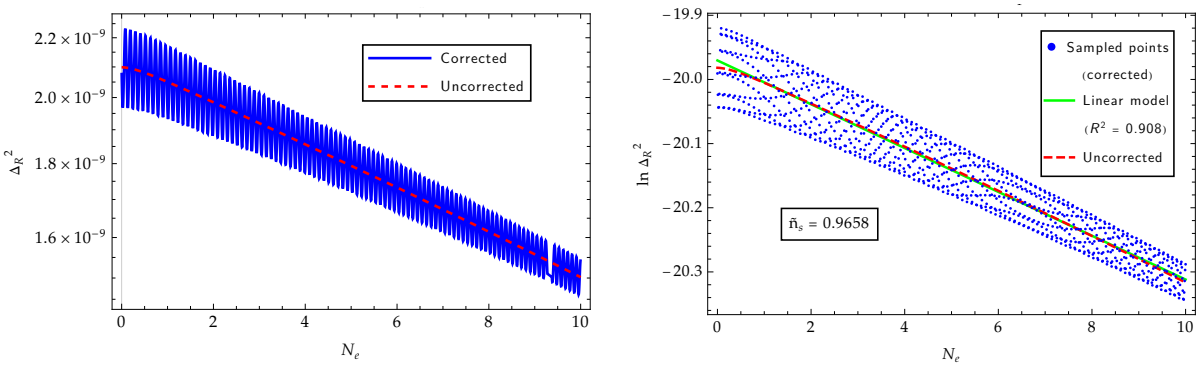

(a)

(b)

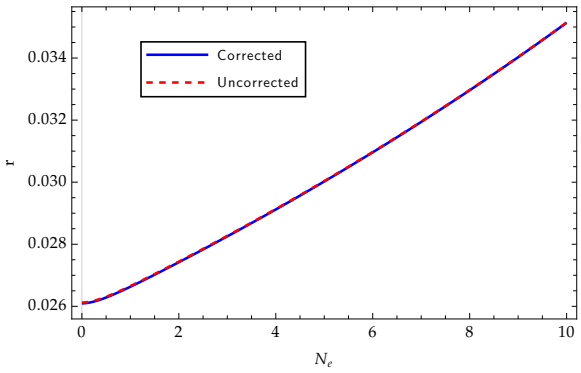

(c)

Figure 3.3.17: Evolution (over the initial 10 e-folds of inflation) of the CMB observables (a) $\Delta^2_{\mathcal{R}}$ and (c) r (both their corrected and uncorrected versions) for the quadratic hilltop potential with $\phi_i = 5\,M_{\rm P}$ and $\kappa = 10^{-2}$, and model parameters $g = 0.2$ and $M = 2 \times 10^{15}$ GeV. In (b) we perform a linear fit to $\ln \Delta^2_{\mathcal{R}}$ and display the obtained R^2 coefficient, as well as the obtained value for $\tilde{n}_s$.

The results of this section seem to show that our model is compatible with the quadratic hilltop potential, producing acceptable values for the considered CMB observables while still allowing for an appreciable production of χ particles, as well as suggesting a graceful exit from inflation.

Quartic hilltop potential $(n = 4)$

The quartic hilltop potential arises from the second-largest contribution to the Abelian Higgs potential [18, 66, 74], corresponding to a ϕ^4-type interaction.

Similarly to the quadratic hilltop, this model allows values for n_s and r that are simultaneously compatible with experimental data [29], which once again is a feature we would like to conserve.

In this case, for $\phi_i = 7\,M_{\rm P}$ and $\kappa = 10^{-4}$, we select the ranges $0 < g < 1$ and 10^{15} GeV $< M < 6 \times 10^{15}$ GeV (the latter being due to the same reasons as in the quadratic hilltop case) and obtain the parameter space at the two instants $\epsilon_V \approx 0.0007$ (corresponding to the value of this parameter at $\phi_i = 7\,M_{\rm P}$ and $\kappa = 10^{-4}$) and $\epsilon_V = 0.5$ (attained later in slow-roll). The plots are displayed in Figure 3.3.18.

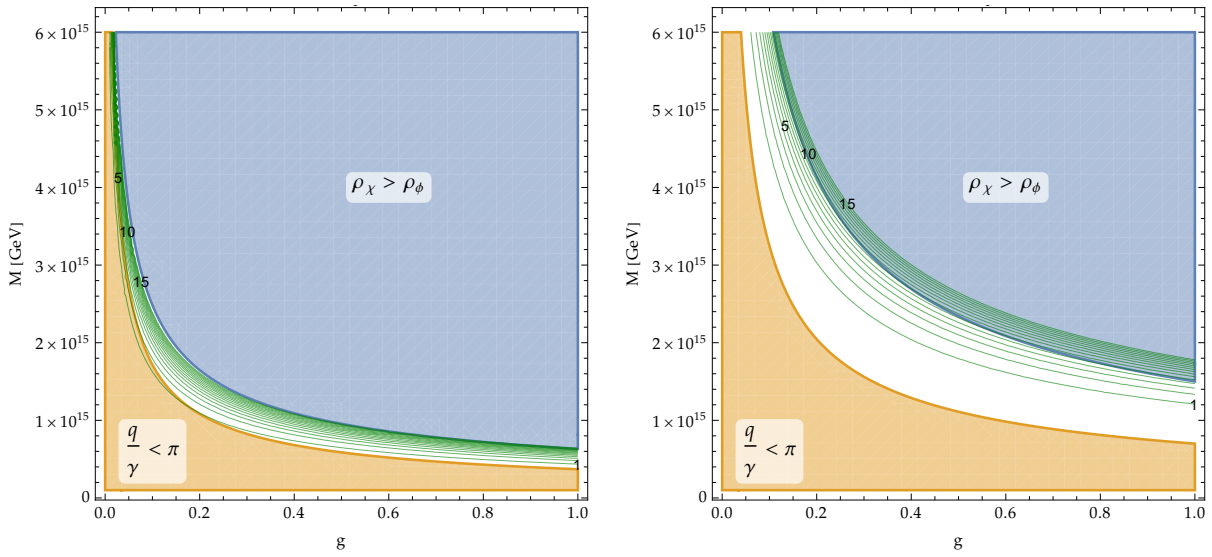

(a) (b)

Figure 3.3.18: Parameter space (g, M) for the quartic hilltop potential with $\phi_i = 7\,M_{\rm P}$ and $\kappa = 10^{-4}$, for two values of the slow-roll parameter ϵ_V: (a) $\epsilon_V \approx 0.0007$ and (b) $\epsilon_V = 0.5$. The acceptable region not excluded by the conditions $\frac{q}{\gamma} < \pi$ (orange) and $\rho_\chi > \rho_\phi$ (blue) is shown in white. Contour lines (as well as some values) for the resonance parameter ξ (for $0 \leqslant \xi \leqslant 15$) are shown in green.

The excluded (shaded) regions refer either to $\frac{q}{\gamma} < \pi$ or $\rho_\chi > \rho_\phi$, while the conditions $\gamma > 1$ and $q > 1$ are again not shown. Contour lines for $0 \leqslant \xi \leqslant 15$ are included. Similarly to the quadratic hilltop case, we see that there exists a significant region of parameter space where all the required conditions are met, including the dominance of the B regime in $\tilde{n}_\chi$, ρ_χ and $\langle\chi^2\rangle$, which, as we go from $\epsilon_V \approx 0.0007$ to $\epsilon_V = 0.5$, gets broader and shifts towards larger values of g

and M. In this case also, we find that if we select a point (g, M) contained within the acceptable region at the start of inflation, as slow-roll develops we may move towards and eventually enter the region where $\frac{q}{\gamma} < \pi$, which is found to generally occur late enough to not invalidate our results (as we saw before, the resonance is efficient only at the beginning of inflation).

As for the time evolution plots, we also take $\phi_i = 7\,M_{\rm P}$ and $\kappa = 10^{-4}$, leading to around 58 e-folds of accelerated expansion in the uncorrected case, resulting in $n_s \approx 0.9647$ and $r \approx 0.011$ (compare with Eqs. (1.2.25b) and (1.2.34a)). We also pick $g = 0.2$ and $M = 1.3 \times 10^{15}$ GeV. The results for this potential are quite similar to those obtained for $n = 2$.

We again obtain decreasing q, γ and ξ, with the latter starting inflation with values larger than unity and evolving to smaller values as slow-roll develops, as can be seen in Figure 3.3.19, where we also see that the energy density of the χ field again increases throughout inflation, becoming, by the end of it, smaller than ρ_ϕ by just one order of magnitude.

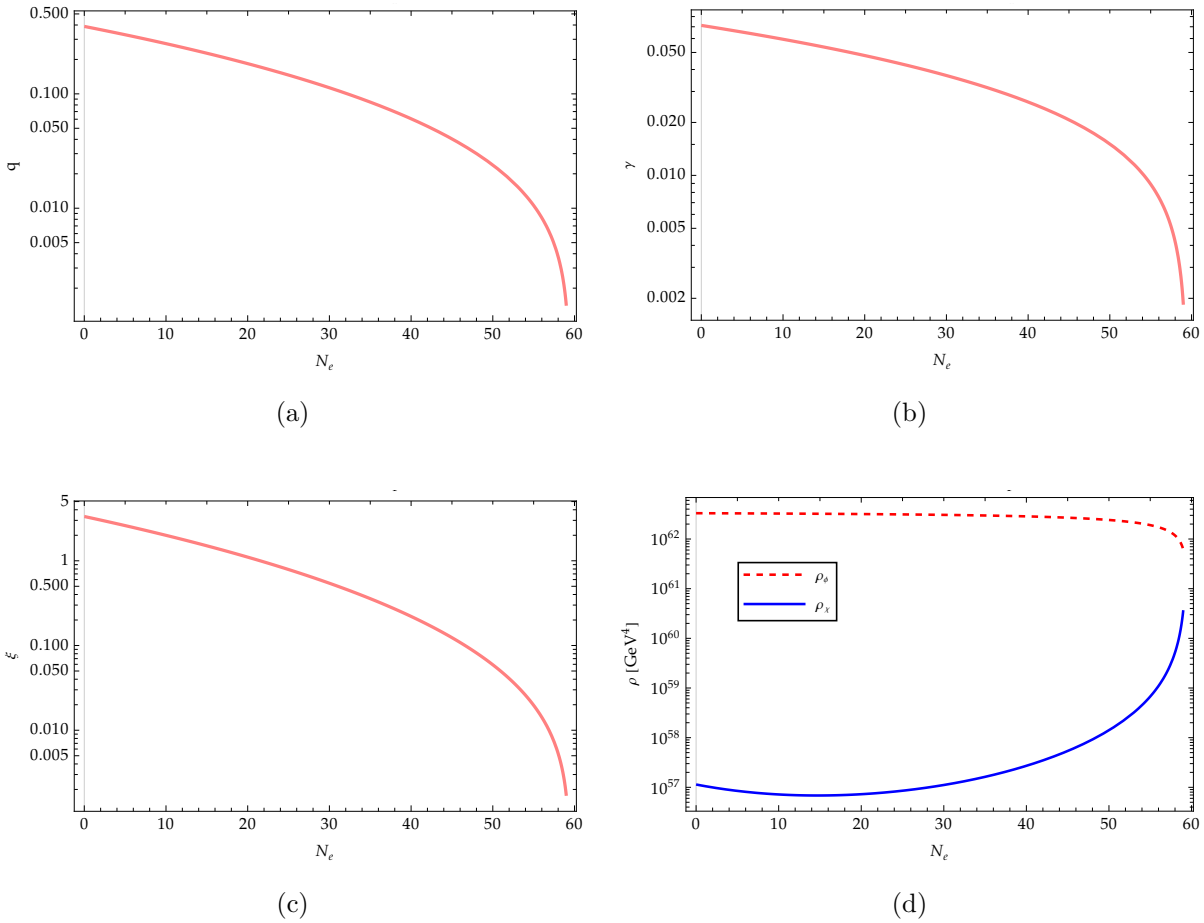

Figure 3.3.19: Evolution of the parameters (a) q, (b) γ and (c) ξ, and of (d) the energy densities ρ_χ and ρ_ϕ for the quartic hilltop potential with $\phi_i = 7\,M_{\rm P}$ and $\kappa = 10^{-4}$, and model parameters $g = 0.2$ and $M = 1.3 \times 10^{15}$ GeV.

Like in the quadratic hilltop case, the corrected and uncorrected inflaton field solutions

follow each other closely, as do the corrected and uncorrected potentials, cf. Figures 3.3.20a and 3.3.20b. The ratios $\left|\frac{\Delta V^{(n)}}{V^{(n)}}\right|_{\max}$ are also plotted in Figure 3.3.20c as functions of N_e; the agreement with Refs. [29, 76, 77] is clear, since indeed $\left|\frac{\Delta V}{V}\right|_{\max} \lesssim 3 \times 10^{-5}$. We are able to improve this accordance by lowering either g or M, while remaining inside the acceptable region of the parameter space.

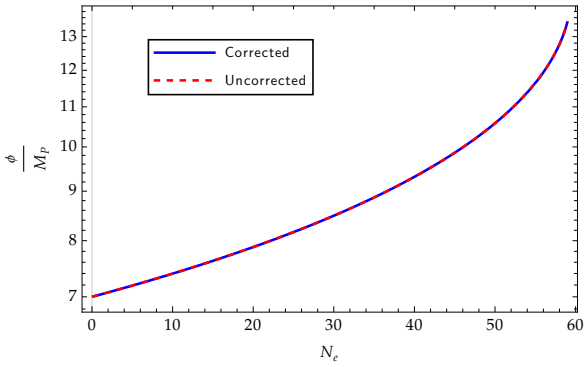

(a)

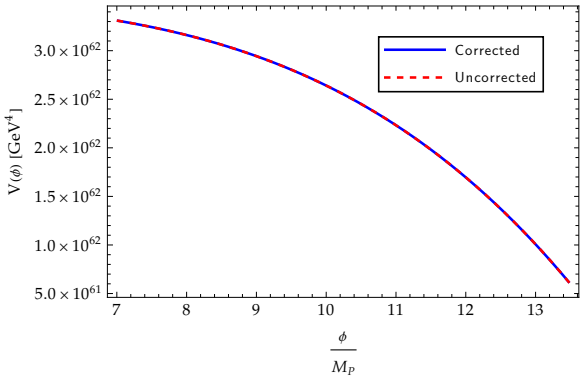

(b)

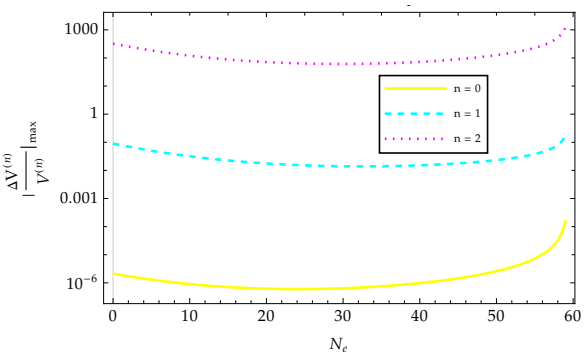

(c)

Figure 3.3.20: Evolution of (a) the corrected and uncorrected ϕ field solutions and of (c) the ratios $\left|\frac{\Delta V^{(n)}}{V^{(n)}}\right|_{\max}$, as well as (b) the corrected and uncorrected potentials plotted as functions of ϕ, for the quartic hilltop potential with $\phi_i = 7\,M_{\rm P}$ and $\kappa = 10^{-4}$, and model parameters $g = 0.2$ and $M = 1.3 \times 10^{15}$ GeV.

The effective Hubble slow-roll parameters and their respective average corrections are also plotted in Figure 3.3.21, with the latter allowing us to conclude that inflation is once again not ended prematurely due to the backreaction.

The "globally corrected" curvature power spectrum from Eq. (2.4.65) is plotted in Figure 3.3.22a, together with its uncorrected version. The corrected scalar spectral index $\tilde{n}_s$ is obtained as the slope of a linear fit on $\ln \tilde{\Delta}^2_{\mathcal{R}}$, cf. Figure 3.3.22b, the latter following the uncorrected curve very closely, as in the previous cases. The value obtained for the index, $\tilde{n}_s \approx 0.9626$,

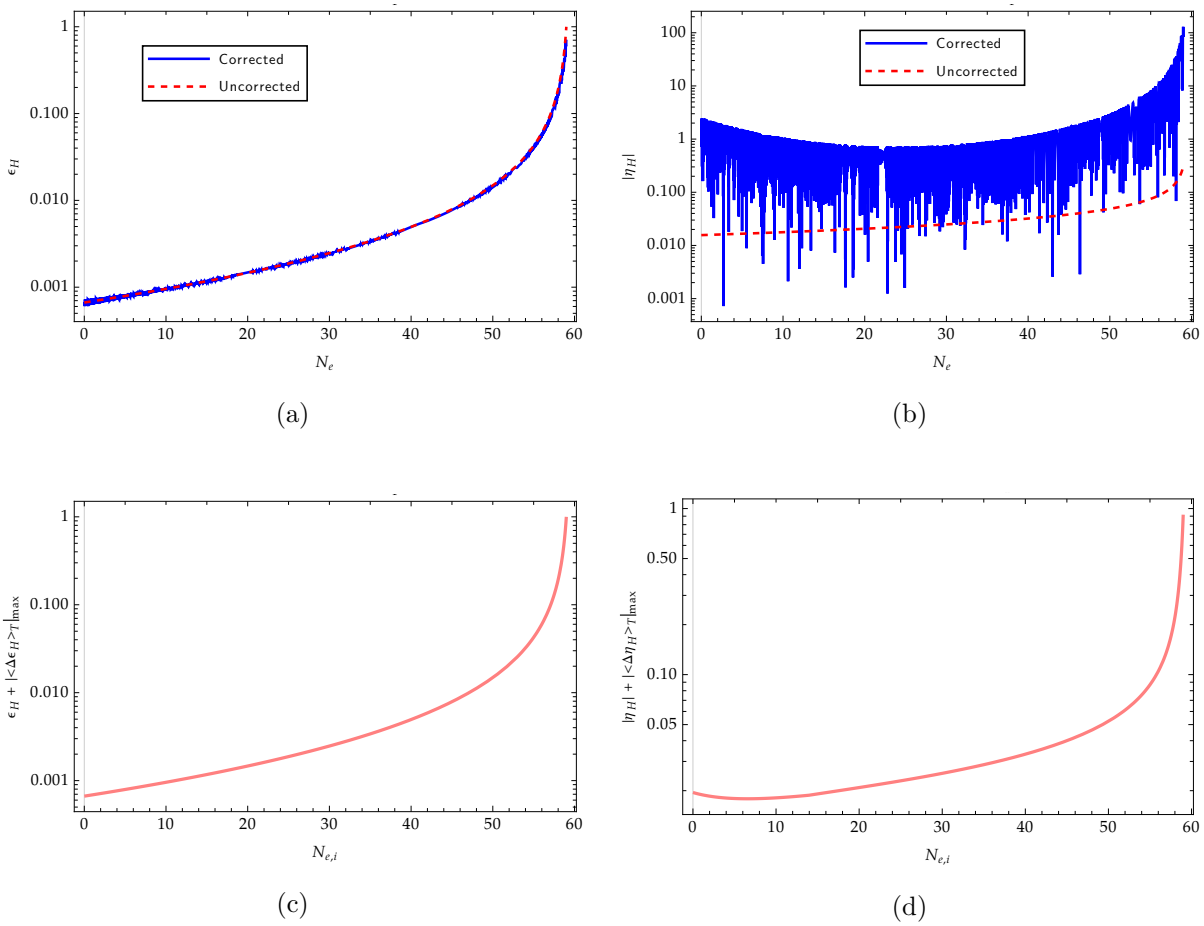

Figure 3.3.21: Evolution of the corrected and uncorrected Hubble slow-roll parameters (a) ϵ_H and (b) $|\eta_H|$, as well as their average corrections (c) $\epsilon_H + |\langle \Delta\epsilon_H \rangle_T|_{\max}$ and (d) $|\eta_H| + |\langle \Delta\eta_H \rangle_T|_{\max}$ plotted as functions of the average centre $N_{e,i}$, for the quartic hilltop potential with $\phi_i = 7\,M_{\rm P}$ and $\kappa = 10^{-4}$, and model parameters $g = 0.2$ and $M = 1.3 \times 10^{15}$ GeV.

is consistent with data from Ref. [29], and it is close to the uncorrected one, indicating again that the effects of the "quantum" and the "classical backreactions" have balanced each other out (although for the selected set of parameters neither of these backreaction effects produced excluded values for $\tilde{n}_s$ when acting isolatedly). In any case, other values for ϕ_i, κ and for the pair (g, M) have been found to produce equally good predictions for the "globally corrected" scalar spectral index. Lastly, the tensor-to-scalar ratio, plotted in Figure 3.3.22c, is also predicted to attain a "quantum-backreacted" value (cf. Eq. (2.4.64)) compatible with the bounds from Ref. [29], that value being essentially equal to the one predicted by the uncorrected model. As before, this was also verified for other values of ϕ_i, κ, g and M.

The results obtained here also point to our model being compatible with the quartic hilltop potential, since we were able to obtain good values for CMB observables, while allowing for a substantial resonance for the χ particles, with a possible graceful exit from inflation due to it.

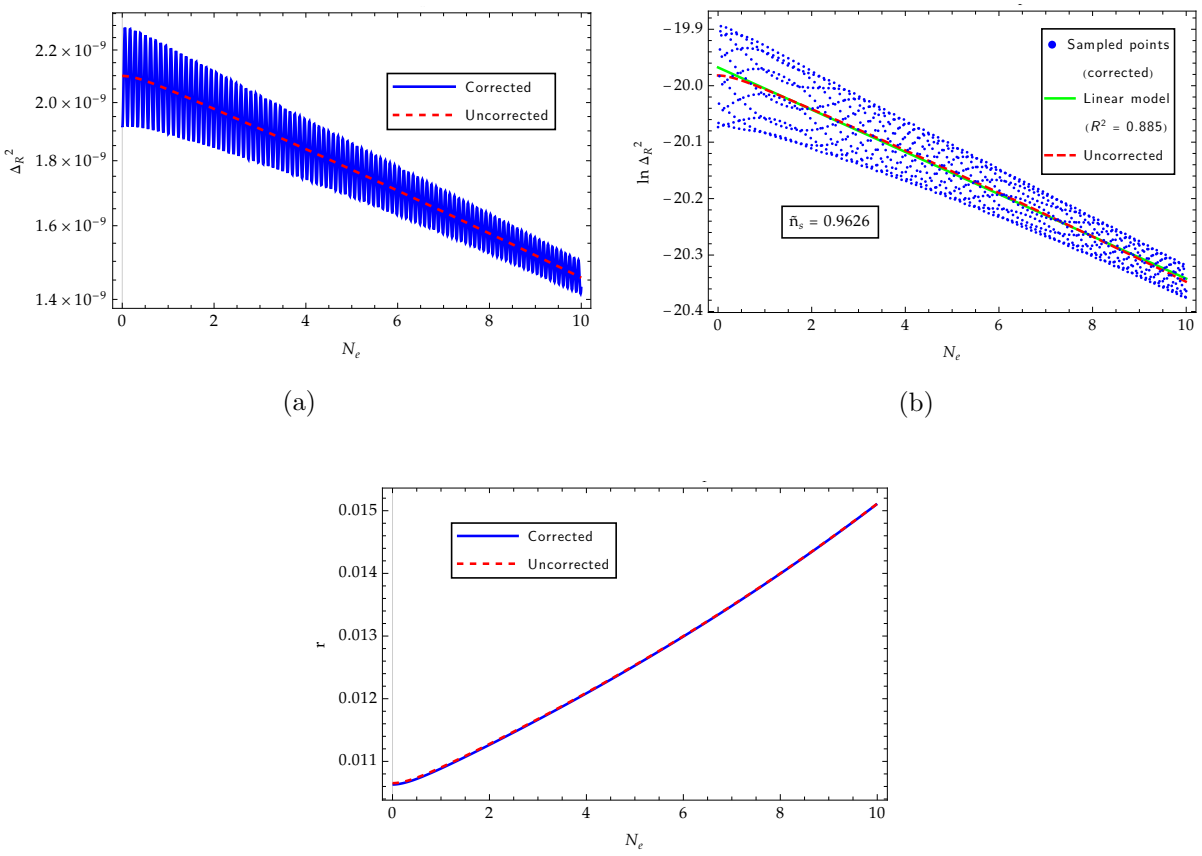

Figure 3.3.22: Evolution (over the initial 10 e-folds of inflation) of the CMB observables (a) $\Delta^2_{\mathcal{R}}$ and (c) r (both their corrected and uncorrected versions) for the quartic hilltop potential with $\phi_i = 7\,M_{\rm P}$ and $\kappa = 10^{-4}$, and model parameters $g = 0.2$ and $M = 1.3 \times 10^{15}$ GeV. In (b) we perform a linear fit to $\ln \Delta^2_{\mathcal{R}}$ and display the obtained R^2 coefficient, as well as the obtained value for $\tilde{n}_s$.

4 Discussion and Conclusion

In this work, we have developed a model for scalar particle production due to a narrow parametric resonance during the inflationary epoch. We checked whether this particle production process can be appreciable while still maintaining the inflaton as the dominant fluid in the Universe, even when the effects of a backreaction are taken into account. There are several conclusions we may draw from our study.

First and foremost, we concluded in § 2.1.2 that the χ particles are relativistic while they are being produced (i.e. while their respective k modes are inside the resonance band), since at such a time their squared physical momentum is essentially equal to $k^2_{c,\mathrm{phys}} = \frac{\langle m_\chi \rangle^2}{2q} \gg \langle m_\chi \rangle^2$, if the resonance is narrow. The fact that all physical momenta of the particles in production at a time z is close to $k_{c,\mathrm{phys}}$, as seen in § 2.2, also allowed us to conclude that the momentum distribution of the χ particles is non-thermal, approximately resembling a Dirac delta function centered at $k_{c,\mathrm{phys}}$, the width of which is roughly $2k_{c,\mathrm{phys}} \sinh\left(\frac{q}{2}\right)$. Moreover, since $k_{c,\mathrm{phys}} = \frac{\langle m_\chi \rangle}{\sqrt{2q}} = \frac{2H}{\gamma}$ varies only due to the slow-roll dynamics, cf. Appendix A, the momentum distribution does not change much in time; rather, it remains roughly the same throughout inflation. In summary, this mechanism leads to the production of relativistic particles with a rather specific value of physical momentum (dependent on the energy scale of inflation via H), which remains essentially unchanged in time.

In §§ 2.2 and 2.3, respectively, we calculated the comoving number density of the χ particles to be given by $\tilde{n}_\chi(z) \approx \frac{2H^3}{3\pi^2\gamma^3}\, a^3(z)\, e^{\frac{\pi q^2}{2\gamma} - \frac{3}{2}q}$ and their physical energy density to be $\rho_\chi \approx \frac{H^4}{\pi^2\gamma^4}\, e^{\frac{\pi q^2}{2\gamma} - 2q}$. In the latter case, we concluded that the energy density of the χ particles is essentially constant in time, only varying adiabatically due to the slow-roll dynamics, and that this was a result of there being an equilibrium between the rate of production and the rate of dilution of these particles, which is a notorious result of our model.

We also concluded (§ 2.4) that the backreaction of the χ particles on the classical inflaton field leads to the appearance of a sinusoidal modulation in the latter's potential, which eventually leads to a similar profile for the classical field solution and (although a little more involved) for the slow-roll parameters. We concluded, however, that despite the large amplitude predicted

for the modulations of, in particular, the backreacted Hubble slow-roll parameters, the backreacted classical inflaton displayed very little change relative to its uncorrected counterpart and was thus able to maintain slow-roll evolution; we explained this phenomenon by the fact that the oscillations of the slow-roll parameters occur very rapidly, so that only the value of these quantities averaged within a period of the oscillation (which we saw led to a great suppression of their amplitudes) would affect the dynamics of the inflaton. Regarding the backreaction on the quantum fluctuations of the inflaton, we concluded that a possible effect was a resonant production of inflaton particles, due to a parametric resonance similar to the one encountered for the χ particles, although typically narrower. We also found the appearance of an additional exponential factor in the power spectrum of the inflaton quantum fluctuations. These effects on the inflaton field induced changes on several CMB observables. In particular, the curvature power spectrum saw the appearance of sinusoidal features and of an exponential factor in its amplitude, with the scalar spectral index and the tensor-to-scalar ratio also being altered due to that (for instance, the latter received an exponential suppression).

In § 3.3, we concluded for three of the four different inflationary potentials we tested (namely, the quadratic monomial and the two hilltop models) that indeed there is a rather significant portion of parameter space that allows us to have an appreciable production of χ particles due to this process of narrow parametric resonance, without this leading to an inevitable dissolution of the underlying inflationary mechanism, i.e. maintaining $\rho_\chi < \rho_\phi$ for the entire slow-roll phase (with an eventual graceful exit from inflation appearing to be possible); on the other hand, the behaviour of the quartic monomial potential did not allow us to draw a suitable conclusion on this regard. Moreover, we found that the resonance is more efficient later in inflation for monomial potentials, whereas for hilltop models this takes place during the first few e-folds. Furthermore, we were able to verify that for the two hilltop models we tested, the predicted values for the considered CMB observables remain compatible with the most recent measurements, even in situations where both the χ and the φ resonances may be considered efficient; however, this agreement was not encountered for the two monomial models. The features on the curvature power spectrum due to the backreaction were also shown to be consistent with current bounds on their amplitude for all considered models. Hence, although the coexistence of our mechanism with the standard inflationary paradigm depends on the inflaton potential we select (with the hilltops displaying the best results), it appears to be plausible, so that our model can be deemed successful in this regard.

Despite the apparently promising results, this model is not a complete description of this system and so we may further improve and refine it. For instance, the full computation of the

effects of the backreaction on the quantum inflaton, including the contribution of the produced inflatons to the energy density, is due. We may too consider the effect of the "classical backreaction" on the value of the tensor-to-scalar ratio, which may either improve or worsen our results, as well as the effect of the backreaction on the running of the scalar spectral index. Moreover, although we mentioned its possible existence, we did not compute the GW spectrum generated by the χ particles [25, 26, 32, 47], whose contribution to the tensor-to-scalar ratio may allow us to restrict even more our parameter space; in fact, this work is currently undergoing and results are expected soon. We can consider as well the possibility of having χ particle production during inflation due to a broad resonance instead and evaluate whether this scenario would ruin inflation or not, as the particle production would surely be more efficient in this case than in the narrow one. Another possibility is the inclusion of additional interaction terms in the Lagrangian from Eq. (2.1.9), for example higher-order terms, interactions with other fields and self-interactions of the χ field, all of which we neglected in our computation; the latter, in particular, allows us to describe the thermal properties of the χ field, including its thermalisation (recall that the momentum distribution of the χ particles is anything but thermal). One can also study the possibility that the particle production during inflation gives rise to a warm inflation regime [52–55], which would surely be an interesting feature of this mechanism if true. All of the obtained results may also be tested for other choices of the inflationary potential.

Additionally, it is important to note that the description of the backreaction via the Hartree approximation is not final. A more rigorous treatment of this, for example more akin to the one done in Refs. [33, 48, 87], is likely required, since other effects which we did not account for may be present (for instance, the appearance of non-local terms in the backreacted EoM [33]).

Another interesting line of work would be to try and devise and analyse an analogous mechanism for other types of fields and particles (vector, spinor, ...), and investigate the repercussions the production of those particles could have for inflation. In particular, it could be of interest to analyse whether standard cosmology can be fully recovered exclusively through particle production during inflation (be it only of scalar particles or of other types as well), or if a post-inflation reheating period is always required, in which case a review of it is relevant. In whichever case, though, a thorough investigation of the thermal properties of the produced fields is also due. Likewise, the decay paths of the produced particles must be investigated in light of the SM; i.e. a theory akin to the elementary theory of reheating [2, 43, 44] must be devised for the particles produced during inflation.

We expect to lead some of these advances ourselves, but we also hope that our results can motivate others to contribute and expand on our work.

Appendices

Appendix A

Time derivatives during inflation

In this appendix, we estimate the time dependence of a few quantities related to our mechanism. For this, we shall consider in particular the derivatives $\frac{q'}{q}$, $\frac{\gamma'}{\gamma}$ and $\frac{\xi'}{\xi}$, where the primes denote differentiation with respect to the number of e-folds, N_e, and $\xi \equiv \frac{\pi q^2}{2\gamma}$. These quantities thus represent the e-fold variation of q, γ and ξ per unit of q, γ and ξ, respectively.

Let us start by determining $\frac{q'}{q}$. From (2.1.31), we have $q = \frac{C_q}{\epsilon_V H^2}$, where C_q is a constant. Differentiating with respect to N_e, we get

$$q' = -C_q \left(\frac{\epsilon_V'}{\epsilon_V^2 H^2} + 2\,\frac{H'}{\epsilon_V H^3} \right) \implies \frac{q'}{q} = -\frac{\dot{\epsilon}_V}{\epsilon_V H} + 2\epsilon_V \,, \tag{A.1}$$

where $dN_e = H dt$ and $-\epsilon_V \approx \frac{\dot{H}}{H^2} = -\epsilon_H$ were used. The latter can be obtained by differentiation of the slow-roll Friedmann equation (1.2.5a) with respect to time

$$2H\dot{H} \approx \frac{V_{,\phi}(\phi)\,\dot{\phi}}{3M_{\rm P}^2} \approx -\frac{[V_{,\phi}(\phi)]^2}{9M_{\rm P}^2 H} \implies \frac{\dot{H}}{H^2} \approx -\frac{[V_{,\phi}(\phi)]^2}{18M_{\rm P}^2 H^4} \approx -\frac{1}{2}M_{\rm P}^2 \left(\frac{V_{,\phi}(\phi)}{V(\phi)}\right)^2 = -\epsilon_V \,, \tag{A.2}$$

where we also used the slow-roll Klein-Gordon equation (1.2.5b), and where the penultimate expression was obtained using the Friedmann equation again. We take the opportunity to show also that $\eta_H \approx \eta_V$, with η_H defined by Eq. (1.2.7b). Since $\epsilon_H \approx \epsilon_V$, we may use the definition of ϵ_V from Eq. (1.2.6) and write

$$\eta_H \;\approx\; 2\epsilon_V - \frac{\epsilon_V'}{2\epsilon_V} \;=\; 2\epsilon_V - \frac{\phi'}{M_{\rm P}^2}\frac{V(\phi)}{V_{,\phi}(\phi)}\,(\eta_V - 2\epsilon_V) \;\approx\; \eta_V \,, \tag{A.3}$$

where we arrived at the second equality by computing the e-fold derivative and using the definitions from Eq. (1.2.6), while the third equality was obtained by using Eqs. (1.2.5a) and (1.2.5b).

Returning to the original derivation, we may thus calculate $\dot{\epsilon}_V \approx \dot{\epsilon}_H$ by using directly the definition of η_H from Eq. (1.2.7b), leading to[25]

$$\frac{\dot{\epsilon}_V}{\epsilon_V H} = -2\left(\eta_V - 2\epsilon_V\right) , \tag{A.4}$$

where we used the fact that $\eta_H \approx \eta_V$, so that

$$\frac{q'}{q} = 2\left(\eta_V - \epsilon_V\right) . \tag{A.5}$$

It is pertinent to note that, since in most inflationary models (and certainly in the ones considered in this work) ϵ_V is strictly increasing during inflation, its growth translating the transition from the slow-roll regime to the post-inflationary period, a relation between η_V and ϵ_V can readily be found by setting $\dot{\epsilon}_V > 0$

$$\eta_V < 2\,\epsilon_V , \tag{A.6}$$

which should thus be valid for most inflaton potentials.

For $\frac{\gamma'}{\gamma}$, taking into account the definition of this quantity $\gamma = C_\gamma \epsilon_V^{-\frac{1}{2}}$, we have

$$\gamma' = -\frac{1}{2} C_\gamma \epsilon_V^{-\frac{3}{2}} \dot{\epsilon}_V H^{-1} \implies \frac{\gamma'}{\gamma} = -\frac{1}{2}\frac{\dot{\epsilon}_V}{\epsilon_V H} = \eta_V - 2\epsilon_V , \tag{A.7}$$

where C_γ is a constant and using (A.4). From (A.6), we immediately see that γ strictly decreases during inflation for the majority of inflationary models.

For $\frac{\xi'}{\xi}$, it's simple to show that

$$\frac{\xi'}{\xi} = \frac{\left(\frac{\pi q^2}{2\gamma}\right)'}{\frac{\pi q^2}{2\gamma}} = 2\,\frac{q'}{q} - \frac{\gamma'}{\gamma} = 3\eta_V - 2\epsilon_V . \tag{A.8}$$

Often, these quantities appear in the form $f \equiv \frac{e^{\alpha\,\xi + \beta\,q}}{\gamma^\delta}$, whose time derivative is then

$$\frac{f'}{f} = \alpha\,\xi\left(3\eta_V - 2\epsilon_V\right) + 2\beta\,q\left(\eta_V - \epsilon_V\right) - \delta\left(\eta_V - 2\epsilon_V\right) . \tag{A.9}$$

Furthermore, considering (2.3.21), we find

$$\frac{\rho_\chi'}{\rho_\chi} = 4(\epsilon_V - \eta_V) + 2q\left(\epsilon_V - \eta_V\right) + \frac{\pi}{2}\xi\left(3\eta_V - 2\epsilon_V\right) , \tag{A.10}$$

[25] It not difficult to show that the usual definition of ϵ_V produces the same result.

such that ρ_χ may either decrease or increase during inflation. Likewise, considering the Friedmann equation (1.2.3), we see that

$$\frac{\rho'_\phi}{\rho_\phi} = -2\epsilon_V < 0\,, \tag{A.11}$$

from which ρ_ϕ always decreases during inflation.

Since the slow-roll parameters are small during inflation, we see that none of these quantities should vary considerably in this period.

Appendix B

Derivation of the Hartree approximation for the backreaction

In this appendix we go through a brief and simple derivation of the effective equation of motion for $\bar{\phi}$, i.e. the classical and homogeneous part of the inflaton, due to χ (cf. § 2.4.1). This is by no means a rigorous calculation, but merely serves as an accurate-enough motivation for the Hartree approximation, i.e. setting $\chi^2 \to \langle \chi^2 \rangle$ in the action (2.4.3), although similar methods can be used to obtain a more thorough description of the backreacted system [33, 71, 73, 87, 88]; we will not concern ourselves with such an analysis here, but some possible paths to follow are briefly discussed in Chapter 4. In order to compute the effects of χ production on the background inflaton field, one may resort to the effective action functional approach, established within the path integral formulation of QFT [18, 66, 69–72]. This functional may be computed by the method due to Jackiw, which uses a saddle-point evaluation in the path integral of the generating functional $Z[J]$, as described in Refs. [18, 66, 69, 87–90], or equivalently by Weinberg's tadpole method [73, 87, 91]. We will consider the former.

We again define the action functional for ϕ and χ as in Eq. (2.4.3),

$$S[\phi, \chi] = \int d^4x \sqrt{-g}\, \mathcal{L}_{\phi\chi}\,, \tag{B.1}$$

where the Lagrangian is given by Eq. (2.4.2) as

$$\mathcal{L}_{\phi\chi} = \frac{1}{2}\partial_\mu\phi\,\partial^\mu\phi + \frac{1}{2}\partial_\mu\chi\,\partial^\mu\chi - \frac{1}{2}m_\chi^2(\phi)\,\chi^2 - V(\phi)\,. \tag{B.2}$$

Using integration by parts, it is simple to show that

$$S[\phi,\chi] \;=-\int d^4x\,\sqrt{-g}\left[\frac{1}{2}\,\phi\,\Box\,\phi+\frac{1}{2}\,\chi\,\Box\,\chi+\frac{1}{2}m_\chi^2(\phi)\,\chi^2+V(\phi)\right]. \tag{B.3}$$

where we discarded a surface integral (obtained using a 4-dimensional version of the divergence theorem) on the assumption that the fields vanish at infinity [18, 66].

We may now define the generating functional of the sources J_ϕ and J_χ

$$Z[J_\phi,J_\chi] \;\equiv\; \int \mathcal{D}\phi\,\mathcal{D}\chi\; e^{i\left[S[\phi,\chi]+(J_\phi,\phi)+(J_\chi,\chi)\right]}, \tag{B.4}$$

where $(f_1,f_2)\equiv\int d^4x\sqrt{-g}\,f_1(x)\,f_2(x)$ is the inner product on the spacetime defined by the metric $g_{\mu\nu}$ [88]. In the saddle point approximation, we write the full inflaton field as $\phi=\bar{\phi}+\varphi$, as we did before, but we now consider the classical background inflaton $\bar{\phi}$ to be a stationary point of the integral in Eq. (B.4); that is

$$\left.\frac{\delta\left(S[\phi,\chi]+(J_\phi,\phi)+(J_\chi,\chi)\right)}{\delta\phi(x)}\right|_{\substack{\phi=\bar{\phi}\\ \chi=0}} \;=\; 0\,. \tag{B.5}$$

With this, we Taylor expand $S[\phi,\chi]$ in the exponent of Eq. (B.4) around $\phi=\bar{\phi}$ and to second-order in φ and χ (we consider the background value of χ to be zero), leading to

$$\begin{aligned}
S[\phi,\chi]+(J_\phi,\phi)+(J_\chi,\chi) \;=\; & S[\bar{\phi},0]+\int d^4x\,\left.\frac{\delta S[\phi,\chi]}{\delta\phi(x)}\right|_{\substack{\phi=\bar{\phi}\\ \chi=0}}\varphi(x)+\int d^4x\,\left.\frac{\delta S[\phi,\chi]}{\delta\chi(x)}\right|_{\substack{\phi=\bar{\phi}\\ \chi=0}}\chi(x)\\
&+\;\frac{1}{2}\int d^4x\int d^4y\,\left.\frac{\delta^2 S[\phi,\chi]}{\delta\phi(x)\delta\phi(y)}\right|_{\substack{\phi=\bar{\phi}\\ \chi=0}}\varphi(x)\,\varphi(y)\\
&+\;\frac{1}{2}\int d^4x\int d^4y\,\left.\frac{\delta^2 S[\phi,\chi]}{\delta\chi(x)\delta\chi(y)}\right|_{\substack{\phi=\bar{\phi}\\ \chi=0}}\chi(x)\,\chi(y)\\
&+\;(J_\phi,\bar{\phi})+(J_\phi,\varphi)+(J_\chi,\chi)\,,
\end{aligned} \tag{B.6}$$

where we did not include terms with mixed derivatives, as they vanish upon considering the condition $\chi=0$. Moreover, we see from Eq. (B.5) that the second and third terms of Eq. (B.6) cancel the last two, respectively, while the remaining terms, upon computing the second-order functional derivatives, eventually lead to the following expression for the generating functional

$$
\begin{aligned}
Z[J_\phi] &= e^{i\left[S[\bar{\phi},0]+(J_\phi,\bar{\phi})\right]} \int \mathcal{D}\varphi\, e^{-\frac{1}{2}\int d^4x\,\varphi\left[i\sqrt{-g}\left(\Box+\bar{V}''\right)\right]\varphi} \int \mathcal{D}\chi\, e^{-\frac{1}{2}\int d^4x\,\chi\left[i\sqrt{-g}\left(\Box+\bar{m}_\chi^2\right)\right]\chi} \\
&= e^{i\left[S[\bar{\phi},0]+(J_\phi,\bar{\phi})\right]} \left[\det\left(\sqrt{-g}\left(\Box+\bar{V}''\right)\right)\right]^{-\frac{1}{2}} \left[\det\left(\sqrt{-g}\left(\Box+\bar{m}_\chi^2\right)\right)\right]^{-\frac{1}{2}} ,
\end{aligned}
\tag{B.7}
$$

where we set $\mathcal{D}\phi \to \mathcal{D}\varphi$; the bars indicate that the functionals and functions are to be evaluated at the classical, homogeneous inflaton field $\bar{\phi}$, and the primes denote derivatives with respect to that field. Notice that we have removed the source J_χ from the argument of the functional, since we no longer have such a dependence (at least explicitly). Moreover, to obtain the second line we used the path integral definition of the functional determinant (see Refs. [18, 66, 88]), which allowed us to cast our generating functional in a more compact and useful form. Taking into account the relation $\det A = e^{\mathrm{Tr}\ln A}$ and the definitions of the connected generating functional, $W[J_\phi] = -i\ln Z[J_\phi]$, and of the effective action, $\Gamma[\bar{\phi}] = W[J_\phi] - (J_\phi,\bar{\phi})$, it is simple to see that [18, 66, 88]

$$
\Gamma[\bar{\phi}] = S[\bar{\phi},0] + \frac{i}{2}\,\mathrm{Tr}\ln\left(\Box+\bar{m}_\chi^2\right) + \frac{i}{2}\,\mathrm{Tr}\ln\left(\Box+\bar{V}''\right) , \tag{B.8}
$$

up to an additive constant in $\bar{\phi}$; this result is known as the *one-loop* effective action, due to it being computable via Feynman diagrams with a single loop [18, 70, 87, 88]. This quantity, which is a Legendre transformation of the connected generating functional, is itself a functional of the classical background field $\bar{\phi}$, which allows us to obtain its equation of motion taking into account quantum corrections [18, 66, 70, 87, 88]. Since we are only interested in the correction due to χ, we may drop the third term in the expression altogether.

The effective equation of motion for $\bar{\phi}$ is then obtained via the condition

$$
\frac{\delta\Gamma[\bar{\phi}]}{\delta\bar{\phi}(x)} = 0 , \tag{B.9}
$$

resulting in

$$
\Box_x\bar{\phi} + \bar{V}' + \frac{i}{2}\,\mathrm{Tr}_y\left[(\bar{m}_\chi^2)'\left(\Box_y+\bar{m}_\chi^2\right)^{-1}\frac{1}{\sqrt{-g}}\,\delta^4(x-y)\right] = 0 , \tag{B.10}
$$

which was computed via the limit definition of the functional derivative [18, 66].

Since the propagator of the field χ is defined as $i\Delta_\chi(x-y) = \left(\Box_y+\bar{m}_\chi^2\right)^{-1}\frac{1}{\sqrt{-g}}\,i\delta^4(x-y)$, we can rewrite the equation as

$$
\Box_x\bar{\phi} + \bar{V}' + \frac{1}{2}\,\mathrm{Tr}_y\left[(\bar{m}_\chi^2)'i\Delta_\chi(x-y)\right] = 0 . \tag{B.11}
$$

The Hartree approximation can be obtained if we assume that the trace satisfies $\mathrm{Tr}_y\left[(\bar{m}_\chi^2)' i\Delta_\chi(x-y)\right] \approx (\bar{m}_\chi^2)'\,\mathrm{Tr}_y\left[i\Delta_\chi(x-y)\right]$.[26] Since the Fourier transform is a unitary transformation, under which the trace is invariant, we may go to momentum space, where we compute the trace as a sum (in this case, an integral) of the eigenvalues of the propagator transform in that space, which are given by [33]

$$i\tilde{\Delta}_\chi(k^\mu) = \frac{ia^{-4}}{k_\mu^{\mathrm{phys}} k^\mu_{\mathrm{phys}} - \bar{m}_\chi^2} + 2\pi\,\frac{\tilde{n}_k}{a^3}\,\delta(k_\mu^{\mathrm{phys}} k^\mu_{\mathrm{phys}} - \bar{m}_\chi^2)\,, \tag{B.12}$$

where $k^\mu = (k^0, \mathbf{k})$ is the comoving 4-momentum, $\frac{\tilde{k}^\mu}{a} \equiv k^\mu_{\mathrm{phys}} = (k^0_{\mathrm{phys}}, \mathbf{k}_{\mathrm{phys}})$ is the physical 4-momentum and $k_\mu^{\mathrm{phys}} k^\mu_{\mathrm{phys}} = (k^0_{\mathrm{phys}})^2 - k^2_{\mathrm{phys}}$, with $k^2_{\mathrm{phys}} = |\mathbf{k}_{\mathrm{phys}}|^2$. The quantity $\tilde{n}_k$ is just the comoving occupation number of k-momentum χ particles. We see that two terms appear to contribute to the propagator, the first term is the CW term [70], corresponding to the usual vacuum propagator for scalar fields, while the second term corresponds to the excitations of the χ field from its vacuum state, i.e. to the produced χ particles (notice that if $\tilde{n}_k = 0$, we are left with the vacuum propagator only). The expression in Eq. (B.12) can be obtained from the following definition of the real-space propagator $i\Delta_\chi(x-x')$, which uses the Fourier expansion of $\hat{\chi}$ from Eq. (2.1.14),

$$\begin{aligned} i\Delta_\chi(x,x') &= \langle 0|\,T\{\hat{\chi}(x)\,\hat{\chi}(x')\}\,|0\rangle \\ &= \theta(t-t')\int \frac{d^3k}{(2\pi)^3}\,\chi_k(t)\,\chi_k^*(t')\,e^{i\mathbf{k}\cdot(\mathbf{x}-\mathbf{x}')} \\ &\quad + \theta(t'-t)\int \frac{d^3k}{(2\pi)^3}\,\chi_k(t')\,\chi_k^*(t)\,e^{-i\mathbf{k}\cdot(\mathbf{x}-\mathbf{x}')}\,, \end{aligned} \tag{B.13}$$

where T is a time-ordering operator and $\theta(t-t')$ is a Heaviside step function [66], and by using the expansion of the field modes $\chi_k(t)$ in terms of Bogoliubov coefficients (see Eq. (2.4.8)). Usually, this definition of $i\Delta_\chi(x,x')$ refers to the vacuum propagator; however, the usage of a Bogoliubov expansion for the mode functions allows us to extend this definition to out-of-vacuum (i.e. excited) states. We consider that the interval $|t-t'|$ is small enough to allow us to approximate $a(t) \approx a(t')$ and so $\omega_k(t) \approx \omega_k(t')$, which greatly simplifies the $\chi_k(t)$ expansion; moreover, we identify $\tilde{n}_k = |\beta_k|^2$ as in § 2.4.1. Using contour integration techniques [66] and the properties of the Dirac delta function, it is then possible to show that the real-space propagator can be written as

[26] In principle, a more rigorous treatment should then require the computation of the full trace from Eq. (B.11).

$$
\begin{aligned}
i\Delta_\chi(x,x') &= \int \frac{d^4k}{(2\pi)^4}\left[\frac{ia^{-4}}{k^{\rm phys}_\mu k^\mu_{\rm phys}-\bar{m}^2_\chi}+2\pi\,\frac{\tilde{n}_k}{a^3}\,\delta(k^{\rm phys}_\mu k^\mu_{\rm phys}-\bar{m}^2_\chi)\right]e^{-ik\cdot(x-x')} \\
&\equiv \int \frac{d^4k}{(2\pi)^4}\,i\tilde{\Delta}_\chi(k^\mu)\,e^{-ik\cdot(x-x')}\,,
\end{aligned}
\tag{B.14}
$$

from where Eq. (B.12) follows directly. Hence, the momentum space trace simply becomes

$$
{\rm Tr}_k\left[i\tilde{\Delta}_\chi(k^\mu)\right] = \int \frac{d^4k}{(2\pi)^4}\left[\frac{ia^{-4}}{k^{\rm phys}_\mu k^\mu_{\rm phys}-\bar{m}^2_\chi}+2\pi\,\frac{\tilde{n}_k}{a^3}\,\delta(k^{\rm phys}_\mu k^\mu_{\rm phys}-\bar{m}^2_\chi)\right], \tag{B.15}
$$

where the integration is, as usual, done on the comoving momentum. We readily identify the same two terms as in Eq. (B.12): the first one is the CW term, and it corresponds to the vacuum contribution to the trace of propagator; the second term is the contribution of the produced χ particles to this trace. As was stated in the main text, upon $\overline{\rm MS}$ renormalisation [55, 74] of the CW term, we found that its contribution to the trace in Eq. (B.15) is subdominant for all the inflationary models we considered, with the term containing $\tilde{n}_k$ providing the leading contribution; hence, the CW term may be neglected. Moreover, we also ignore the vacuum subtraction coming from the expression $\tilde{n}_k = \frac{1}{2}\frac{\omega_k}{\omega^0_k}\,e^{2\mu_k z}-\frac{1}{2}$, so that we are left only with the exponential contribution, in which case Eq. (B.15) may be further simplified by performing the k^0 integration (considering that $k^{\rm phys}_\mu k^\mu_{\rm phys} = (k^0_{\rm phys})^2 - k^2_{\rm phys} = (k^0_{\rm phys})^2 - \omega_k^2 + \bar{m}^2_\chi$), ridding it of the delta function and thus resulting in

$$
{\rm Tr}_k\left[i\tilde{\Delta}_\chi(k^\mu)\right] = \frac{1}{a^3}\int\frac{d^3k}{(2\pi)^3}\,\frac{e^{2\mu_k z}}{2\omega_k} = \langle\chi^2\rangle\,. \tag{B.16}
$$

Equation (B.11) thus becomes

$$
\Box\bar{\phi} + \bar{V}' + \frac{1}{2}(\bar{m}^2_\chi)'\,\langle\chi^2\rangle = 0\,, \tag{B.17}
$$

just as we had obtained in Eq. (2.4.6) under the Hartree approximation.

Appendix C

Approximations

C.1 Variation of $X_k(t) = a^{3/2}(t)\,\chi_k(t)$

In this appendix, we shall demonstrate relation (2.3.9) from § 2.3. We start by writing ρ_k as we did in (2.3.6)

$$\rho_k \equiv \frac{1}{2}|\dot{\chi}_k|^2 + \frac{k^2}{2a^2}|\chi_k|^2 + \frac{1}{2}m_\chi^2|\chi_k|^2\,. \tag{C.1}$$

If we use $\chi_k(t) = X_k(t)\,a^{-3/2}(t)$, we can easily arrive at $\dot{\chi}_k = \left(\dot{X}_k - \frac{3}{2}HX_k\right)a^{-3/2}$, where $H = \frac{\dot{a}}{a}$. With this, we can calculate

$$|\dot{\chi}_k|^2 = a^{-3}\left[|\dot{X}_k|^2 + \frac{9}{4}H^2|X_k|^2 - 3H\,\mathfrak{Re}(\dot{X}_k X_k^*)\right]\,. \tag{C.2}$$

Substituting in (C.1) and using $\omega_k^2 = \frac{k^2}{a^2} + m_\chi^2$, we get

$$\rho_k \equiv \frac{a^{-3}}{2}\left[|\dot{X}_k|^2 + \omega_k^2\,|X_k|^2 + \frac{9}{4}H^2|X_k|^2 - 3H\,\mathfrak{Re}(\dot{X}_k X_k^*)\right]\,. \tag{C.3}$$

We may use (2.2.6) and estimate $\omega_k \sim \frac{2H}{\gamma}$ and $\mu_k(z) \sim \mu_k^{\max} = \frac{q}{2}$ for modes near the resonance band, making

$$X_k(t) \;\propto\; e^{-i\omega_k t}\,e^{\frac{2H}{\gamma}\mu_k(t)\,t} \;\sim\; e^{\left(-i\frac{2H}{\gamma}+\frac{H}{\gamma}q\right)t} \;\approx\; e^{-i\frac{2H}{\gamma}t}\,, \tag{C.4}$$

where the last approximation is attained by comparing the absolute value of each term inside the parentheses and by taking $q \ll 1$ and $\gamma \ll 1$. This means that $\dot{X}_k \sim -\frac{2H}{\gamma}X_k$, and so

$$|\dot{X}_k|^2 \sim \left(\frac{2H}{\gamma}\right)^2 |X_k|^2 \tag{C.5a}$$

$$\omega_k^2 |X_k|^2 \sim \left(\frac{2H}{\gamma}\right)^2 |X_k|^2 \tag{C.5b}$$

$$3H\,\mathfrak{Re}(\dot{X}_k X_k^*) \sim -3H\frac{2H}{\gamma}|\chi_k|^2 = -\frac{6H^2}{\gamma}|\chi_k|^2\,, \tag{C.5c}$$

such that $|\dot{X}_k|^2$ and $\omega_k^2 |X_k|^2$ dominate over $\frac{9}{4}H^2|X_k|^2$ and $3H\,\mathfrak{Re}(\dot{X}_k X_k^*)$. Hence,

$$\rho_k \approx \frac{a^{-3}}{2}\left(|\dot{X}_k|^2 + \omega_k^2 |X_k|^2\right)\,. \tag{C.6}$$

As in Eq. (2.2.3), we define the comoving energy of the k modes, $\tilde{\rho}_k$, as

$$\tilde{\rho}_k \equiv \frac{1}{2}\left(|\dot{X}_k|^2 + \omega_k^2 |X_k|^2\right)\,, \tag{C.7}$$

and the comoving particle number, $\tilde{n}_k$, as

$$\tilde{\rho}_k \equiv \omega_k\left(\tilde{n}_k + \frac{1}{2}\right) \iff \tilde{n}_k \equiv \frac{\tilde{\rho}_k}{\omega_k} - \frac{1}{2}\,, \tag{C.8}$$

which of course allows us to write

$$\rho_k \approx \frac{\tilde{\rho}_k}{a^3} \tag{C.9}$$

and, using $\rho_k \equiv \omega_k\left(n_k + \frac{1}{2}\right)$,

$$n_k + \frac{1}{2} \approx \frac{1}{a^3}\left(\tilde{n}_k + \frac{1}{2}\right)\,. \tag{C.10}$$

C.2 Backreacted potential and equation of motion

In this appendix, we demonstrate some relations used or mentioned when discussing the back-reaction on the classical inflaton, in § 2.4.1.

We start by showing that $\left|\frac{\Delta V}{V}\right|_{\max} \ll \left|\frac{\Delta V'}{V'}\right|_{\max} \ll \left|\frac{\Delta V''}{V''}\right|_{\max}$, where $\Delta V^{(n)} \equiv \mathcal{V}^{(n)} - V^{(n)}$, with $\mathcal{V}$ given by Eq. (2.4.15), and where V is written using the uncorrected slow-roll Friedmann equation (1.2.5a). The primes denote derivatives with respect to the uncorrected classical inflaton, with which we will work in this appendix. We denote this field as ϕ_0 and the uncorrected Hubble parameter as H. From the definitions of ϵ_V and η_V in Eq. (1.2.6), we readily find

$$|V'| = \frac{\sqrt{2\epsilon_V}}{M_\mathrm{P}}\, V \tag{C.11a}$$

$$|V''| = \frac{|\eta_V|}{M_\mathrm{P}^2}\, V\,. \tag{C.11b}$$

Moreover, since we are assuming Λ^4 to vary adiabatically, we neglect its derivatives (as per the discussion following Eq. (2.4.14)), which leads to

$$\left|\Delta V^{(n)}\right|_\mathrm{max} \approx \left(\frac{2}{M}\right)^n |\Delta V|_\mathrm{max}\,, \tag{C.12}$$

from where

$$\left|\frac{\Delta V'}{V'}\right|_\mathrm{max} \approx \sqrt{\frac{2}{\epsilon_V}}\,\frac{M_\mathrm{P}}{M}\,\left|\frac{\Delta V}{V}\right|_\mathrm{max} \gg \left|\frac{\Delta V}{V}\right|_\mathrm{max} \tag{C.13a}$$

$$\left|\frac{\Delta V''}{V''}\right|_\mathrm{max} \approx \frac{4}{|\eta_V|}\left(\frac{M_\mathrm{P}}{M}\right)^2 \left|\frac{\Delta V}{V}\right|_\mathrm{max} \gg \left|\frac{\Delta V'}{V'}\right|_\mathrm{max} \gg \left|\frac{\Delta V}{V}\right|_\mathrm{max}\,, \tag{C.13b}$$

assuming that $M < M_\mathrm{P}$ (which is indeed verified, cf. in particular § 3.1), proving our claim.

Next, we briefly show that $\left|\frac{\mathcal{V}'}{V}\,\phi_1\right| \ll 1$ and $|\Lambda^4| \ll \left|\frac{M}{2}\,V'\right|$. For the former, using the above relations, it is simple to see that

$$\left|\frac{\mathcal{V}'}{V}\,\phi_1\right| \leqslant \frac{|V'| + |\Delta V'|}{|V|}\,|\phi_1| \leqslant \left[\frac{\sqrt{2\epsilon_V}}{M_\mathrm{P}} + \left(\frac{2}{M}\right)\left|\frac{\Delta V}{V}\right|_\mathrm{max}\right]|\phi_1| \ll 1\,, \tag{C.14}$$

since $|\phi_1| \ll \frac{M}{2}$ and $\left|\frac{\Delta V}{V}\right|_\mathrm{max} \ll 1$, as we know from §§ 2.4.1 and 3.3. The latter relation is not as straightforward to prove; considering the quantity

$$\left|\frac{\Lambda^4}{V'}\right| = \frac{M_\mathrm{P}}{\sqrt{2\epsilon_V}}\left|\frac{\Delta V}{V}\right|_\mathrm{max}\,, \tag{C.15}$$

it is not immediately clear whether it is smaller than $\frac{M}{2}$. However, we show in § 3.3 that for all tested inflationary potentials $\left|\frac{\Delta V}{V}\right|_\mathrm{max} \sim 10^{-5}$, in agreement with the bounds encountered by Refs. [29, 76, 77] (the most stringent one being $\left|\frac{\Delta V}{V}\right|_\mathrm{max} \lesssim 3 \times 10^{-5}$, from Ref. [76]), whereas ϵ_V is usually greater than $\mathcal{O}(10^{-3})$ during inflation. Thus,

$$\left|\frac{\Lambda^4}{V'}\right| \lessapprox 10^{-4}\, M_\mathrm{P} \lesssim \frac{M}{2}\,, \tag{C.16}$$

considering the typical ranges for M (cf. § 3.3).

Lastly, we show that $|A\,\frac{M}{2}| \ll 1$, $|B\,\frac{M^2}{4}| \ll 1$ and $A^2 \gg |B|$, with $A = -\frac{3}{M_{\rm P}}\,\frac{1}{\sqrt{2\epsilon_{V_*}}}$ and $B = \frac{3}{2M_{\rm P}^2}\left(\frac{\eta_{V_*}}{\epsilon_{V_*}} - 1\right)$. Starting with the first relation, we have

$$\left|A\,\frac{M}{2}\right| \;=\; \frac{3}{2\sqrt{2}}\,\frac{1}{\sqrt{\epsilon_{V_*}}}\,\frac{M}{M_{\rm P}} \;\ll\; 1\,, \tag{C.17}$$

given that $\epsilon_{V_*} \gtrsim 10^{-3}$ for most inflationary models and $\frac{M}{M_{\rm P}} \lesssim 10^{-3}$. For the second expression, we find

$$\left|B\,\frac{M^2}{4}\right| \;=\; \frac{3}{8}\left|\frac{\eta_{V_*}}{\epsilon_{V_*}} - 1\right|\left(\frac{M}{M_{\rm P}}\right)^2 \;\ll\; 1\,, \tag{C.18}$$

since for the models we are considering $\left|\frac{\eta_{V_*}}{\epsilon_{V_*}} - 1\right| \lesssim 10^3$ (cf. § 3.3 and references therein). Lastly, for the third expression we obtain

$$A^2 \;=\; \frac{9}{2}\,\frac{1}{M_{\rm P}^2}\,\frac{1}{\epsilon_{V_*}} \;\gg\; \frac{9}{2}\,\frac{1}{M_{\rm P}^2}\,\frac{1}{\epsilon_{V_*}}\,|\eta_{V_*} - \epsilon_{V_*}| \;\sim\; |B|\,. \tag{C.19}$$

References

[1] S. Dodelson and F. Schmidt, *Modern Cosmology*. Elsevier Science, 2020. [Online]. Available: https://doi.org/10.1016/C2017-0-01943-2

[2] D. Baumann, "The Physics of Inflation: A Course for Graduate Students in Particle Physics and Cosmology," 2011, ICTS. [Online]. Available: https://www.icts.res.in/sites/default/files/baumann_icts_dec2011.pdf

[3] E. Kolb and M. Turner, *The Early Universe*. CRC Press, 2018. [Online]. Available: https://doi.org/10.1201/9780429492860

[4] N. Aghanim, Y. Akrami, F. Arroja, M. Ashdown, J. Aumont, C. Baccigalupi *et al.*, "Planck 2018 results: I. Overview and the cosmological legacy of Planck," *Astronomy & Astrophysics*, vol. 641, p. A1, Sep. 2020. [Online]. Available: https://arxiv.org/abs/1807.06205

[5] N. Aghanim, Y. Akrami, M. Ashdown, J. Aumont, C. Baccigalupi, M. Ballardini *et al.*, "Planck 2018 results: VI. Cosmological parameters," *Astronomy & Astrophysics*, vol. 641, p. A6, Sep. 2020. [Online]. Available: https://arxiv.org/abs/1807.06209

[6] S. M. Carroll, *Spacetime and Geometry: An Introduction to General Relativity*. Cambridge University Press, 7 2019. [Online]. Available: https://doi.org/10.1017/9781108770385

[7] A. Riotto, "Inflation and the theory of cosmological perturbations," *ICTP Lect. Notes Ser.*, vol. 14, pp. 317–413, 2003. [Online]. Available: https://arxiv.org/abs/hep-ph/0210162

[8] S. Weinberg, *Cosmology*. Oxford University Press, 02 2008. [Online]. Available: https://doi.org/10.1093/oso/9780198526827.001.0001

[9] R. Pathria and P. Beale, *Statistical Mechanics*. Elsevier Science, 2021. [Online]. Available: https://www.sciencedirect.com/book/9780081026922/statistical-mechanics

[10] R. Brawer, "Inflationary Cosmology and Horizon and Flatness Problems: The Mutual Constitution of Explanation and Questions," Master's thesis, MIT, 1996. [Online]. Available: https://inspirehep.net/literature/1476684

[11] D. Baumann, "TASI Lectures on Inflation," in *Theoretical Advanced Study Institute in Elementary Particle Physics: Physics of the Large and the Small*, 2011, pp. 523–686. [Online]. Available: https://arxiv.org/abs/0907.5424

[12] A. Linde, "Particle physics and inflationary cosmology," 2005. [Online]. Available: https://arxiv.org/abs/hep-th/0503203

[13] A. Linde, "Inflationary Cosmology," *Lect. Notes Phys.*, vol. 738, pp. 1–54, 2008. [Online]. Available: https://doi.org/10.1007/978-3-540-74353-8_1

[14] A. Linde, "A new inflationary universe scenario: A possible solution of the horizon, flatness, homogeneity, isotropy and primordial monopole problems," *Physics Letters B*, vol. 108, no. 6, pp. 389–393, 1982. [Online]. Available: https://doi.org/10.1016/0370-2693(82)91219-9

[15] A. H. Guth, "Inflationary universe: A possible solution to the horizon and flatness problems," *Phys. Rev. D*, vol. 23, pp. 347–356, Jan 1981. [Online]. Available: https://link.aps.org/doi/10.1103/PhysRevD.23.347

[16] A. D. Linde, "Chaotic Inflation," *Physics Letters B*, vol. 129, pp. 177–181, 1983. [Online]. Available: https://inspirehep.net/literature/196244

[17] S. Weinberg, *The Quantum Theory of Fields. Vol. 1: Foundations.* Cambridge University Press, 6 2005. [Online]. Available: https://doi.org/10.1017/CBO9781139644167

[18] L. H. Ryder, *Quantum Field Theory.* Cambridge University Press, 1996. [Online]. Available: https://doi.org/10.1017/CBO9780511813900

[19] D. Benisty, E. I. Guendelman, E. N. Saridakis, H. Stoecker, J. Struckmeier, and D. Vasak, "Inflation from fermions with curvature-dependent mass," *Phys. Rev. D*, vol. 100, no. 4, p. 043523, 2019.

[20] A. Golovnev, V. Mukhanov, and V. Vanchurin, "Vector inflation," *Journal of Cosmology and Astroparticle Physics*, vol. 2008, no. 06, p. 009, Jun. 2008. [Online]. Available: http://dx.doi.org/10.1088/1475-7516/2008/06/009

[21] L. H. Ford, "Inflation driven by a vector field," *Phys. Rev. D*, vol. 40, p. 967, 1989. [Online]. Available: https://inspirehep.net/literature/278867

[22] J. Martin, C. Ringeval, and V. Vennin, "Encyclopædia Inflationaris," *Phys. Dark Univ.*, vol. 5-6, pp. 75–235, 2014. [Online]. Available: https://arxiv.org/abs/1303.3787

[23] R. Flauger and E. Pajer, "Resonant non-gaussianity," *Journal of Cosmology and Astroparticle Physics*, vol. 2011, no. 01, p. 017–017, Jan. 2011. [Online]. Available: http://dx.doi.org/10.1088/1475-7516/2011/01/017

[24] A. R. Liddle, P. Parsons, and J. D. Barrow, "Formalizing the slow-roll approximation in inflation," *Physical Review D*, vol. 50, no. 12, p. 7222–7232, Dec. 1994. [Online]. Available: http://dx.doi.org/10.1103/PhysRevD.50.7222

[25] C. Caprini and D. G. Figueroa, "Cosmological backgrounds of gravitational waves," *Classical and Quantum Gravity*, vol. 35, no. 16, p. 163001, Jul. 2018. [Online]. Available: http://dx.doi.org/10.1088/1361-6382/aac608

[26] M. C. Guzzetti, N. Bartolo, M. Liguori, and S. Matarrese, "Gravitational waves from inflation," *Riv. Nuovo Cim.*, vol. 39, no. 9, pp. 399–495, 2016. [Online]. Available: https://arxiv.org/abs/1605.01615

[27] M. Sasaki, "Large Scale Quantum Fluctuations in the Inflationary Universe," *Progress of Theoretical Physics*, vol. 76, no. 5, pp. 1036–1046, 11 1986. [Online]. Available: https://doi.org/10.1143/PTP.76.1036

[28] V. F. Mukhanov, "Gravitational Instability of the Universe Filled with a Scalar Field," *JETP Lett.*, vol. 41, pp. 493–496, 1985. [Online]. Available: https://inspirehep.net/literature/222017

[29] Y. Akrami, F. Arroja, M. Ashdown, J. Aumont, C. Baccigalupi, M. Ballardini *et al.*, "Planck 2018 results: X. Constraints on inflation," *Astronomy & Astrophysics*, vol. 641, p. A10, Sep. 2020. [Online]. Available: http://dx.doi.org/10.1051/0004-6361/201833887

[30] G. Domenech, "Scalar induced gravitational waves review," *Universe*, vol. 7, no. 11, p. 398, Oct. 2021. [Online]. Available: http://dx.doi.org/10.3390/universe7110398

[31] D. Baumann, P. Steinhardt, K. Takahashi, and K. Ichiki, "Gravitational wave spectrum induced by primordial scalar perturbations," *Physical Review D*, vol. 76, no. 8, Oct. 2007. [Online]. Available: http://dx.doi.org/10.1103/PhysRevD.76.084019

[32] L. A. Boyle and P. J. Steinhardt, "Probing the early universe with inflationary gravitational waves," *Physical Review D*, vol. 77, no. 6, Mar. 2008. [Online]. Available: https://arxiv.org/abs/astro-ph/0512014

[33] L. Kofman, A. Linde, and A. A. Starobinsky, "Towards the theory of reheating after inflation," *Physical Review D*, vol. 56, no. 6, pp. 3258–3295, Sep 1997. [Online]. Available: https://doi.org/10.1103%2Fphysrevd.56.3258

[34] L. Kofman, A. Linde, and A. A. Starobinsky, "Reheating after inflation," *Physical Review Letters*, vol. 73, no. 24, pp. 3195–3198, Dec 1994. [Online]. Available: https://doi.org/10.1103%2Fphysrevlett.73.3195

[35] J. Braden, L. Kofman, and N. Barnaby, "Reheating the universe after multi-field inflation," *Journal of Cosmology and Astroparticle Physics*, vol. 2010, no. 07, p. 016–016, Jul. 2010. [Online]. Available: http://dx.doi.org/10.1088/1475-7516/2010/07/016

[36] N. McLachlan, *Theory and Application of Mathieu Functions*. Clarendon Press, 1947. [Online]. Available: https://api.semanticscholar.org/CorpusID:118459732

[37] M. Abramowitz and I. Stegun, *Handbook of Mathematical Functions: with Formulas, Graphs, and Mathematical Tables*, ser. Dover Books on Mathematics. Dover Publications, 2012. [Online]. Available: https://api.semanticscholar.org/CorpusID:121782574

[38] F. Olver, D. Lozier, R. Boisvert, and C. Clark, *The NIST Handbook of Mathematical Functions*. Cambridge University Press, New York, NY, 2010-05-12 00:05:00 2010. [Online]. Available: https://www.nist.gov/publications/nist-handbook-mathematical-functions

[39] "*NIST Digital Library of Mathematical Functions*," Release 1.2.1 of 2024-06-15, f. W. J. Olver, A. B. Olde Daalhuis, D. W. Lozier, B. I. Schneider, R. F. Boisvert, C. W. Clark, B. R. Miller, B. V. Saunders, H. S. Cohl, and M. A. McClain, eds. [Online]. Available: https://dlmf.nist.gov/

[40] J. G. Rosa and J. March-Russell, "Resonant particle production in branonium," *Physical Review D*, vol. 77, no. 12, Jun 2008. [Online]. Available: https://doi.org/10.1103%2Fphysrevd.77.126004

[41] P. B. Greene and L. Kofman, "Preheating of fermions," *Physics Letters B*, vol. 448, no. 1-2, pp. 6–12, Feb 1999. [Online]. Available: https://doi.org/10.1016%2Fs0370-2693%2899%2900020-9

[42] J. T. Deskins, J. T. Giblin, and R. R. Caldwell, "Gauge Field Preheating at the End of Inflation," *Phys. Rev. D*, vol. 88, no. 6, p. 063530, 2013. [Online]. Available: https://arxiv.org/abs/1305.7226

[43] L. F. Abbott, E. Farhi, and M. B. Wise, "Particle production in the new inflationary cosmology," *Physics Letters B*, vol. 117, no. 1-2, pp. 29–33, Nov. 1982. [Online]. Available: https://ui.adsabs.harvard.edu/abs/1982PhLB..117...29A

[44] A. D. Dolgov and A. D. Linde, "Baryon Asymmetry in Inflationary Universe," *Physics Letters B*, vol. 116, p. 329, 1982. [Online]. Available: https://inspirehep.net/literature/178480

[45] A. Albrecht, P. J. Steinhardt, M. S. Turner, and F. Wilczek, "Reheating an inflationary universe," *Phys. Rev. Lett.*, vol. 48, pp. 1437–1440, May 1982. [Online]. Available: https://link.aps.org/doi/10.1103/PhysRevLett.48.1437

[46] D. J. H. Chung, E. W. Kolb, A. Riotto, and I. I. Tkachev, "Probing Planckian physics: Resonant production of particles during inflation and features in the primordial power spectrum," *Phys. Rev. D*, vol. 62, p. 043508, 2000. [Online]. Available: https://inspirehep.net/literature/508964

[47] J. L. Cook and L. Sorbo, "Particle production during inflation and gravitational waves detectable by ground-based interferometers," *Phys. Rev. D*, vol. 85, p. 023534, 2012, [Erratum: Phys.Rev.D 86, 069901 (2012)]. [Online]. Available: https://inspirehep.net/literature/926106

[48] P. Creminelli, S. Kumar, B. Salehian, and L. Santoni, "Dissipative inflation via scalar production," *JCAP*, vol. 08, p. 076, 2023. [Online]. Available: https://arxiv.org/abs/2305.07695

[49] R. Durrer, O. Sobol, and S. Vilchinskii, "Backreaction from gauge fields produced during inflation," *Physical Review D*, vol. 108, no. 4, Aug. 2023. [Online]. Available: http://dx.doi.org/10.1103/PhysRevD.108.043540

[50] N. Barnaby and Z. Huang, "Particle production during inflation: Observational constraints and signatures," *Physical Review D*, vol. 80, no. 12, Dec. 2009. [Online]. Available: http://dx.doi.org/10.1103/PhysRevD.80.126018

[51] Z. Yu, C. Fu, and Z.-K. Guo, "Particle production during inflation with a nonminimally coupled spectator scalar field," *Phys. Rev. D*, vol. 108, no. 12, p. 123509, 2023. [Online]. Available: https://arxiv.org/abs/2307.03120

[52] A. Berera, "Warm inflation," *Physical Review Letters*, vol. 75, no. 18, p. 3218–3221, Oct. 1995. [Online]. Available: http://dx.doi.org/10.1103/PhysRevLett.75.3218

[53] A. Berera and L.-Z. Fang, "Thermally induced density perturbations in the inflation era," *Physical Review Letters*, vol. 74, no. 11, p. 1912–1915, Mar. 1995. [Online]. Available: http://dx.doi.org/10.1103/PhysRevLett.74.1912

[54] A. Berera, "The warm inflation story," *Universe*, vol. 9, no. 6, p. 272, Jun. 2023. [Online]. Available: http://dx.doi.org/10.3390/universe9060272

[55] M. Bastero-Gil, A. Berera, R. O. Ramos, and J. G. Rosa, "Warm Little Inflaton," *Phys. Rev. Lett.*, vol. 117, no. 15, p. 151301, 2016. [Online]. Available: https://arxiv.org/abs/1604.08838

[56] M. Bastero-Gil, A. Berera, R. Hernández-Jiménez, and J. G. Rosa, "Warm inflation within a supersymmetric distributed mass model," *Phys. Rev. D*, vol. 99, no. 10, p. 103520, 2019. [Online]. Available: https://inspirehep.net/literature/1709820

[57] M. Bastero-Gil, A. Berera, R. O. Ramos, and J. G. Rosa, "Towards a reliable effective field theory of inflation," *Physics Letters B*, vol. 813, p. 136055, Feb. 2021. [Online]. Available: https://arxiv.org/abs/1907.13410

[58] P. B. Ferraz and J. G. Rosa, "Shrinking the Warm Little Inflaton," *JHEP*, vol. 12, p. 176, 2023. [Online]. Available: https://arxiv.org/abs/2308.00564

[59] J. G. Rosa and L. B. Ventura, "Warm Little Inflaton becomes Dark Energy," *Phys. Lett. B*, vol. 798, p. 134984, 2019. [Online]. Available: https://inspirehep.net/literature/1742007

[60] J. G. Rosa and L. B. Ventura, "Warm Little Inflaton becomes Cold Dark Matter," *Phys. Rev. Lett.*, vol. 122, no. 16, p. 161301, 2019. [Online]. Available: https://arxiv.org/abs/1811.05493

[61] M. Levy, J. G. Rosa, and L. B. Ventura, "Warm inflation, neutrinos and dark matter: a minimal extension of the Standard Model," *JHEP*, vol. 12, p. 176, 2021. [Online]. Available: https://inspirehep.net/literature/1835336

[62] M. Schmaltz, "Physics beyond the standard model (theory): Introducing the little Higgs," *Nucl. Phys. B Proc. Suppl.*, vol. 117, pp. 40–49, 2003. [Online]. Available: https://arxiv.org/abs/hep-ph/0210415

[63] M. Schmaltz and D. Tucker-Smith, "Little Higgs review," *Ann. Rev. Nucl. Part. Sci.*, vol. 55, pp. 229–270, 2005. [Online]. Available: https://arxiv.org/abs/hep-ph/0502182

[64] M. Perelstein, "Little Higgs models and their phenomenology," *Prog. Part. Nucl. Phys.*, vol. 58, pp. 247–291, 2007. [Online]. Available: https://arxiv.org/abs/hep-ph/0512128

[65] S. Weinberg, "General Theory of Broken Local Symmetries," *Phys. Rev. D*, vol. 7, pp. 1068–1082, 1973. [Online]. Available: https://inspirehep.net/literature/83745

[66] M. Peskin and D. Schroeder, *An Introduction to Quantum Field Theory*, ser. Advanced Book Program. CRC Press LLC, 2019. [Online]. Available: https://doi.org/10.1201/9780429503559

[67] J. Berges, "Introduction to nonequilibrium quantum field theory," in *AIP Conference Proceedings*, vol. 739. AIP, 2004, p. 3–62. [Online]. Available: http://dx.doi.org/10.1063/1.1843591

[68] M. Kachelriess, *Quantum Fields — From the Hubble to the Planck Scale*. Oxford University Press, 10 2022. [Online]. Available: https://doi.org/10.1093/oso/9780198802877.001.0001

[69] S. Weinberg, *The Quantum Theory of Fields. Vol. 2: Modern Applications*. Cambridge University Press, 8 2013. [Online]. Available: https://doi.org/10.1017/CBO9781139644174

[70] S. Coleman and E. Weinberg, "Radiative corrections as the origin of spontaneous symmetry breaking," *Phys. Rev. D*, vol. 7, pp. 1888–1910, Mar 1973. [Online]. Available: https://link.aps.org/doi/10.1103/PhysRevD.7.1888

[71] D. J. Toms, *The Schwinger Action Principle and Effective Action*, ser. Cambridge Monographs on Mathematical Physics. Cambridge University Press, 2007. [Online]. Available: https://doi.org/10.1017/CBO9780511585913

[72] O. Cheyette, "Derivative expansion of the effective action," *Phys. Rev. Lett.*, vol. 55, pp. 2394–2397, Nov 1985. [Online]. Available: https://link.aps.org/doi/10.1103/PhysRevLett.55.2394

[73] C. Armendariz-Picon, "On the expected backreaction during preheating," *Journal of Cosmology and Astroparticle Physics*, vol. 2020, no. 05, p. 035–035, May 2020. [Online]. Available: http://dx.doi.org/10.1088/1475-7516/2020/05/035

[74] M. D. Schwartz, *Quantum Field Theory and the Standard Model*. Cambridge University Press, 2013. [Online]. Available: https://doi.org/10.1017/9781139540940

[75] A. Caravano, K. Inomata, and S. Renaux-Petel, "The inflationary butterfly effect: Non-perturbative dynamics from small-scale features," 2024. [Online]. Available: https://arxiv.org/abs/2403.12811

[76] C. Pahud, M. Kamionkowski, and A. R. Liddle, "Oscillations in the inflaton potential?" *Physical Review D*, vol. 79, no. 8, Apr. 2009. [Online]. Available: https://arxiv.org/abs/0807.0322

[77] M. Aich, D. K. Hazra, L. Sriramkumar, and T. Souradeep, "Oscillations in the inflaton potential: Complete numerical treatment and comparison with the recent and forthcoming cmb datasets," *Physical Review D*, vol. 87, no. 8, Apr. 2013. [Online]. Available: https://arxiv.org/abs/1106.2798

[78] R. Flauger, L. McAllister, E. Pajer, A. Westphal, and G. Xu, "Oscillations in the cmb from axion monodromy inflation," *Journal of Cosmology and Astroparticle Physics*, vol. 2010, no. 06, p. 009–009, Jun. 2010. [Online]. Available: https://arxiv.org/abs/0907.2916

[79] R. Flauger, L. McAllister, E. Silverstein, and A. Westphal, "Drifting oscillations in axion monodromy," *Journal of Cosmology and Astroparticle Physics*, vol. 2017, no. 10, p. 055–055, Oct. 2017. [Online]. Available: https://arxiv.org/abs/1412.1814

[80] A. Achúcarro, M. Biagetti, M. Braglia, G. Cabass, R. Caldwell, E. Castorina *et al.*, "Inflation: Theory and Observations," 2022. [Online]. Available: https://arxiv.org/abs/2203.08128

[81] H. G. Lillepalu and A. Racioppi, "Generalized hilltop inflation," *The European Physical Journal Plus*, vol. 138, no. 10, Oct. 2023. [Online]. Available: http://dx.doi.org/10.1140/epjp/s13360-023-04512-1

[82] L. Boubekeur and D. H. Lyth, "Hilltop inflation," *Journal of Cosmology and Astroparticle Physics*, vol. 2005, no. 07, p. 010–010, Jul. 2005. [Online]. Available: http://dx.doi.org/10.1088/1475-7516/2005/07/010

[83] K. Dimopoulos, "An analytic treatment of quartic hilltop inflation," *Physics Letters B*, vol. 809, p. 135688, Oct. 2020. [Online]. Available: http://dx.doi.org/10.1016/j.physletb.2020.135688

[84] W. R. Inc., "Mathematica, Version 12.0," champaign, IL, 2019.

[85] C. Gomes, O. Bertolami, and J. G. Rosa, "Inflation with planck data: A survey of some exotic inflationary models," *Physical Review D*, vol. 97, no. 10, May 2018. [Online]. Available: http://dx.doi.org/10.1103/PhysRevD.97.104061

[86] A. R. Liddle and D. H. Lyth, *Cosmological Inflation and Large-Scale Structure*. Cambridge University Press, 2000. [Online]. Available: https://doi.org/10.1017/CBO9781139175180

[87] S. J. N. Mooij, "Effective Theories in Cosmology," Ph.D. dissertation, U. Amsterdam, IHEF, 2013. [Online]. Available: https://inspirehep.net/literature/1265038

[88] J. Guven, "Calculating the effective action for a self-interacting scalar quantum field theory in a curved background spacetime," *Phys. Rev. D*, vol. 37, p. 2182, 1988. [Online]. Available: https://doi.org/10.1103/PhysRevD.37.2182

[89] R. Jackiw, "Functional evaluation of the effective potential," *Phys. Rev. D*, vol. 9, p. 1686, 1974. [Online]. Available: https://inspirehep.net/literature/95439

[90] J. M. Cornwall, R. Jackiw, and E. Tomboulis, "Effective Action for Composite Operators," *Phys. Rev. D*, vol. 10, pp. 2428–2445, 1974. [Online]. Available: https://inspirehep.net/literature/1295

[91] S. Weinberg, "Perturbative Calculations of Symmetry Breaking," *Phys. Rev. D*, vol. 7, pp. 2887–2910, 1973. [Online]. Available: https://inspirehep.net/literature/83740